Contributions to a Meteorology of the Tibetan Highlands

By
H. Flohn

Department of Atmospheric Science
Colorado State University
Fort Collins, Colorado

Prepared with the support under Grant E-10-68G from the
National Environmental Satellite Center, ESSA
Project leader: E.R. Reiter
(H, Flohn was on leave from the University of Bonn, Institute of Meteorology)
August, 1968

Colorado State University

Department of Atmospheric Science

Paper No. 130

CONTRIBUTIONS TO A METEOROLOGY OF THE TIBETAN HIGHLANDS

by

H. Flohn[1]

This report was prepared with support
under Grant E-10-68G from the
National Environmental Satellite Center, ESSA
Project Leader: E. R. Reiter

Department of Atmospheric Science
Colorado State University
Fort Collins, Colorado

August 1968

Atmospheric Science Paper Number 130

[1] On leave from: University of Bonn, Institute of Meteorology

ABSTRACT

Summer meteorological conditions in the Tibetan Highlands are evaluated from the analyses of all available surface and aerological data and the detailed examination of NIMBUS and ESSA satellite cloud photographs. Persistent conditionally unstable lapse rates in the middle troposphere over the highlands account for a very high frequency of afternoon cumulonimbus activity which continues into the night in the eastern regions. Wind data show a marked diurnal circulation. The daytime ascending flow over the highlands is maintained during the night about 30% of the time by the dominant seasonal component of the regional circulation which is driven by the high tropospheric warm cell even through periods of weak uplift and rainfall.

During the summer the Tibetan Highlands act as a heat engine with an enormous convective chimney in the southeastern sector where giant cumulonimbus cells play a major role in continuously carrying heat upward into the high troposphere. This regional circulation is established in the spring when the initiation of the diurnal circulation of the highlands together with the pre-monsoon rains of NE India, produce a gradual warming of the middle and upper troposphere above the Himalayas. This warming weakens and finally eliminates the subtropical jet stream and establishes the tropical easterly jet. Thus, there is a complex interaction between the formation of the high tropospheric Tibetan anticyclone and the development of the Indian Monsoon.

TABLE OF CONTENTS

LIST OF FIGURES AND PLATES

LIST OF TABLES

LIST OF TABLES CONT'D.

CHAPTER 1
INTRODUCTION

Until very recent years, the Tibetan Highlands had to be included among the unknown continental areas of our globe. During the 19th Century and at the beginning of the 20th Century, a number of scientific travelers-- like the Schlagintweit brothers, Prshevalsky and Sven Hedin--collected regular meteorological observations. However, these data were measured at various locations, at different altitudes and under a variety of local conditions; thus their evaluation could be made only in an approximate way, even more approximate than maritime observations from moving ships. The results from a very few climatic stations in the southern valleys--Leh, Lhasa, Gyangtse--have been published. Most of the available data have been evaluated and compiled with other short records in a comparative study (Flohn 1958, 1959). One of the remarkable results obtained was that the valleys of southern Tibet, at altitudes between 3500 and 3700 m, enjoy higher summer temperatures than the once famous "Hill Stations" in the Himalayas, at altitudes of 2100-2300 m. At least during the warm season, the surface temperatures axe definitely higher than the latitudinal average in the free atmosphere at similar heights. Furthermore, a large frequency of .showers and thunderstorms, often with snowfall and hail, has been reported from all sources, lasting during the whole warm season, i. e. without being limited to the time period of the Indian summer monsoon.

At the time when these studies were submitted for publication, only the first data had become available from the network of meteorological and aerological stations which has been installed by the military occupation forces of the Chinese People's Republic since 1956. These data--used in two more recent publications (Flohn 1964, 1965)--confirmed the occurrence of a quasi-stationary warm anticyclone centered above SE Tibet, which is responsible for the remarkable intensity and persistency of the Tropical Easterly Jet (Koteswaram 1958) above the Indo-Pakistan subcontinent. However, the exact position of the warmest air has been argued, as well as the role of this warm anticyclone in the complex mechanism of the Indian summer monsoon. While at first the cause of this seasonal high-tropospheric anticyclone was suggested in the transport of sensible heat from a large-scale elevated heating surface (about 2×10^6 km^2 with

an average elevation of 4500 m), more recently it has been assumed that the large amount of latent heat released in the strong orographic rainfall zone of Assam, Bengal, Upper Burma and SE Tibet (triggered by the eastern section of the Himalayas) is of even greater importance. A comprehensive review of the monsoon problem in its different aspects has recently been given by Orgill (1967) and Riehl (1967).

The purpose of the present study is to check these working hypotheses with the much better observational data now available (cf. Chapter 2). Since the investigation has been started from large-scale questions of dynamic climatology, it is essentially limited to the warm season; only few data from the winter and spring seasons have been collected for comparison. A complete surface and upper air climatology of the Tibetan area is not intended here, in spite of the growing need for filling this gap. However, some important aspects of the heat and water budget will be mentioned, using data from the marginal mountain areas. The bulk of the climatological results are contained in Tables 1-23 (cf. Appendices D-H).

CHAPTER 2
DATA AND DATA SOURCES

The present study is based on nearly all of the sources now available. Since about 1956 the Meteorological Service of the Chinese People's Republic has installed a number of meteorological stations in Tibet with trained observers. Synoptic surface data from 16 such stations (cf. Table 1, Appendix B) are used here; they had been partly evaluated (1200 GMT only) from available publications (Appendix A, Sources 12 and 14), while the largest portion has been evaluated from unpublished records of the National Weather Records Center, Asheville, North Carolina. Not less than 12 of these stations are situated above an altitude of 3000 m; however, only two are situated at the average level of the highlands near 4500 m, and none above 4800 m. Most stations are located in the sheltered valleys of eastern and southern Tibet, which-- according to Kingdon Ward and other experienced travelers--do not represent the harsh climate of the mountain ridges and passes, especially not that of the great Changtang Plateau in northern and west-central Tibet. These extensive areas are only insufficiently represented by the short and incomplete record from Shensa Dzong and by the Italian expedition observations at Depsang (5362 m) just east of the Karakorum ranges. However, the excellent observations at Heiho supply many most interesting (and sometimes rather unusual) results from the central part of Tibet. Unfortunately the vast area between longitudes 80°E and 88°E is not covered by any available station. The essential results are collected in Appendix D.

From nine of these stations aerological data are available, although incomplete and not without errors. In addition to the incompletely published data (Appendix A, Sources 12 and 14) for the years 1956-61, unpublished records from the National Weather Records Center, Asheville, North Carolina have been used. The quality of the radiosonde observations is apparently quite satisfactory. Since only data received by telecommunication are available, many gaps and errors are unavoidable. Unfortunately, upper wind data are only available at Tibetan stations from optical theodolites; they are therefore strongly biased by the selection of cases with few

clouds and by other systematic errors. In order to study the diurnal (and seasonal) circulation induced by the Tibetan highlands, it was also necessary to use aerological data from adjacent territories (India, Pakistan, Afghanistan, U.S.S.R., Sinkiang, Szechwan). The essential results and station coordinates are given in Appendix E, as well as some critical remarks.

In addition to these data, many climatological data have been collected during the last twenty years from the available literature, including unpublished (or only partly published) records. Since such data from the marginal high mountain ranges are little known--especially from Afghanistan, northernmost Pakistan, Nepal and Sikkim--a collection has been given in Appendices F and G, together with a list of coordinates (Table 21). Here the average temperatures have been reduced to certain altitudes (2300, 3300 and 4000 m above sea level) in order to facilitate comparisons.

A major objective of this investigation involved the use of satellite cloud photographs as a primary data source. While TIROS pictures have not been used--because of gridding difficulties--a detailed study of a few NIMBUS I pictures (during late summer 1964) and of a more complete set of NIMBUS II pictures (May 25 to July 31, 1966) has been carried out. Due to the relatively lower quality of the pictures from the central AVCS camera of NIMBUS II more quantitative studies of convective cells had to be excluded. These data were supplemented by a comparative survey of ESSA 3 and 5 pictures in their rectified and gridded version available since November 1966 and mainly used for Summer 1967. For comparison, such pictures have also been examined for January and April 1967, as well as (in a preliminary manner) for February and March 1968 (ESSA 6). Since these ESSA pictures are given on a smaller scale and with a lower resolution, no details have been studied. All of these satellite photographs were taken shortly before noon (between 1030 and 1200 local time, 90E), thus they represent only one part of the marked diurnal circulation (cf. Chapter 6). As a supplement, a few HRIR records from NIMBUS I have also been surveyed, but no detailed study of these excellent sources could be made.

It was not intended to study individual cases in detail; therefore, only short descriptions of the days with satisfactory satellite information (NIMBUS) are given (Appendix C). For comparison, two series of weather maps have been used: the Japanese maps mainly for 500 and 700 mb, and the hemispherical maps of the Free University of Berlin (Scherhag and coll.) for surface and 300 mb (Appendix A, Sources 11 and 12). These series are not quite internally consistent, they are also incomplete due to telecommunication deficiencies. Surface analysis of such an area--where most stations are situated between 700 mb and 600 mb--is certainly not very satisfactory, not even on a hemispherical scale; nevertheless, some useful hints could be derived from these sources.

CHAPTER 3

SUMMER WEATHER ACCORDING TO SATELLITE PICTURES

Cloud photographs from the NIMBUS AVCS camera have been evaluated for seven cases in 1964 (August 31-September 21) and 28 cases between May 25 and July 31, 1966; the descriptions of the individual cases are given in Appendix C and examples are shown in Plates 1 -5. Furthermore, rectified pictures from ESSA 3 and 5, on a much smaller scale, have been used for a comparative study of summer conditions during 1967 (e. g. Plates 6-7). All these data reveal a fairly persistent cloud pattern above the whole area during summer, which contrasts strongly with the large day-to-day variations in the area of the extratropical westerlies (extending to Sinkiang and northern Tibet) as well as in the Indian Monsoon region. The main features of this climatic cloud pattern are the following:

a) The western mountains, particularly Hindukush, Pamir, Alai, and to a lesser degree also the NW Himalayas west of 78E, Karakorum and central Kuenlun (78-83E) are unusually clear and cloudfree. Only a few convective systems can be seen along the ridges, especially visible from NIMBUS I with its excellent resolution (e. g. Plate 1). The larger valleys (Amu-Darja and Indus with its tributaries) are clearly distinguishable in almost every picture. Lakes Karakul and Panggong, the great bend in the Indus, together with the valleys of the Gilgit, Hunza and Astor Rivers, the marked Shyok Valley, and the Kunar River in central Hindukush are excellent landmarks, as well as the Wakhan and Alai Valleys in the Pamir region. Only south of about 36N do large-scale cloud systems occasionally hide the topography and increase the snow-cover. During the summer, the snow-cover disappears due to the high radiation; melting and evaporation into the dry air may both contribute to this result. However, the large extension of glaciers is sufficient to outline the orographical features. The decrease of visual albedo during July 1966 was clearly discernible.

b) In the high plateaus of western Tibet (west of about 82E) cloudiness is relatively weak, not infrequently occurring as small-scale cumuli (especially in the Upper Sutlej Basin west of Lake Manasarovar) or mountain

wave clouds in the lee of the Karakorum Range (cf. Plate 3, July 4-5, 1966). Giant Cb cells are not rare, but less frequent and less intense than above central and eastern Tibet. Some lakes (especially Lake Lighten, south of Kuenlun) are often seen. The synoptic data of Gar Dzong confirm this result.

c) In central and southern Tibet most pictures are characterized by a large number of giant Cb cells, even at this early time of the day (around 1100 local time, cf. Plates 4-7). This is confirmed by the quite exceptional number of Cb clouds, showers and thunderstorms in the afternoon hours at all stations of this area; Heiho may serve as the most typical example (Tables 2, 3, 5). Frequently these giant cells are arranged according to topography. Many of the lakes — especially Seling-Tso and Nam-Tso (or Tengri-Nor)--are visible. At this early time anvils are only rarely developed. Extended Cs sheets are frequent north of about 33N, while the upper Tsangpo Basin (west of Shikatse) can be frequently distinguished as more or less cloudfree.

d) Eastern Tibet south of about 33N exhibits much more cloudiness than the other parts. But here again giant cells and other convective clouds prevail, and the large NW-SE oriented valleys (especially Yangtsekiang and Yalung) are mostly visible. In the northeastern part of Tibet the cloudiness decreases and convective cells are frequently replaced by extensive Cs sheets.

e) The central and southern Himalayas (between Garhwal and Sikkim, i.e., about 78-89E) are frequently covered by convective clouds, but also-- from the southern side--by intense cloud systems from active or decaying monsoon disturbances. However, the northern flank is much less affected and the dark valleys crossing the Himalayan ranges from north to south, reaching with their source tributaries right to the southern edge of the dry highlands, are frequently cloudfree.

f) East of 89E, the Himalayas and especially the Assam Arc on both sides of the Tsangpo Gorge are mostly cloud covered, frequently with dense, apparently stable, Ns systems (cf. Plates 4 and 6). Sometimes a dense Cs-As sheet covers a number of indistinct, bright convective cells. North

of the main mountain chain the character of the cloud pattern changes rapidly, stable Ns dissolving into a dense network of more convective types of cells. While the lower Tsangpo Gorge is frequently covered, the upper portions and its tributaries are sometimes discernible.

g) The region of the Meridional Gorges (Irawaddy to Yangtse) is characterized by extensive, but mostly convective, cloudiness; the gorges are partly discernible, but only as a chain of cellular gaps in the extensive cloud cover (cf. Plate 5). Because of the low quality of the pictures from the central camera of NIMBUS II, those of the side cameras have been used, which do not allow more detailed studies.

In order to obtain an internally consistent picture of the average summer weather conditions in the Tibetan Highlands, two maps have been tentatively drawn:

A) Average cloudiness at 1100 local time (33 days with satellite pictures)--Figure 1;
B) Percentage of convective clouds (Cu, Cb at 1100 local time, 33 days) compared with the total cloud amount--Figure 2.

Both maps are derived from estimates for each 2° lat. x 2° long, area, allowing for the apparent increase of cloudiness with distance from the subsatellite point, but disregarding gridding errors. These gridding errors could not be rectified in such a comparative study of many cases. In most cases--except the portions viewed under large angles from the vertical (> 30°)--these errors are less than 0. 5° latitude (= 55 km).

Figure 1 shows a marked maximum of cloudiness in the area of the Assam Arc; here the highest cloudiness is found along the mountains to the north and east, which are nearly completely covered. From this center, the average cloudiness (in percent) decreases slowly towards the north and east. The figures for central Tibet (40-50 percent) and for eastern Tibet (near 60 percent) are consistent with the values derived from expeditionary observations (averages for June-July: central Tibet 42%, eastern Tibet 67%). In contrast to this, the western mountains (Pamir, Hindukush, NW Himalayas) are apparently cloudfree in most

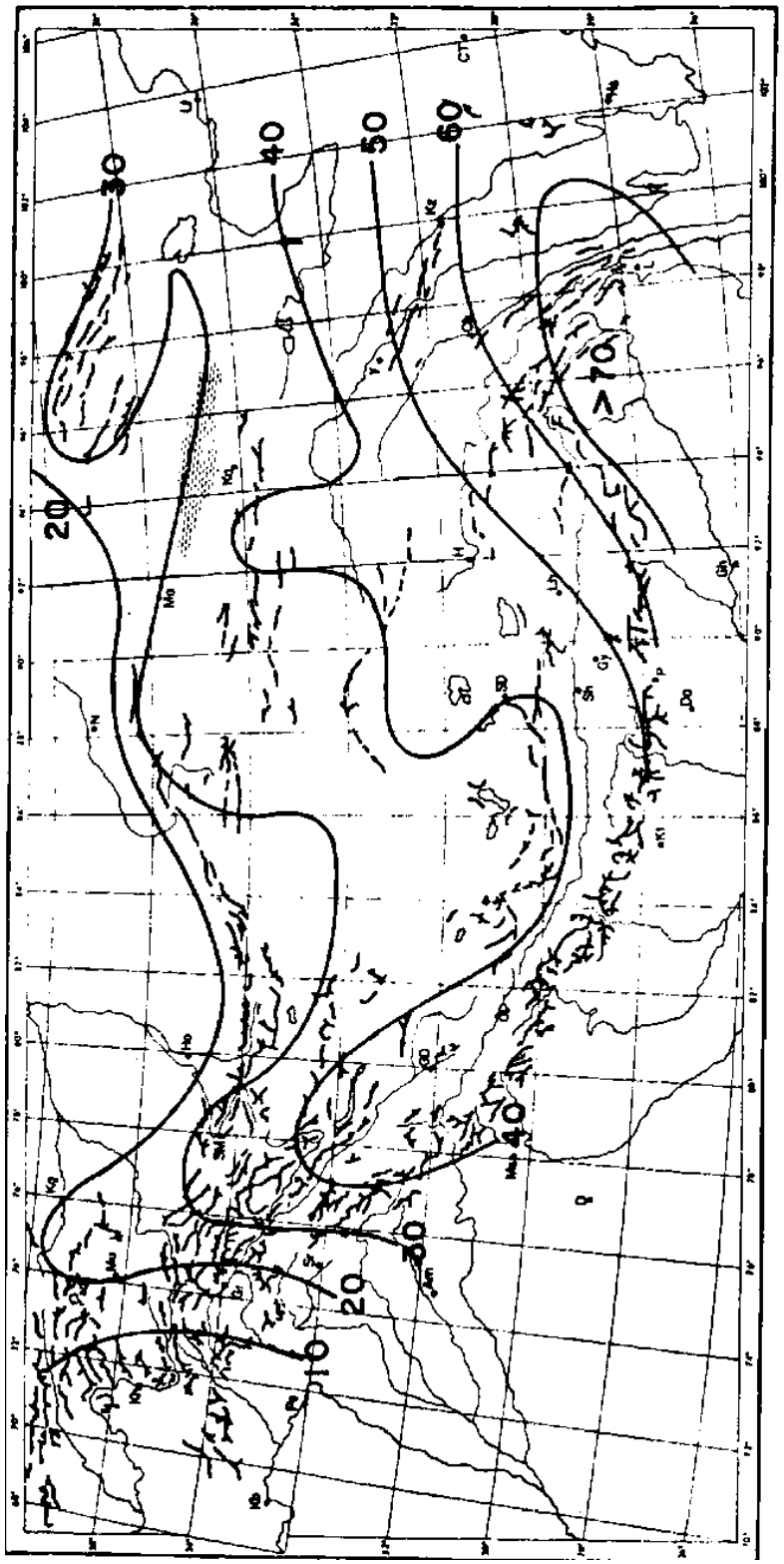

Fig. 1. Average cloudiness (percent), 1100 LT, satellite data, 33 days.

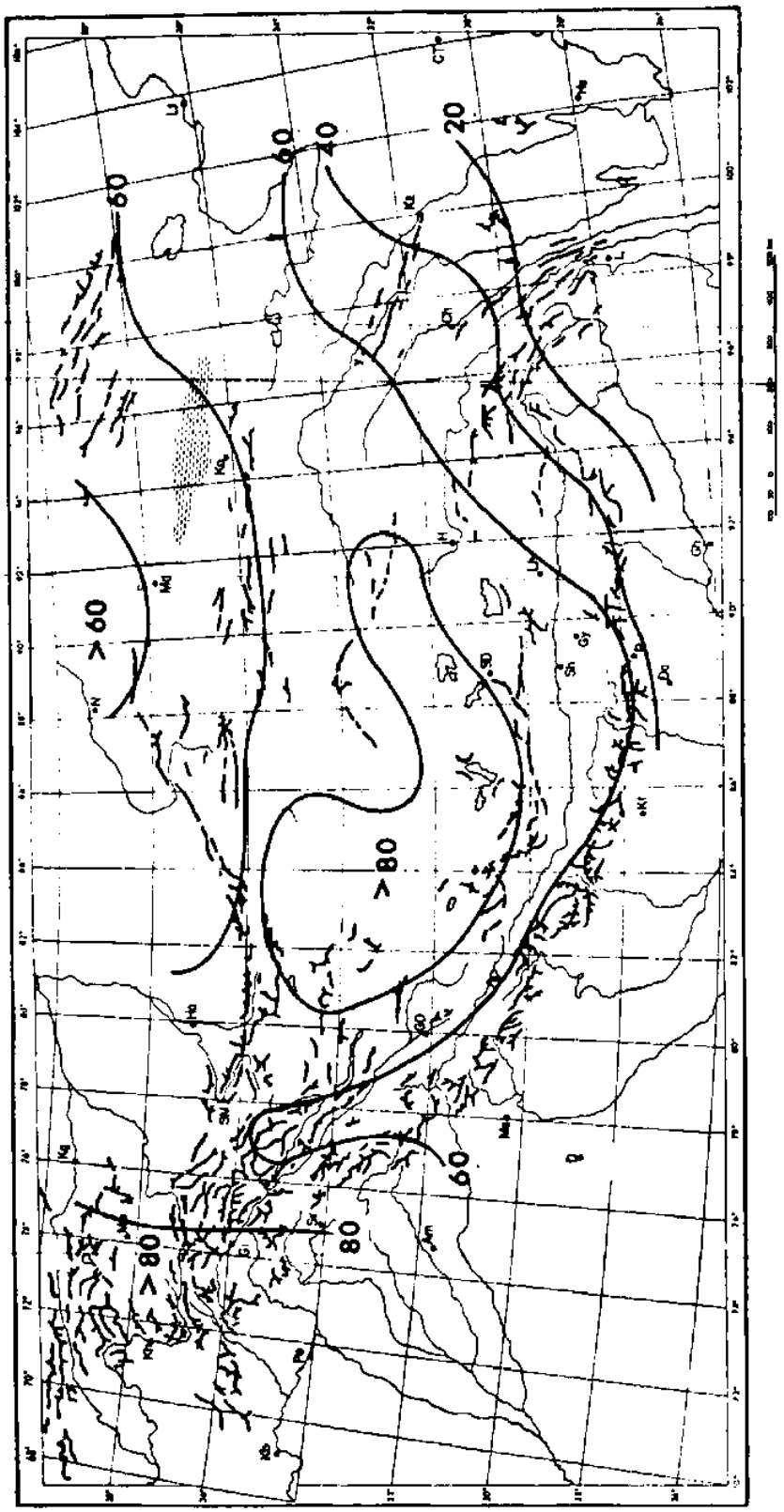

Fig. 2. Percentage of convective cells (Cu and Cb) contributing towards the total cloudiness, 1100 LT, 33 days.

satellite pictures. This seems to be inconsistent with the available cloud statistics: Karakorum expeditions 48%, Murgab (Pamir) 38%, Misgar (NW Karakorum) 08^h 26%, 17^h 38%. However, a clear distinction between small-scale cumuli--developing before noon along the mountain ridges-- and snow-cover or glaciers is only possible from some NIMBUS I pictures, while the quality of the NIMBUS II pictures is insufficient for such discrimination. Especially in the glaciated central parts of Karakorum and Kunelun, any clear distinction between the orographical pattern of Cu convection and the distribution of snow and ice was unfortunately not possible. Furthermore it was necessary to take into account the frequent shallow cirrus veils--with a vertical extension of only few decameters (as judged from many airplane observations in other areas)--which are invisible from the satellite, as well as an overestimate of clouds near the horizon by less experienced surface observers.

Figure 2 is derived from a subjective classification of stable clouds (Ns, As, Cs streaks), unstable clouds (Cu, Cb) and partly unstable clouds (mountain waves, Cb cells covered by extended As and Cs streaks, Sc, Ac. (Here only Cu/Cb cells have been selected.) It demonstrates clearly that in western and central Tibet (as well as in the western mountains) convective clouds are dominant. Nearly every picture displays a great collection of bright developing Cb cells; high albedo seems to indicate great vertical extension. Due to the early time of the day--one hour before noon—the development of anvils is rare. From several counts the density of such cells can be estimated at 20-50 per 10^5 km^2 ; the average dimension is then on the order of 50-80 km. This result coincides very well with the exceptionally high frequency of afternoon showers and thunderstorms, and Cb clouds as revealed by Tables 3 and 4. The results at the marginal mountains in both western and eastern sections are not sufficiently reliable, since they are frequently derived from the side cameras of NIMBUS II with their oblique view and low resolution. Only the area between 7 6E and 96E can be considered as fairly trustworthy.

Similar to the cloudfree annulus around a heated island--as described by Malkus (1955) and others--a daytime cloudfree divergence zone is often observed around heated mountains. The author has observed--during

several automobile journeys—such zones along the eastern sides of the Venezuelan Andes and the Rocky Mountains, along the northern side of the Alps and along the southern side of the Hindukush Mountains in Pakistan and Afghanistan; one should expect them also along the Himalayas. Using enlargements of rectified ESSA photographs--with a scale of about $1:42 \times 10^6$--for a sample of 37 days between June 27 and August 6, 1967, the frequent occurrence of an elongated divergence zone just south of the Himalayas shortly before noon is quite conspicuous (e. g. Plate 7). Marked exceptions are the well-known "break conditions" of the monsoon, where a monsoon disturbance has been displaced in the-forward section of a trough of the upper westerlies northward into the Himalayas. Estimating the length of this divergence zone for each of these 37 days in percent of the total length of the Himalayas (from 74E to 95E), the net result is 60 percent in the average. Since this zone coincides with a belt of increased precipitation amount and frequency along the mountains, one may interpret this belt to be caused by the orographic effect on monsoon disturbances, and/or by nocturnal rains (cf. Assam, Chapter 5).

From all investigated satellite pictures during Summer 1966 (NIMBUS II) and 1967 (ESSA 5), a number of cases have been found-- cf. Appendix C, June 28 and July 24, 25 and Plate 5--in which the convective cloud systems are apparently arranged in a more or less complete anti-cyclonic pattern. Because of their scale, the rectified ESSA pictures were better suited for finding such a large-scale pattern, after which the NIMBUS pictures were re-examined. Here all cases have been omitted in which the orographic orientation of the mountain ridges in the vicinity of the Assam Arc suggests an incomplete anticyclonic circulation north of 29N, 95E. Figure 3 shows the distribution of anticyclonic centers for 21 cases, together with the average position of the anticyclonic center at 31.8N, 90.6E, i.e. very near the position suggested by earlier aerological evidence. A nearly vertical structure of such a center between about 150 and 500 mb may be expected when considering the strong vertical exchange of momentum in Cb cells.

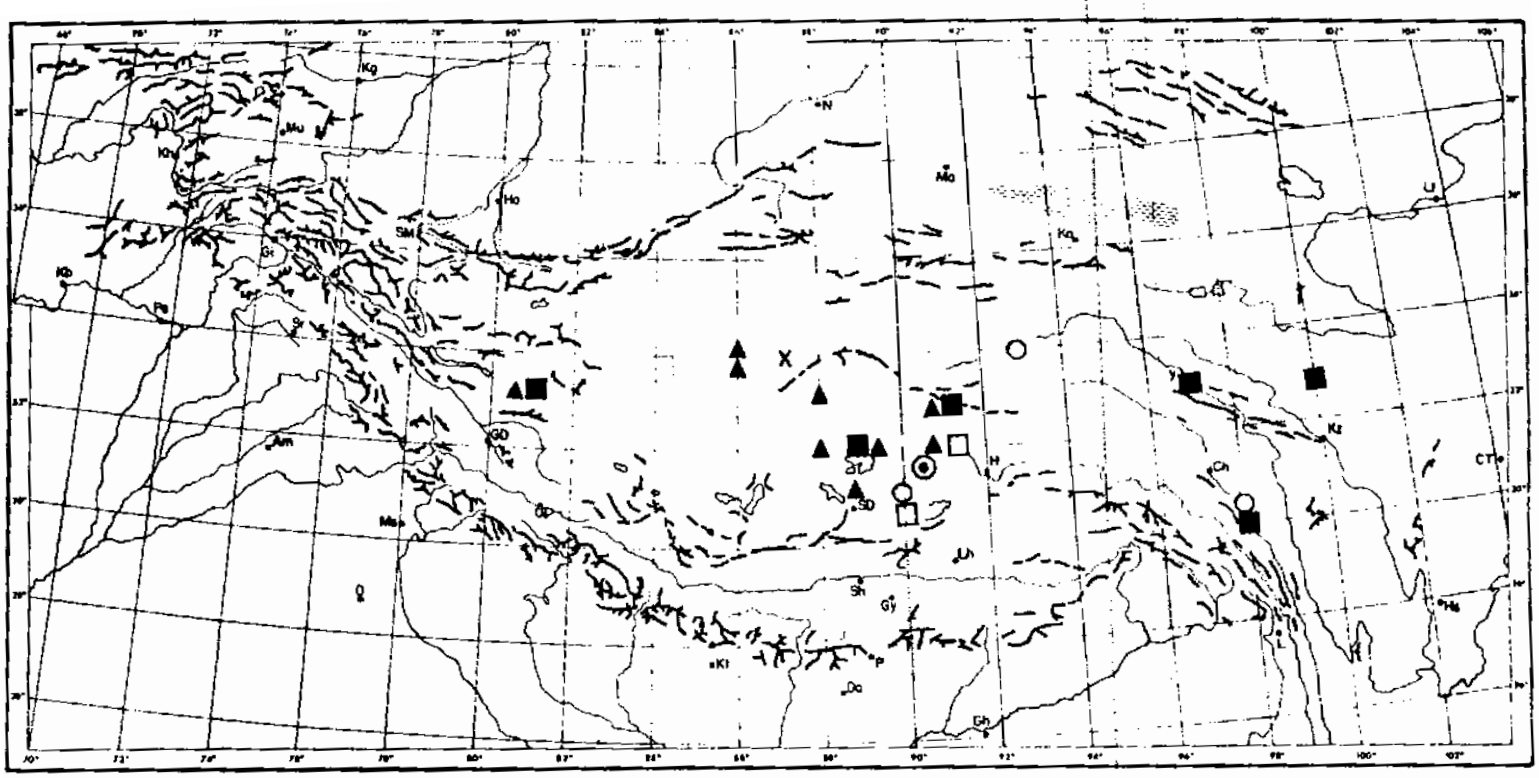

Fig. 3. Positions of anticyclonic centers (from satellite pictures).

CHAPTER 4

SYNOPTIC AND AEROLOGICAL CONDITIONS DURING SUMMER

As a necessary complement to the satellite studies, surface data from sixteen stations and aerological data from nine stations have been investigated for varying periods, mainly between 1960 and 1966. Careful checks have shown that during summer the differences between individual years are sufficiently small so as not to prohibit the use of short records from different years. However, from the climatological viewpoint, the results can only be taken as first approximations.

The surface data (Appendix D) are given in a condensed form in Tables 2-6. Here all data for the period June-September are taken together in spite of the fact that in central and southern Tibet, July and August are slightly more humid and cloudy than June and September. Most striking is the unusually high frequency of afternoon showers, thunderstorms and Cb clouds at all stations of central, southern and southeastern Tibet, thus confirming the high frequency of giant convective cells derived from the satellite pictures shortly before local noon. In one single hour (1700-1800 LT, cf. Table 2), the relative frequency of showers and thunderstorms rises at four stations to 59-72%; the frequency of afternoon thunderstorms between 1200 and 1800 LT (i. e. thunder heard) at six stations reaches 32-45% which may belong to the highest observed values. The frequency of Cb clouds at 1800 LT varies, at seven stations, between 60 and 81%. The convective activity above western and northern Tibet is less spectacular. The highly arid Tsaidam Basin (cf. Karmu) is apparently subject to local divergence with very little convective activity in spite of the high vertical lapse rate (Table 11).

Unfortunately, no data of rainfall amounts are available, and the very scanty available data in the literature are restricted to southern and southeastern Tibet. South of 33N and east of 90E the summer rains seem to be fairly frequent and reliable; the climate of this region is only semi-arid during winter, but mostly humid during four-six summer months (cf. Appendix G). It strongly contrasts with that of the Changtang Plateau in the central,

northern and western sections of Tibet where, in spite of the high convective activity, most precipitation evaporates before reaching the surface. This is certainly true at the stations in the west and north, where the relative humidity during the afternoon remains below 30-40% (Table 19) and where the cloud bases are higher than 2000 m above the surface (Table 5). It should be noted further that the observations of convective cloud bases (h) and those of humidity do not always seem to be quite consistent; however, the humidity measurements at a valley station may not be representative for the convective clouds triggered over the adjacent mountains.

The aerological data (Appendix E, Tables 7-12) demonstrate a marked warm ridge along about lat. 30N (cf. Figure 4); the exact position of the heat center will be discussed in Chapter 7. It is important to stress the high humidity above SE Tibet--unfortunately no aerological data are available from stations like Gar Dzong in SW Tibet--compared to the dryness above the northern flank (Mangya, Karmu, cf. Tables 7, 8). The high summer temperatures are remarkably constant from year to year (Table 9). Of special interest are the average vertical lapse rates during afternoon (Table 11), once more belonging to the highest observed values. The values of Kosharyl may represent the conditions above the arid western highlands where an average lapse rate of 9°/km in the layer 4-7 km, nearly dry- adiabatic, is quite common. In SE Tibet, however, the vertical lapse rate is still 7-8°Q'km, now together with high relative humidities, and thus indicating a super-moist-adiabatic gradient with large conditional instability up to about 200 mb (cf. Chapter 7). Obviously similar conditions also prevail in other parts of central and southern Tibet. The large number of giant convective cells observed as early as 1100 LT (Chapter 3) is quite consistent with these results. The low variance of the mid-tropospheric temperatures (Table 12)--similar to that of the equatorial region--also indicates the remarkable persistency of these conditions from day to day.

A zonal temperature cross-section along lat. 32N (Figure 4)--derived from data source 17 (Appendix A)--shows the center of the positive temperature anomalies above Tibet near the 300 mb level, in marked contrast to the low-level continental heat centers above Africa and western North America. An interpretation of this position will be given in Chapter 7.

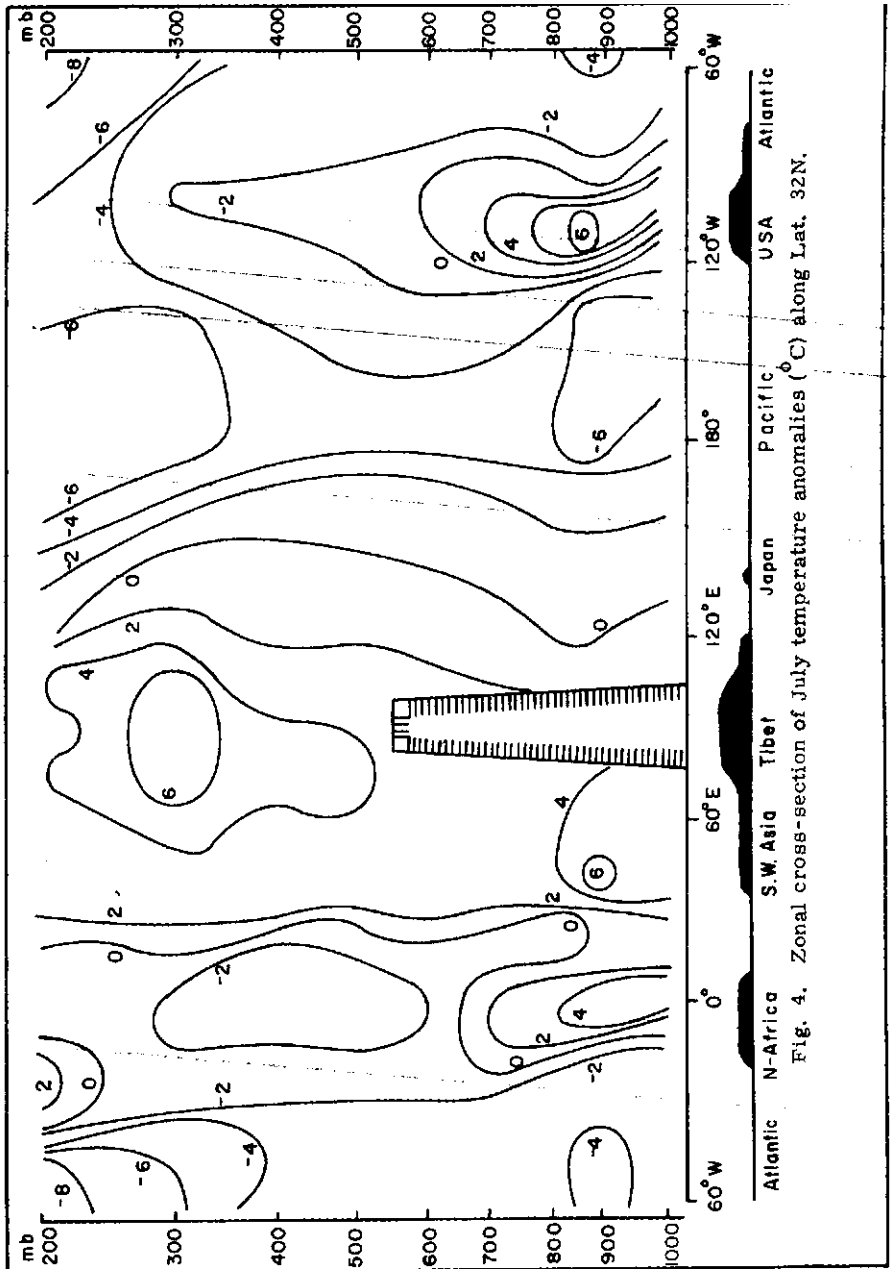

Fig. 4. Zonal cross-section of July temperature anomalies (°C) along Lat. 32N.

CHAPTER 5

SUMMER CONDITIONS IN ASSAM AND THE GORGES COUNTRY

Assam--i. e., the Brahmaputra (Tsangpo) plain including the well- known Khasia Hills (1954 m)--is surrounded on three sides by high mountains. The Himalayan Mountains reach up to 7754 m (Namche Barwa) right at the Tsangpo Gorges and only a few passes are below 4500 m. The eastern mountains between the Tsangpo-Lohit system and the deep meridional Salween Gorge are everywhere higher than 3900 m north of latitude 27.5°. Between latitudes 25° and 27.5°N, the NNE-SSW running ridges between Assam and the catchment areas of Chindwin and Irawaddi have altitudes between 2400 and 2800 m, except for a narrow, hidden pass at about 2000 m.

Under such conditions, the low -level monsoon winds which enter the Assam-Bengal area from the south are forced to flow from WSW to ENE, south of the Indo-Gangetic pressure trough representing the monsoon convergence zone. According to the average surface wind frequencies, this convergence zone--as represented by the stations Dhubri (26.0N, 90.0E), Gauhati and Sibsagar (27.0N, 94.6E) with nearly equal frequency of northeasterly and southwesterly winds--runs from the great bend in the Tsangpo at Dhubri to 27.5N, 97E. All stations north of this line have predominantly northeasterly winds (Dibrugarh, Tezpur, Darjiling) while at all other stations southerly winds definitely prevail.

Pilot balloon data in that region--especially under the conditions of the rather persistent monsoon rains--are strongly biased by selection of the rare fine weather situations. With that restriction in mind, recent upper wind maps (Source 4, Appendix A) give the impression that SW flow prevails at the 3 km level up to the Himalayas, including Upper Burma and the Gorges region. However, since there is no outlet below 4 km, it must be concluded that either the air is continuously forced to rise or that it tends to curve cyclonically into the easterly flow along the Himalayan foothills which can be followed up to the Punjab. The latter is evident from the Rawin ascents of Gauhati where the direction of the resultant wind (July/

August) turns from 222° at 850 mb to 187° at 700 mb, 137° at 500 mb and finally to 060-070° in the 300-100 mb layer, i.e., above the highest Himalayan "peaks.

Thus, the meteorological situation above Assam is characterized by a more or less permanent low-level convergence zone and by a similarly permanent cyclonic flow in the layers below 600 mb or at least 700 mb, driven by the persistent southerly monsoon flow over the Gulf of Bengal and forced into curvature by the combined effect of the surrounding mountains.

The effect of these circulation features on precipitation frequency and amount in Assam is quite remarkable. From the Indian Daily Weather Map (April-September 1962-63) one can select ten low elevation stations in the Assam plains, excluding all hill stations like Cherrapunji with its enormous quantities of rainfall. Taking into account the frequency of missing rainfall reports (15 percent), one can evaluate area-averaged frequencies and amounts of rainfall for two periods daily (0830-1730 and 1730-0830 Indian time). These data were statistically evaluated for the monsoon season, June-August, and for the pre-monsoon season, April-May.

The diurnal variation of rainfall is characterized by a minimum during day and a maximum during evening and night, which has been confirmed by a few individual stations like Darjiling and Cherrapunji. During the fifteen hours, 1730-0830 LT (62.5 percent of the total time), 74.3 percent of the daily area rainfall is observed during the monsoon season, and 78.6 percent during the pre-monsoon months. Two physical causes may contribute to this predominance of nocturnal rains: the nocturnal convergence of local circulations (mountain breezes) above the plain, and the net long-wave radiation from the cloud tops during night, when short-wave absorption in the atmosphere vanishes.

In the following table, these data are classified with respect to the area affected by rain in percent of the total area (i.e., the relative frequency of stations with rainfall). Section A gives the probabilities of different classes of area affected by rain; Section B gives the contribution of these classes to the total amount of rainfall; and Section C gives the

effective area-averaged rainfall (i.e., the average rainfall per station with rain); n = number of cases.

	Percent of Area Affected by Rain						
A)	90-100	>70	>50	>30	No Rainfall	Total Average	n
Assam, April-May	2.5	9	29	59	7%		122
Assam, June-August	10	34	74	92	0		184
N. Germany, June-August	21	47	63	75	10		1104
B)							
Assam, April-May	10	23	49	82	0%	8. 8mm/d*	
Assam, June-August	22	53	89	98	0	15.7mm/d*	
N. Germany, June-August	45	74	91	97	10	3.0mm/d*	
C)							
Assam, April-May	37.5	25.8	23.6	24.0	0%	23.8mm/d	
Assam, June-August	39.1	29.9	26.3	__	0	26.1mm/d	
N. Germany, June-August	6.3				10	5.0mm/d	

* Average daily area rainfall (with respect to all stations)

On the average, the portion of the total area of Assam affected by rain increases from 37% during the pre-monsoon to 60% during the monsoon season. In contrast, the same statistic for northern Germany (Ungewitter) is 57% during spring and 59% during summer. Due to the convective character of the major rainfall events in Assam, the probability of very widespread rain is smaller in Assam than in central Europe. Further, on 74% of all days at least half of the area is affected by rainfall, and no rainless days exist. Similarly, the intensity of rainfall per station affected (effective area average) does not vary substantially with an expansion of the rainfall area. The contribution of the individual days to the seasonal amount of rainfall varies mainly with the areal extension of rainfall.

Certainly the area-averaged rainfall over Assam varies with time. As usual, the contribution of a few days with large widespread rainfall amounts is much greater than that of many days with scattered or isolated showers. In thirteen percent of all cases, the daily area-averaged rainfall over Assam is larger than 200 percent of the average daily area-averaged rainfall; while in twenty percent of all cases, the daily area-averaged rainfall over Assam is larger than 150 percent of the average. These cases yield 31 and 44 percent, respectively, of the total amount. The latter figures compare well with northern Germany, where 21 percent of all days yield 45 percent of the total rainfall. However, during the monsoon no 24-hour dry period exists and the percentage contribution of the few days with very widespread rainfall to the total amount is substantially less than in middle latitudes. Therefore, the monsoon rainfall in the Assam area must be considered a semi-permanent feature. During the pre-monsoon season, the rainfall is produced mainly by showers while only relatively few disturbances produce widespread and intense rain.

Very few meteorological data are available from the area of the Meridional Gorges, between longitudes 98E and 102E. There is a long climatological record at Tengchung (25.1N, 98.5E) (located south of the Gorges area proper, which is limited to about latitudes 26-30N). To the north there is a transition to the broad NW-SE oriented valleys of eastern Tibet. After many journeys, the experienced botanist Kingdon Ward distinguished between an upper and a lower River Gorge Country. In the upper part (inside the main mountain ranges crossing the gorges at latitudes 28-28.5N and reaching to altitudes above 6000 m) the valleys are arid and the plateaus are relatively dry, while the lower gorges are much more moist with densely forested mountain ridges. Crossing a great mountain range towards the south, "the arid, treeless Salween Valley passes abruptly into a forested region within a few miles, through a magnificent gorge" (Kingdon Ward).

According to the satellite pictures used, the summer weather in the Gorges country should be cloudy, with frequent showers and thunderstorms along the mountain ridges. In the gorges themselves intense heating and strong southerly winds prevail during daytime, and only a few showers reach the ground before evaporating. During night, at least in some of the broader valleys, the converging down-slope breezes produce further

showers in the thermodynamically unstable air. At Hsihchang and Lawang the frequency of any kind of precipitation has its minimum between 0600 and 1200 local time, with a weak peak in the afternoon only at Lawang (Table 4). The average cloud base at both stations is at 1500-2000 m above the station, i.e., at 3000-3500 m above sea level. The high frequency of precipitation shows, however, that neither of these stations represents the arid part of the gorges. It is remarkable that at nighttime (dawn) southerly winds still prevail at Lawang (cf. Chapter 6). Because of the complex orographic pattern, however, no substantiated interpretation of the diurnal circulation can be given from map studies alone. At 700 mb, the prevailing northeasterlies show that the monsoon convergence lies south of this latitude.

The satellite pictures confirm Kingdon Ward's reports on the climatic effect of the divide between the catchments of Lohit-Tsangpo and Salween which "cannot be crossed by the clouds". The extremely heavy and persistent precipitation over all mountain ranges surrounding Assam, especially those at the northern and eastern sides, is replaced east of the divide by frequent sunshine and only convective showers. The number and intensity of these showers obviously increases toward the south, especially south of the main mountain range near 28N. It seems almost certain that the rainy season here also coincides with that of Assam; however, the cool season is by no means continuously dry (cf. Table 20).

CHAPTER 6
DIURNAL AND SEASONAL CIRCULATION

A comparative investigation of surface winds at representative stations (Appendix H, Table 22) was expected to demonstrate the usual diurnal change of wind direction, as produced by strong ascending valley breezes at noon and afternoon and by weaker descending mountain breezes during night and early morning. However, the results were not as expected. At least in a number of representative cases--disregarding here the most frequent cases with calms at dawn--the nighttime flow at 0600 LT was predominantly in the same direction as during the day (at Mangya and Shahiullah Mazar on the northern flank, at Phari Dzong, Lawang and Hsihchang on the southern flank). Here a large-scale ascending flow apparently overwhelms the nocturnal mountain breeze. From data given in Source 8 (Appendix A), we find the same is true for Indian stations like Kalimpong (near Darjiling) and Mussoorie. During summer, the early morning mountain breezes—in this case at 0830 LT--from the north are replaced, in about 30 percent of all cases, by an ascending southerly flow. A different example is given at Shikatse and Gar Dzong, both situated in valleys descending from the Himalayas towards the NNW. Here the expected daytime valley breeze is, in about half of the cases, replaced by a down-valley flow from the SE indicating likewise the remarkable extension and intensity of a large-scale southerly flow, ascending from India across the Himalayas into the Tibetan Highlands and overwhelming the local valley breezes in some cases.

If these data may be considered representative, during daytime (1200-1800 LT) above the Tibetan Highlands, a convergence between large-scale ascending flow from both north and south is expected (cf. Fig. 5), while the reversed nocturnal circulation--with descending motions diverging from the highlands—is at least much weaker than the daytime flow. Furthermore, in 10-30 percent of all cases ascending motion from both north and south--thus also converging above the axis of the highlands--seems to prevail even at dawn.

These surface winds suggest that the highlands trigger a complex regional-scale circulation consisting of two parts:

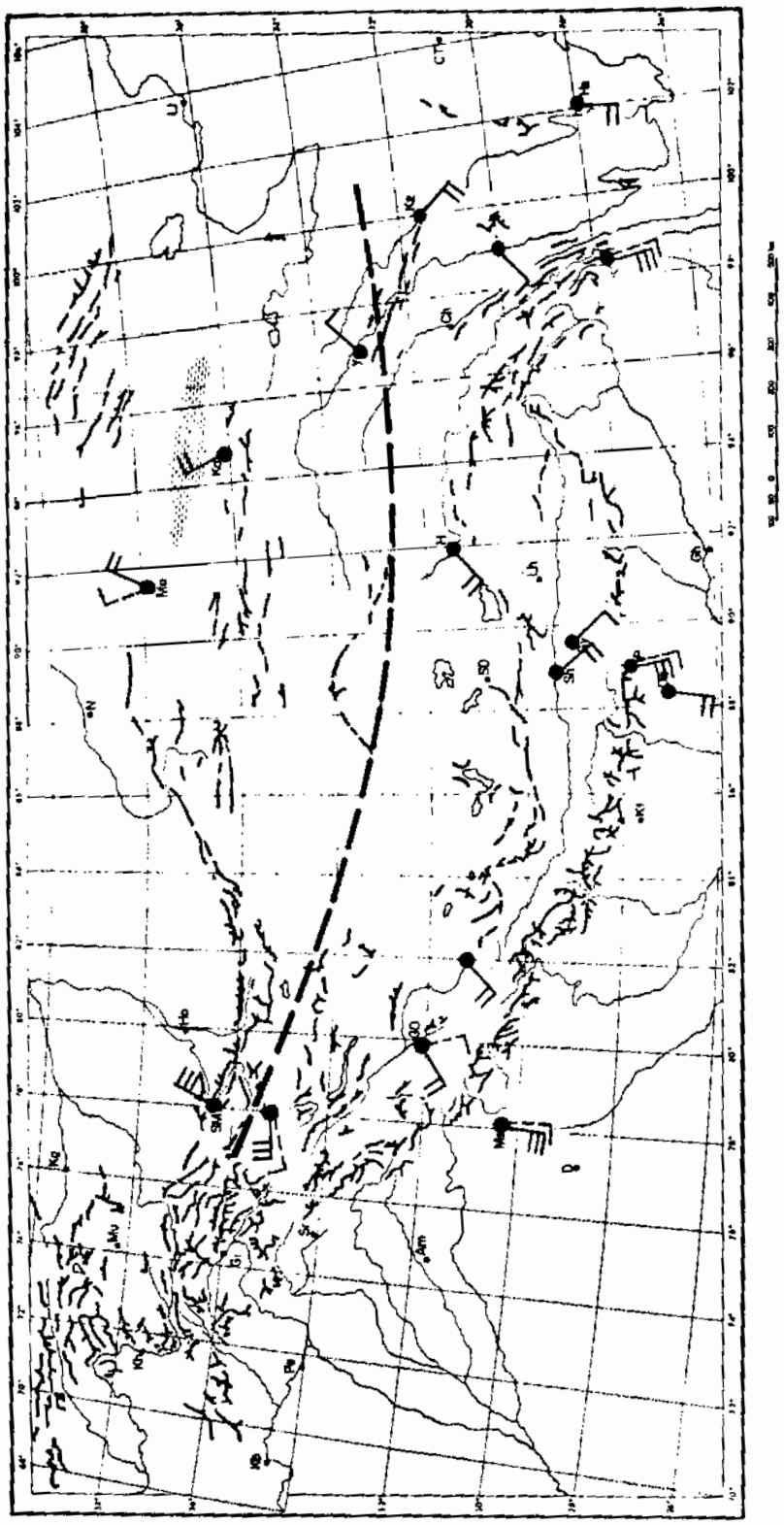

Fig. 5. Surface winds at 1800 LT (solid) and 0600 LT (dashed).

a) The "diurnal" circulation, reversing from day to night, which can be numerically estimated on the base of the vector differences between 0600 and 1800 LT (cf. Yeh and Koo 1956).

b) A constant or "seasonal" circulation, which can be estimated only by an evaluation of the horizontal divergence of the wind field averaged from 0600 and 1800 data as a function of height. Unfortunately, the available upper wind data are hardly adequate for that purpose. Additional evidence for this seasonal circulation is given by the high frequency of night showers (cf. Table 3).

A fairly realistic estimate of the magnitude of the diurnal part of the circulation can be given using a simple model. The following table contains the time differences (0600 minus 1800 LT) of the wind vector for the lower layer (950-700 mb or 850-700 mb, depending on the station elevation) and an upper layer (500-200 mb or 500-300 mb, depending on the available data).

	Lower Layer	Upper Layer*
Kosharyl	--	104° 0. 34 m sec^{-1}
Nochiang	23° 1.3 m sec^{-1}	229° 3. 3 m sec^{-1}
Karmu	--	234° 1. 45 m sec^{-1}
Chengtu	69° 0. 67 m sec^{-1}	270° 0. 28 m sec^{-1}
Gauhati	177° 0. 38 m sec^{-1}	18° 0. 95 m sec^{-1}
Allahabad	71° 0. 39 m sec^{-1}	354° 0. 95 m sec^{-1}
Peshawar	117° 1.6 m sec^{-1}	--

* cf. Figure 6

At most stations the reversal of this difference wind with height is well marked; the upper divergence of the difference wind (Figure 6) is easily seen while the lower difference winds are sometimes distorted by local influences (Allahabad; Peshawar). Averaging of the raw data yields for the lower (upper) layer 102 (121) cm sec^{-1}. The results of the upper layer are much more representative and shall, therefore, be adopted here.

Now let us assume a circular mountain region with an area $A = 2 \times 10^6$ km^2, i.e. with a radius R of about 800 km. Taking the level of non-divergence--

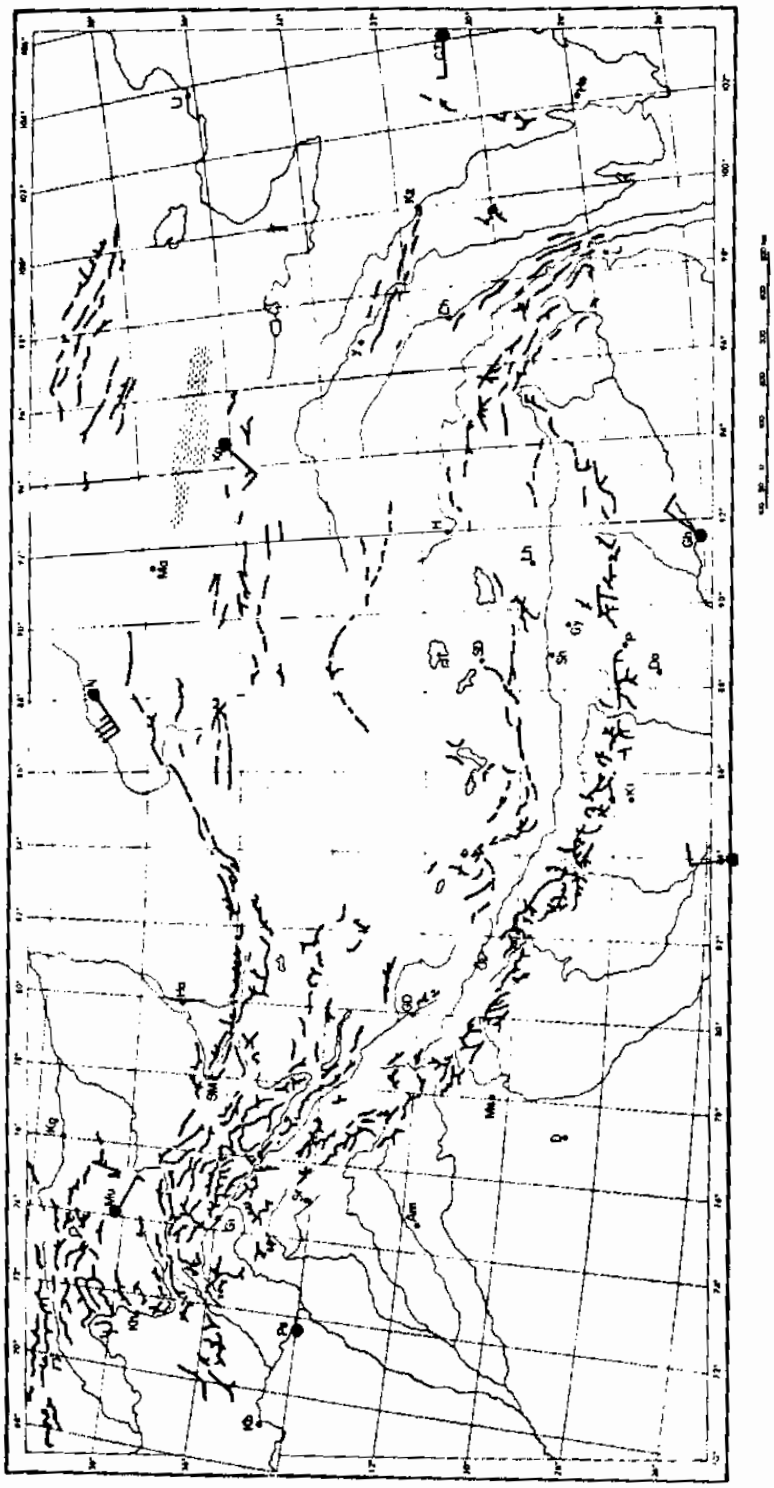

Fig. 6. Divergence of the daytime circulation, upper troposphere (0600 minus 1800 LT wind vector).

which separates the reversed flow patterns of the lower and upper layers--at 500 mb and assuming stationary conditions, an estimate obtained for the difference wind in the 200-500 mb layer (0.3 of the mass, M = 1013 g cm^{-2}, of the atmosphere) is 120 cm sec^{-1}, diverging during the day and converging at night. In the lower layer, 500-900 mb (0.4M), the difference wind is then 90 cm sec^{-1} converging during the day and diverging at night. During the day (between 0600 and 1800 LT) this is equivalent to a lower convergence of 90 cm sec^{-1}/800 km = $1.1 \times 10^{-6} sec^{-1}$, while the upper divergence amounts to 120 cm sec^{-1}/800 km = $1.5 \times 10^{-6} sec^{-1}$.

Assuming that the vertical flow is zero through the surface and the 200 mb level, the horizontal outflow, F_u, in the 200-500 mb layer must be balanced by an equivalent inflow, F_ℓ, in the 500-900 mb layer and by an ascending mean transport, F_z, through the 500 mb layer produced by a vertical wind component w_{500}.

$$F_\ell = 90 \times 0.4M \times 2\pi R \qquad (g sec^{-1})$$

$$F_u = 120 \times 0.3M \times 2\pi R = F_\ell$$

$$F_z = W_{500} \times \rho_{500} \times \pi R^2 \qquad (g sec^{-1})$$

(ρ_{500} = density at 500 mb = 0.65×10^{-3} g cm^{-3})

Since $F_z = F_u = F_\ell$, the resulting vertical motion is

$$w_{500} = \frac{36M \times 2\pi R}{\rho_{500} \times \pi R^2} = \frac{72 \times 1013}{0.65 \times 8 \times 10^4} = 1.40 \text{ cm sec}^{-1}$$

equivalent to nearly 600 m or 37 mb per 12h, which seems to be fairly realistic. Since the lower inflow can reach the interior highlands (with an average elevation near 4300 m) only above 600 mb, F must increase in the 500-600 mb layer (0.1M) to 360 cm sec^{-1}. Assuming the total width of the mountain gaps and passes to be 30 percent of the circumference, the average wind velocity at these gaps is 12 m sec^{-1}. In view of the many reports of strong stormy valley winds in the Himalayas, this high value does not seem to be unrealistic. This daytime circulation model is shown schematically in Figure 7 (with F_ℓ = 72 cm sec^{-1} for the layer 500-1000 mb).

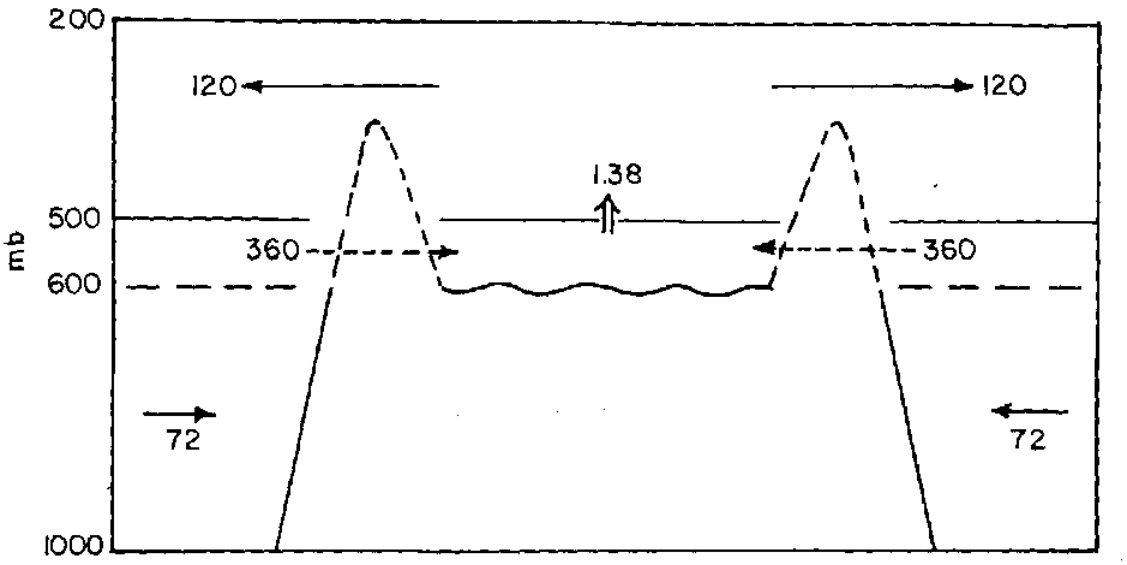

Fig. 7. Model of the diurnal (daytime) circulation, cm s^{-1}.

The ascending motion above the Tibetan Highlands is probably concentrated in the giant convective cells. Assuming (cf. Chapter 3) over 50 percent of the total area (A = 2 $x10^6 km^2$) an average density of 30 such cells per 10^5 km^2, a total of 300 cells exist simultaneously. Further, assuming a central core diameter of 6 km (~1/10 of the average distance), the total area of the active parts of the cells would be 8500 km^2 or 0.42 percent of the area A. Then the average vertical motion of 1.40 cm sec^{-1} would be equivalent to an average ascent in the active area of the convective cells of 325 cm sec^{-1}. The real value should be even higher because of the sinking motion around the cells, and average values of 4-5 m sec^{-1} have frequently been reported elsewhere. Due to the high cloud base (often more than 2000 m above the surface) much of the rain evaporates before reaching the ground.

Computing the thermal wind in the 500-300 mb layer (5.4-9.0 km) for 0600 and 1800 LT separately (Table 15), comparison shows that there are practically no significant differences between the two samples which would represent the "diurnal" circulation component; neither in direction nor in intensity. Only above Hsihchang does a relatively large variation occur between dawn and sunset; however, the 1800 LT sample at Hsihchang

consists only of n = 25 ascents (to be compared with n = 70 at 0600 LT) and, therefore, cannot be considered as sufficiently reliable. The constancy of the thermal wind around the Tibetan Highlands between day and night presents more evidence that the heating of the air centered above southeastern Tibet is not a daytime, but a seasonal, phenomenon.

The continued maintenance of the regional daytime circulation through the night can hardly be considered an effect of the large scale of the highlands alone. The thermally induced circulation between the Indonesian Islands (Borneo, Sumatra, etc.) and the adjacent seas is of the same order of magnitude, but reverses twice daily. However, it must be taken into account that the nocturnal cooling of the interior highlands ($\Delta T = T_{max} - T_{min} \approx 15\text{-}18°C$, cf. Table 16) is restricted to a shallow inversion layer mm while in SE Tibet at least the release of latent heat in the giant Cb cells is maintained during the greater part of the night (cf. Tables 4, 6), the lifetime of large clusters of Cb cells being on the order of 6-12 hours.

An attempt has been made to estimate the "seasonal" component of the circulation using the 700 mb winds from seven stations (Peshawar, Amritsar, Gauhati, Hsihchang, Chengtu, Karmu and Nochiang) averaged for 0000 GMT and 1200 GMT (cf. Table 14). Here the data from Allahabad were omitted since they gave no contribution to the net inflow at the 700 mb level. Only the data at Amritsar show a weak outflow. After weighting the 700 mb components perpendicular to the boundary and taking into account the varying length of the boundary elements, the average "seasonal" inflow through the boundary is + 134 cm sec^{-1}. Using the above-mentioned circular model, this is equivalent to a net convergence ($div_2\vec{v} = -1.68 \times 10\ sec^{-1}$). If this net inflow at 700 mb represents the lower branch of the circulation in the 500-1000 mb layer, this "seasonal" circulation is slightly stronger than the 12-hour "diurnal" circulation; this would explain the maintenance of the lower converging and ascending flow even during nighttime. A similar computation for the 300 mb failed to give reliable results, because of the unrepresentative distribution of the stations along the western and eastern boundaries.

Since the nocturnal branch of the diurnal circulation is to a large extent suppressed by the "seasonal" circulation averaged over 24 hours, the daytime

branch may be used as a first guess of the magnitude of the average "seasonal" circulation[1].

[1] The results outlined here and in Chapter 7 seem to coincide in substance with the results of T. Ch. Yeh (Acta Meteorologica Sinica 28, 1957, 108-121, in Chinese) based on earlier pilot-balloon data.

CHAPTER 7

THE TIBETAN SUMMER ANTICYCLONE AND ITS EFFECT ON THE ATMOSPHERIC CIRCULATION

The nearly simultaneous occurrence of a high tropospheric subtropical anticyclone above the Tibetan Highlands and the Indian summer monsoon (cf. Chapter 8) has been the subject of much debate in scientific circles, especially since the Monsoon Symposium held in New Delhi in February 1958 (cf. Koteswaram and Rao 1963, Proc. Symp. Meteor. Results IIOE 1965). In this chapter the position of this anticyclone and its physical origin shall be discussed, together with an outlook to other seasons.

It has been pointed out by Indian meteorologists--e.g., Rangarajan 1963--that the high temperatures of this warm anticyclone do not occur above Tibet, but in an elongated belt extending along latitudes 25-30N from Egypt across southern Asia and northern India towards SW China. This is only partly true, since several systematic errors must be taken into account (cf. Appendix E). A critical study of all existing aerological data (Flohn 1964, 1965) revealed that the highest temperatures in the layer between 500 and 150 mb are in fact observed above the Himalayas, i.e., above northern India and southern Tibet. In this investigation a careful reexamination of all available data has been carried out, with the following objectives:

a) Collecting all available aerological data from the network of the Chinese P. R.;
b) Restricting and/or correcting the temperature data to 0000 GMT = 0600 LT in order to exclude the diurnal variation of temperature;
c) Using the thermal wind equation, at least qualitatively, to check the horizontal gradient of the average temperature field; and
d) Correcting as far as possible the uncertain altitudes of Tibetan stations (Appendix B) by aerological comparisons.

The results are shown for the 300-500 mb layer in Figure 8 which contains all thickness values and thermal winds. The thickness values have been computed from the data of Table 7, taking into account the difference

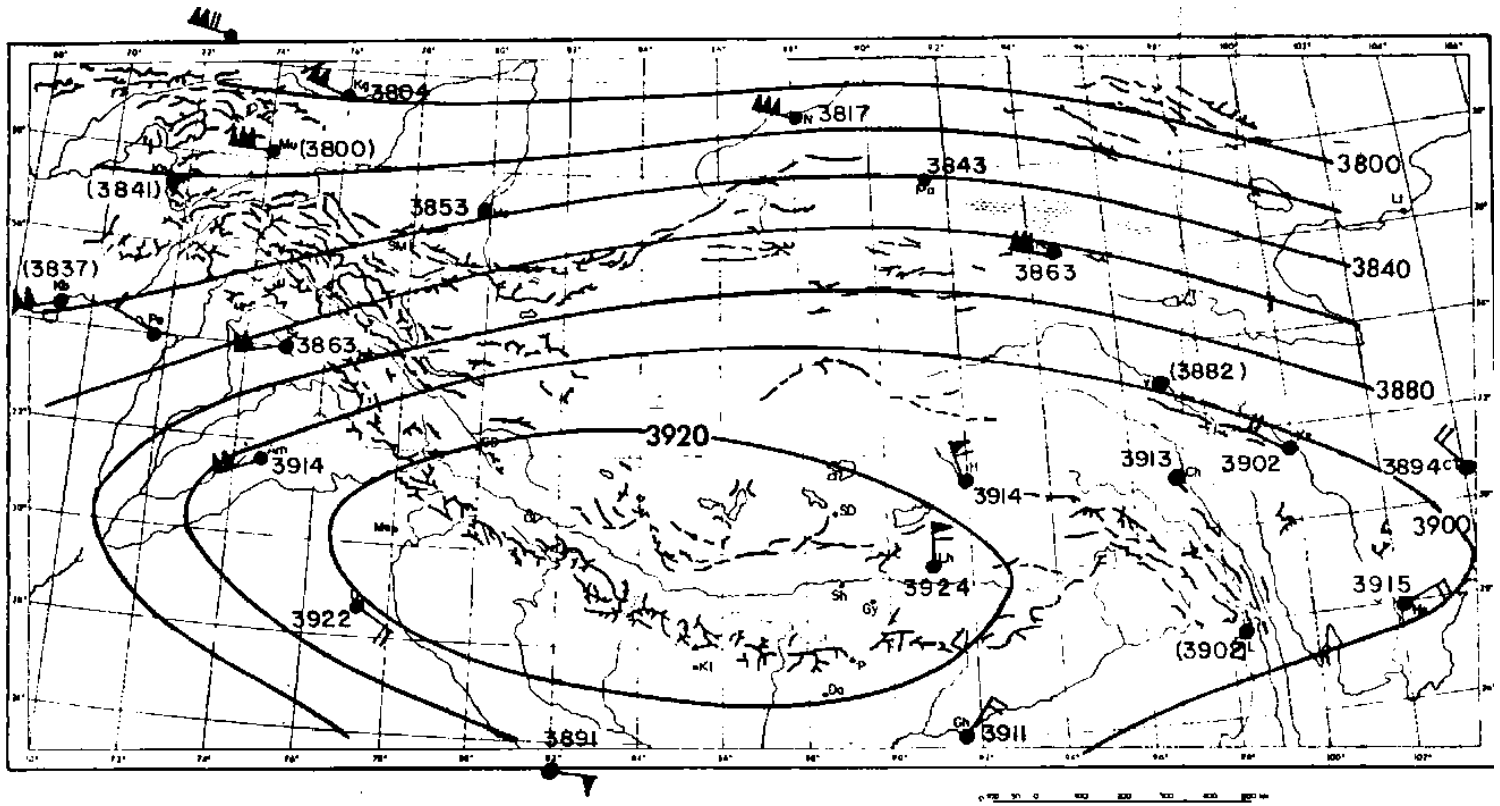

Fig. 8. Thickness pattern, 300-500 mb layer, and thermal winds. Scale on right converts thickness into mean temperature of layer (^{o}C).

between virtual and actual temperature and correcting the values of Srinagar (only 1200 GMT available) by using the average diurnal differences in Table 10. Short-period averages are given in brackets (Kabul, Khorog, Lawang). With the exception of the difference between Kosharyl (exact position unknown) and Kashgar the data are apparently internally consistent.

Below 300 mb the thermal winds at Kosharyl, Nochiang, Chengtu, Gauhati, Allahabad, New Delhi and Amritsar (Table 15) are not significantly biased by any selection and shall, therefore, be adopted as reliable. However, similar results for the stations of eastern and central Tibet (Heiho, Lhasa, Kantze, and Hsihchang) are certainly not an adequate representation. Nevertheless, Figure 8 seems to indicate that these data together-- except for the northwestern margin--present a sufficiently consistent pattern. The warmest area in this layer (between about 5.8 and 9.7 gpt km) is situated between latitudes 27N and 33N and longitudes 76E and 94E, centered near 30N, 85E, i.e., in the upper Tsangpo Basin about 150 km north of the Himalayas. It should, however, be pointed out that two possible sources of error have been neglected here: (1) a systematical difference between the radiosondes of India and the Chinese P. R., and (2) the bias of the thermal winds of Heiho and Lhasa in an anticyclonic sense. A systematic temperature deviation of not more than 0.7°C would result in a thickness difference of about 10 gpt m. If the Indian radiosondes are still only 0.7°C warmer than those of the Chinese network--which is hardly more than the attainable accuracy of routine instruments--this would result in a displacement of the warm cell by about 3° longitude toward the east, still consistent with the thermal winds of Heiho and Lhasa (cf. also Fig. 3 and page 12).

The average position of this warm cell coincides roughly with the average position of the highly persistent 100 mb anticyclone above southern Asia (Mason and Anderson 1963). The carefully analyzed maps of Source 11 (Appendix A) showed this center, for the period June-September 1962-63, to be situated near 30N, 88E (cf. Flohn 1965). Scherhag has published a hemispheric thickness map of the 100-850 mb layer for July 1966 with the warm center near 30N, 80E, based on thermal winds from a smaller number of stations. Earlier estimates of the position of the anticyclonic center are: 29N, 98E (Flohn 1950, 225 mb level) and 30N, 96E (Staff Member Ac. Sinica,

500 mb level); model computations by Murakami (input of sensible heat) resulted in a position near 31N, 98E. Although the present data are much more complete, no attempt is made to extend this evaluation up to 100 mb because of the decreasing reliability of the data with height. If the heat center is identified with the 3920 gpt m thickness isoline, about two-thirds of its area is situated above the Tibetan Plateau.

The physical origin of this heat center was originally attributed to the input of sensible heat above the elevated heat source of the Tibetan Plateau (Flohn 1950, 1958). Later this idea was revised (e. g., Flohn 1963, cf. also Riehl 1959) by taking into account the release of latent heat by the enormous monsoon rains, especially above the central and eastern Himalayas and their southern approaches. This source of energy, however, is available only if, and insofar as, the vertical lapse-rate is greater than moist adiabatic. If the air is conditionally stable, vertical exchange can only cool the upper layers. Table 11 shows that the air above the Tibetan Plateau is, on the average, conditionally unstable; latent heat irreversibly released by rain reaching the ground is, therefore, one of the sources of energy. Here only part of the energy sources and sinks can be discussed numerically; a more complete evaluation shall be given at a later opportunity.

The surface heat budget is given by

$$Q = U_L + LE + U_S$$

Q = net radiation in ly d^{-1}, U_L = heat loss due to long wave radiation, L = heat of condensation, E = evaporation in g cm^{-2} d^{-1}, U_S = heat flux into the soil. During the summer months (mainly August) the following values have been observed (a_s = surface albedo) in the Alai-Pamir Mountains as reported by Aizenshtat (1966).

	Height	a_s	Q	U_L	LE	U_s
Sary-Tash, Alai Valley, dry grass	3150 m	17%	321	178	89	54 ly d^{-1}
Lake Karakul, Pamir, sandy gravel	3990 m	22%	324	243	29	52 ly d^{-1}

	Height	a_s	Q	U_L	LE	U_s
Fedtchenko Glacier, Pamir, snow	4900 m	66%	142	-37	116	7 ly d^{-1}
Kosharyl, E Pamir (Aksu valley)	3710 m	21%	294	244	0	50 ly d^{-1}
For Comparison:						
Repetek, Karakum Desert	~200 m	24%	330	276	0	54 ly d^{-1}
Shafrikan, Kysylkum, Saksaul steppe.	~200 m	20%	381	255	88	38 ly d^{-1}

These carefully measured data demonstrate that the input of sensible heat into the atmosphere from an elevated semi-arid surface is of the same order as that above a sea level desert at the same latitude (39N) and averages around 250 ly d^{-1} (75-80 percent of Q). In more humid areas where the bulk of Q is used for evaporation, U_L drops to a few percent of Q. The observations from upper Fedtchenko Glacier (apparently not complete) indicate the role of the surface albedo in lowering Q and the reversal of the sensible heat flux; while still evaporating into the dry air, the glacier acts as a heat sink. The role of U_L in the dry western parts of the Tibetan Highlands is illustrated by the extremely high mid-tropospheric lapse-rate at Kosharyl (Table 11); here the heating effect has not had sufficient time to extend from the elevated surface (near 650 mb) into the upper troposphere.

Over Assam and especially over the eastern Himalayas and the Assam Arc the release of latent heat of precipitation, LP, is a nearly continuous, uninterrupted process during the months of June-August (cf. Chapter 5). The same is probably also true for southeastern Tibet up to about longitude 90E and latitude 33N, as suggested by the high frequency of convective activity and rainfall (Table 4) together with the high water vapour content of the atmosphere.

In order to obtain a realistic comparison of the magnitude of the heating terms, the thermodynamic processes during the ascent of monsoon air in the Assam region are considered, which are mainly due to orographic effects. The average atmospheric properties may be represented by combining the ascents of Gauhati (below 500 mb = 5. 85 km) and Lhasa (above 500 mb, cf. Table 7 and Fig. 9). An ascending parcel of undiluted

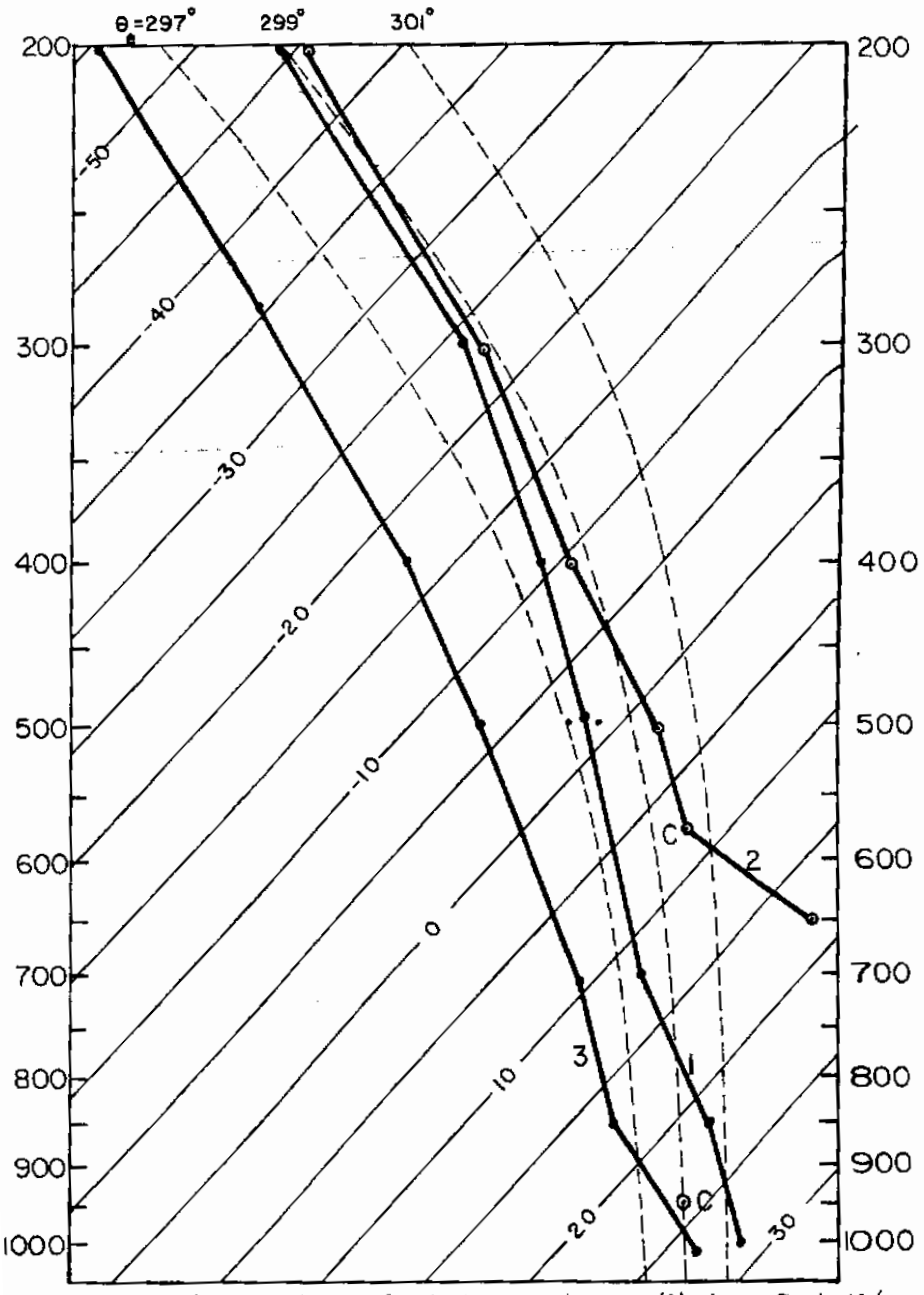

Fig. 9. Average tropospheric temperatures: (1) above Gauhati/ Lhasa combined at 0600 LT, (2) above Lhasa at 1800 LT, and (3) tropical standard atmosphere (C=condensation level).

monsoon air reaches the condensation level at 950 mb with $T = T_d = 24.3°C$. It intersects the environmental ascent curve at 77 5 mb (+17.2°C) and at 205 mb (-44°C), with an average excess temperature in this layer, 775-205 mb (=0.57M), of +1.6°C. Averaged below 200 mb, this combined ascent is 5.4°C warmer than the tropical standard atmosphere (cf. Fig. 9). The decrease in water vapour content of ascending saturated monsoon air between 950 and the average mountain ridge level of 500 mb is 20.1 - 6.6 = 13.5 g kg^{-1}. The precipitable water content in a column of saturated monsoon air is 75 mm compared with 44-48 mm above equatorial Africa.

Since the average flow component toward the mountains at Gauhati is only on the order of 40 cm sec^{-1} or 35 km per day (cf. Chapter 6), the forced ascent by the Himalayas over a distance of 210 km may last six days, equivalent to an average lifting of about 1 km/day. Assuming that each kg of air ascends with this speed during six days, the average rain-fall rate amounts to 135/6 = 22.5 mm/day or about 700 mm/month (cf. Table 20, E-G). In the Assam plains, the average daily amount of rain-fall per station affected is 26 mm (cf. Chapter 5). This amount of precipitation would release as much as 1350 ly d^{-1}, which would be sufficient to heat the layer between 950 and 200 mb (=0. 75M) by 7.5°C per day. The energy needed for heating an ascending parcel of undiluted monsoon air by 1.6°C in the super-moist adiabatic layer is only 220 ly d^{-1} or about 16 percent of the total release of latent heat. However, this heat source is obviously most effective in the upper troposphere, due to the strong upward heat flux maintained by the ascending motion in the hot towers. This effect may be used to interpret the position of the positive temperature anomaly at 32N near 300 mb, above Tibet, in marked contrast to the low-level position of similar anomalies above Africa and North America (Fig. 4).

It should be pointed out here that strong orographic (i.e., at least seasonally permanent) rainfall occurs above large parts of southeastern Asia (e. g., the west coasts of both Indian peninsulas, the mountain ranges of Sumatra, Borneo, Java, Celebes and New Guinea) mainly at elevations below 2000 m. The level of maximum rainfall in the Tropics is situated everywhere near 1200 m. This area can be estimated on the order of 6×10^5 km^2, thus the same order of magnitude as the active rain area estimated by Riehl and Malkus (1958) at $4 \times 10^{15} cm^2$. In these areas of orographic rain, undiluted ascent of unstable equatorial air may occur quite often; this

may add to the role of the comparatively few hot towers above the oceans.

Combining the cloud observations from satellites with the aerological data and some qualitative considerations of the heat budget, it may be concluded that the occurrence of the heat center of the Tibetan summer anticyclone in the upper troposphere is caused by a combination of the following effects with horizontally varying intensities:

a) Flux of sensible heat into the air, mainly in the arid western portion of the Tibetan Highlands;
b) Release of latent heat of condensation, mainly above the Himalayas and (with a marked degree of persistency) above Assam, Bengal and the adjacent mountains, i.e., between longitudes 86E and 98E;
c) Upward transport of heat in orographic and cumulonimbus up- drafts;
d) Radiative processes (which deserve a more quantitative treatment).

As a whole, the Tibetan Highlands act as a heat engine with a giant chimney in their southeastern corner, where heat is carried upward. The nearly stationary heat center in the middle and upper troposphere continues to maintain the thermally induced "seasonal" circulation during nighttime and during periods of weaker uplift and rainfall. During the passage of a deep westerly trough—together with the well-known "monsoon breaks" (Ramaswamy 1962)--the center of the thermal anticyclone can be weakened and zonally displaced; however, it usually rebuilds after two or three days.

CHAPTER 8

THE INDIAN SUMMER MONSOON AND THE TIBETAN HIGHLANDS

The recent renewal of the discussion on the Indian summer monsoon is largely hampered by different definitions of the term "monsoon" which has caused many misinterpretations. The original (Arabic) word was used by Arab seafarers on their travels between the Arabian peninsula (especially from its fertile southwestern part "Arabia felix") and India where they experienced the seasonal change of winds; its meaning is "season". In the western part of the Arabian Sea and in southern Arabia itself the summertime SW winds are usually not accompanied by rain, with exception of the highlands of Yemen, where the diurnal wind systems from the Red Sea and the Gulf of Aden converge and produce., under unstable conditions, regular afternoon showers as shown by many satellite pictures. The classical description of Halley (1685) deals mainly with the winds and gives a remarkable map of the prevailing directions during summer.

In contrast to this, in India the term monsoon is only used for the main rain period, including that of late fall and early winter on the SE coast of the Indian peninsula. It has been pointed out in the meteorological literature that the seasonal shift of prevailing winds does not necessarily coincide with the beginning and end of the rainy season. Since the last century it has been known that above the Indian peninsula westerly winds occur during April and May at the southern flank of a heat-low system which gradually intensifies with increased heating and moves toward the north and northwest. These shallow westerlies, named in earlier descriptions in a somewhat misleading way as "sea breezes", are not accompanied by rain which is, in rare cases, induced by intense upper troughs. The low-level westerlies eventually merge with the perennial equatorial westerlies expanding north and towards the southern tip of the peninsula; monsoon rains along the west coast do not occur before this system has reached sufficient vertical thickness and thermal instability.

In northeast India (Assam, Bengal, East Pakistan) the summer rain period starts much earlier than in the peninsula (except at its southern tip)

and very much earlier than in the Punjab. In fact, the frequency and amount of rainfall during April and May in Assam and especially in the Himalayas is remarkable. Mountain stations east of 88E (including Sikkim) receive 200-500 mm of rain in these two months alone, disregarding here the isolated maximum around Cherrapunji (618 and 1280 mm for April and May, respectively). The number of rainy days (>2.5 mm) reaches 12-19 per month at many places as shown in a recent publication of Domroes (1968). It is now well established that these pre-monsoon rains occur in connection with an upper wind regime which is, above 800 mb, identical with that of winter. However, near the surface the dry, subsiding "NE "monsoon"--here equivalent to the NE trades--has been replaced at the eastern flank of the above-mentioned heat low above the peninsula by a southerly flow of moist air from the Gulf of Bengal. This shallow flow carries moisture into the advanced part of the quasi-stationary, orographically produced, Bengal Trough (near 90E) of the upper westerlies. Due to the divergence aloft and low-level convergence of this situation (Ramaswamy 1956), the convective activity increases rapidly, enhanced by orographic lifting at the eastern end of the Assam plain.

During May and early June, the gradual warming of the air at the northern flank of the subtropical jet geostrophically weakens its intensity until finally the Tibetan anticyclone develops, reversing the direction of the flow in the upper troposphere (500-100 mb). The physical cause of this event is discussed in Chapter 7. As pointed out recently by Ramaswamy and Ananthakrishnan, the onset of the summer rain period in NE India (or at Kerala at the southernmost tip of the peninsula) can never be attributed to the occurrence of the Tibetan anticyclone. In fact, this anticyclone is partly caused by the orographically reinforced early summer (pre-monsoon) rains of NE India (Flohn 1963). Its formation is in any case correlated with (and responsible for) the sudden reversal of the upper flow, i.e., with the replacement of the subtropical (westerly) jet by the tropical easterly jet during summer.

Thus, the facts of the situation are that above the peninsula the monsoonal wind shift toward the west and southwest occurs one to two months earlier than the onset of the summer rainy season, while in the northeastern part of the subcontinent the summer rains precede the monsoonal wind shift

by one or two months. It must certainly be understood that in a large continental area suffering under seasonal or permanent lack of adequate water supply, the role of the summer rain period is most important from the practical point of view, while the weak surface winds are hardly noticed. The viewpoint of meteorologists engaged in large-scale problems of the atmospheric circulation must, however, be quite different, looking primarily at the vagaries and displacements of the atmospheric flow. In any discussion of the "monsoon" problem, it is necessary to distinguish clearly between the monsoon winds and monsoon rains and to realize the lack of coincidence of the two.

The early onset of the summer rain period in Assam--long before the reversal of the wind pattern--obviously also occurs in Tibet, at least in the eastern, southeastern and central parts of the highlands. This is not only shown in the climatological data on rainfall and rain frequency (Flohn 1958) but can also be conjectured from satellite data.

An instructive preliminary study of 21 rectified ESSA 3 pictures (April 23-May 13, 1967) showed on each particular day a large amount of convective activity in central, eastern and southeastern Tibet, together with extensive cloudiness in the western mountains (Hindukush, Karakorum, Alai-Pamir), as expected from climatological data (e. g. Plate 6). On 13 days western and southern Tibet (west of about 90E) was also mostly covered by cellular clouds. In marked contrast to this, the plains of northern India remained nearly cloudfree, with the exception of northern Assam which was also cloudy or overcast nearly every day (cf. Chapter 5).

This study suggests that during late April and May, i.e., during a period of strong insolation and seasonal warming, the highlands already begin to trigger strong convective activity together with the summertime regional circulation described above (Chapter 6). Even if at this time the development of a high tropospheric cell in the area (and to the north) of the subtropical jet (i.e., north of about 25N) is very rare, this circulation contributes to the gradual warming above Assam and the Gorges area, which eventually--after a period of six to eight weeks--leads to the reversal of the wind pattern. These early showers probably do not produce much rain (and, consequently, latent heat release) above SE Tibet, at least when

compared with July and August. The role of this circulation during springtime needs further quantitative investigation. The Himalayan foothills, on the other hand, already receive 250-450 mm rain in 15-20 days per month (Table 20).

The role of the Tibetan Plateau in the development of the Indian summer monsoon is obviously much more complex than hitherto apprehended.

a) The early occurrence of the summer rains above northeastern India results from the combined effect of: an orographically produced trough in the subtropical jet; the establishment of a shallow low-level current from the south and southeast carrying moist maritime air from the Gulf of Bengal into the plains of northeast India where it is trapped; and the initiation of a regional diurnal circulation along the Himalayas, resulting in strong convective activity over SE Tibet. While the last two effects are more or less stationary, the trough of the high-level westerlies is obviously only quasi-stationary. If during this period tropical disturbances develop over the Bengal Gulf (or enter that area), they can be steered northward and intensify in the advanced section of such an upper trough. This creates widespread rainfall and sometimes winds of hurricane intensity along the coasts and plains of Bengal and East Pakistan.

b) The combined effects of the direct heating from the elevated surface and the release of latent heat in the ascending air and in the giant cells of SE Tibet during spring (especially May), together with the other processes described in Chapter 7, cause high tropospheric warming and consequently weakening of the upper westerlies. Finally--in most cases not before the first ten days of June--the wind pattern in the 18-30N latitude belt reverses its direction, coinciding with the strengthening of the SW monsoon of the Arabian Sea and the onset of strong rainfall along the central and northern parts of the west coast of the peninsula.

With exception of the western coastlines and NE India as outlined above, there is no doubt that the bulk of the monsoon rains are produced by moving disturbances (cf. Plate 7), some of them best recognizable at the 850 mb level, others near the 500 mb level (Miller and Keshavamurthy). Between these disturbances the rains cease; not infrequently monsoon "breaks" (cf. Ramaswamy 1962) with a duration of four to eight days occur, and prolonged regional droughts are by no means rare in large areas of the subcontinent. Over NE India, SE Tibet and in the Himalayan foothills east of about 86E such disturbances are certainly not absent; however, due to the continuously forced ascent of monsoon air in. the Assam area and the thermodynamically induced (diurnal and seasonal) circulation of the Tibetan Highlands practically no rainless periods occur. During April and early May this is a frequent, but interrupted process; from late May to early September it is a quasi-permanent process varying only in intensity.

It has been pointed out by Raman and Ramanathan (1964) that periods of intense rainfall are locally followed by an intensification of the tropical easterly jet. This process should encompass a larger scale, varying the intensity of the baroclinic field between the edge of the Tibetan Highlands and the equatorial "cool" air. A systematic investigation of the correlation between the area-averaged rainfall above NE India, using virtually all records obtainable from synoptic stations, and the area-averaged speed of the easterlies near 200 mb may yield statistically significant results.

On the basis of the above-mentioned results, it should be stressed that the establishment of a high-tropospheric anticyclone above the southern part of the Tibetan Highlands, during late May or early June, effectively reverses the tropospheric wind field above the Indo-Pakistan subcontinent thus producing the seasonal or monsoonal wind shift. The eastern part of this unique anticyclone is, in turn, partly produced by the orographically intensified and locally fixed pre-monsoon and monsoon rains of NE India and SE Tibet, and partly by the flux of sensible heat from the elevated heat source of the western highlands. The Tibetan anticyclone is the center of a large-scale, very nearly stationary anticyclonic belt extending from the western tropical Pacific across Asia and Africa to the eastern tropical Atlantic. Additional, but definitely weaker, contributions are made to this system from the highlands of southern Iran and Baluchistan to the region of quasi-permanent rain-producing

fronts running across central China, together with the export of sensible heat from the thermal anticyclone above southernmost Tibet.

CHAPTER 9
SUMMARY

On the basis of all available surface and aerological data, together with a fair selection of satellite cloud pictures from NIMBUS and ESSA satellites, meteorological conditions during summer in the Tibetan Highlands (and their marginal mountain ranges) were evaluated. During this season, the vertical lapse rates in the middle troposphere above the highlands are conditionally unstable, which results in extremely high frequencies of giant cumulonimbus cells, showers and thunderstorms, mainly during the afternoon hours, but in the eastern parts also maintained at night. Based on radiosonde data from 0000 GMT (0600 LT) together with all available thermal winds, the thickness pattern of the 300-500 mb layer was found to be characterized by a warm cell above southern Tibet and the Himalayas centered near latitude 30N, longitude 85E. A combination of the ascents at Gauhati and Lhasa well represents the atmospheric state in the heat center of the high tropospheric Tibetan anticyclone. Below 200 mb, this ascent is 5.4°C warmer than the tropical standard atmosphere; an ascending parcel of undiluted monsoon air in the 775-205 mb layer is 1.6°C warmer than its environment.

Evaluation of surface and upper wind data revealed a marked diurnal circulation with an average daytime outflow in the 300-500 mb layer of about 120 cm sec^{-1}, equivalent to a divergence of 1.5x10 sec Assuming a simple stationary model, this was equivalent to an average vertical component of +1. 38 cm sec^{-1} at the 500 mb level. Local winds showed that in about 30 percent of all cases this daytime circulation was even maintained during the night. This result was supported by the persistency of the thermal wind pattern in the 300-500 mb layer from day to night.

During the warm season the Tibetan Highlands act as a heat engine with a giant chimney in their southeastern corner where heat is continuously carried upward into the high troposphere. The nearly stationary heat center in the upper troposphere continues to maintain the thermally induced circulation during short periods of weaker uplift and rainfall.

The onset of the Indian summer monsoon rains does not coincide with the seasonal reversal of the wind field. In NE India the rains precede the monsoonal wind shift by one or two months, while above the peninsula low- level westerly winds begin one or two months before the onset of monsoon rains. The early occurrence of pre-monsoon rains in NE India is interpreted as the result of the combined effects of: an orographically produced quasi-stationary trough in the subtropical jet near longitude 90E; the establishment of a shallow southerly inflow of mostly maritime air; and the initiation of the diurnal circulation of the Tibetan Highlands. This circulation causes gradual warming of the middle and upper troposphere above the Himalayas which weakens and finally eliminates the subtropical (westerly) jet which is then replaced by a very permanent tropical easterly jet. The remarkable high-tropospheric Tibetan anticyclone thus produces the seasonal reversal of the flow patterns in the upper troposphere; its eastern section is, in turn, partly produced by the release of heat from the orographically fixed pre-monsoon and monsoon rains.

ACKNOWLEDGEMENTS

The author is highly indebted to many organizations and individuals for the provision of data, both published and unpublished, during the last fifteen years. Due to this long period, only part of this invaluable help can be mentioned here. Synoptic, climatological and pilot balloon data have been furnished by the Directors and Superintendents of the Meteorological Services from Afghanistan, India, Nepal, Pakistan and Thailand; by far the most extensive contribution has been put at our disposal from the National Weather Records Canter^Jinvironinental Science Services Administration, Asheville, North Carolina, including aerological data. Satellite data have been furnished by NASA and ESSA. The evaluation of original data has been done since 1956 by several of my collaborators; among those special credit should be given to Mr. Harbhajan Anand, and Dipl. Meteor. Ernst Dittmann.

The largest part of this investigation has been carried out during a visit to the Department of Atmospheric Science, Colorado State University, Fort Collins, during March-July 1968. I am highly indebted to Professor Elmar R. Reiter and Professor Herbert Riehl for this opportunity and for many stimulating and challenging discussions. Professor William Gray participated significantly in these discussions. Without the untiring help of Mr. Gene Wooldridge and Mr. M. Ryder the work would not have been possible. The laborious computer programs have been contributed by Mr. William Kamm; the manuscript has been thoroughly revised by Mr. R. Dirks, and efficiently prepared by Mrs. P. Stollar and Mrs. S. Olson.

The research performed at Colorado State University was sponsored by the Environmental Science Services Administration under Grant E-10-68G.

SELECTED LIST OF REFERENCES

Aizenshtat, B. in M. I. Budyko, 1966: Problems of Climatology (in Russian language), Leningrad, 87ff.

Anand, H. S., 1964: Unpublished M. Sc. Thesis, Department of Meteorology, McGill University.

Bugaev, V. A., -V. A. Djordjio and Coll., 1957: Synoptic Processes of Central Asia. Ac. Sc. Uzbek, SSR (in Russian) English translation WMO 1962, (645 + XXIV pages).

Domroes, M., 1968: Zur Frage der Niederschlagshaufigkeit auf dem Indisch-Pakistanischen Subkontinent nach Jahresabschnitten. Meteor. Rundsch. , 21, 35-43.

Flohn, H., 1950: Studien zur allgemeinen Zirkulation der Atmosphare III. Ber. D. Wetterdienst, U. S.-Zone, 18, 34-50.

_____, 1958: Beitrage zur Klimakunde von Hochasien. Erdkunde, 12, 294-308.

_____, 1959: Bemerkungen zur Klimatologie von Hochasien (Aktuelle Schneegrenze und Sommerklima. Abh. Ak. Wiss. Lit. Mainz, Math. Nat. Kl., 14, 1409-1431.

_____, 1960: Recent Investigations on the Mechanism of the "Summer Monsoon" of Southern and Eastern Asia. Symposium on Monsoons of the World, New Delhi, 75-88.

_____, 1963: Comments on a Synoptic Climatology of Southern Asia. World Meteor. Org. Techn. Note 69, 245-252.

_____, 1964: Investigations on the Tropical Easterly Jet. Bonner Meteor. Abh. , 4, 83 pp; cf. also Proc. Symposium Tropical Meteorology Rotorua (1963), 160-172.

Flohn, H., 1965: Thermal Effects of the Tibetan Plateau During the Asian Monsoon Season. Austral. Meteor. Mag., 49, 55-57.

Kingdon Ward, H., 1934: A Plant Hunter in Tibet. London.

Koteswaram, P., 1958: The Easterly Jet Stream in the Tropics. Tellus, 10, 43-57.

_____, and N. S. B. Rao, 1963: The Structure of the Asian Summer Moonson. Austral. Meteor. Mag. , 42, 35-56 —

Malkus, J. S., 1955: The Effects of a Large Island Upon the Trade-Wind Air Stream. Quart. J. Roy. Meteor. Soc., 81, 538-550.

Mason, R. B., and C. E. Anderson, 1963: The Development and Decay of the 100 mb Summertime Anticyclone over Southern Asia. Monthly Weather Review, 91, 3-12.

Miller, F. R., and R. N. Keshavamurthy, 1968: Structure of an Arabian Sea Summer Monsoon System. Internat. Ind. Ocean Expedition, Meteor. Monogr. 1.

Murakami, T., 1958: The Sudden Change of Upper Westerlies Near the Tibetan Plateau at the Beginning of Summer Season. J. Meteor. Soc. Japan, 36, 239-247.

Orgill, M. M., 1967: Some Aspects on the Onset of the Summer Monsoon over Southeast Asia. Dept. Atmos. Sci., Colorado State Univ., Final Rpt. Contract DA28-043-AMC-0130 3(E), 75 pp.

Proceedings of the Symposium on Meteorological Results of the Indian Ocean Expedition, 1965, Bombay.

Ramaswamy, C., 1956: On the Subtropical Jet-Stream and Its Role in the Development of Large-Scale Convection. Tellus, 8, 26-60.

Ramaswamy, C. , 1962: Breaks in the Indian Summer Monsoon as a Phenomenon of Interaction Between the Easterly and the Subtropical Westerly Jet Stream. Tellus, 14, 337 -349.

Rangarajan, S., 1963: Thermal Effects of the Tibetan Plateau During the Asian Monsoon Season. Austral. Meteor. Mag.. 42, 24-34.

Riehl, H., and J. S. Malkus, 1958: On the Heat Balance of the Equatorial Trough Zone. Geophysica (Helsinki), 503-538.

_____, 1959: On the Production of Kinetic Energy from Condensation Heating. Rossby Memorial Volume, 381-399.

_____, 1967: Southeast Asia Monsoon Study. Dept. Atmos. Sci., Colorado State Univ., Final Rpt. Contract DA 28-043-AMC-01303(E), 33 pp.

Schweinfurth, U., 1956: Uber klimatische Trockentaler im Himalaja. Erdkunde, 10, 297-302.

Staff Members Academia Sinica, Inst. Geophys. Meteor. Peking, 1957-58: On the General Circulation over Eastern Asia I-III. Tellus, 9, 432-446; Tellus, 10, 58-7 5 and 299-312.

Troll, C., 1967: Die klimatische und vegetationsgeographische Gliederung des Himalaya-Systems. In: Khumbu-Himal (Munchen) Vol. I, 353-388.

Ungewitter, G., 1968: Studien zur Struktur der Gebietsniederschlage in der Bundesrepublik Deutschland. Unpublished Dipl. Thesis, Bonn.

Yeh, T. Ch., and Ch. Ch. Koo, 1956: The Effect of the Tibetan Plateau on the Circulation of the Atmosphere and Weather in China (in Russian). Izv. Ak. Nauk Ser. Geogr., No. 2, 127-139.

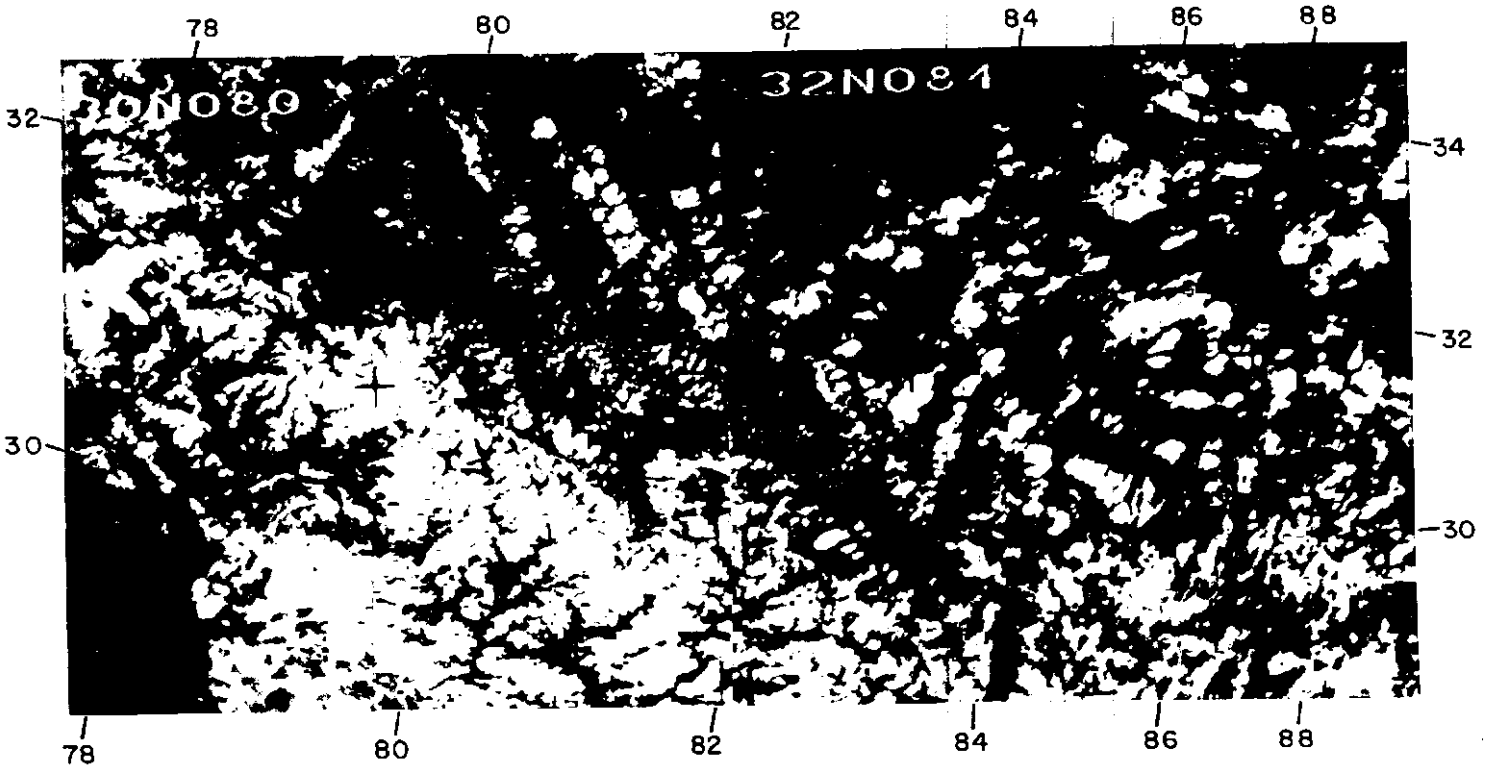

Plate 1. NIMBUS 1, Orbit 160, Sept. 8, 1964. Convective clouds in different scale over SW Tibet, mostly oriented from S-SW.

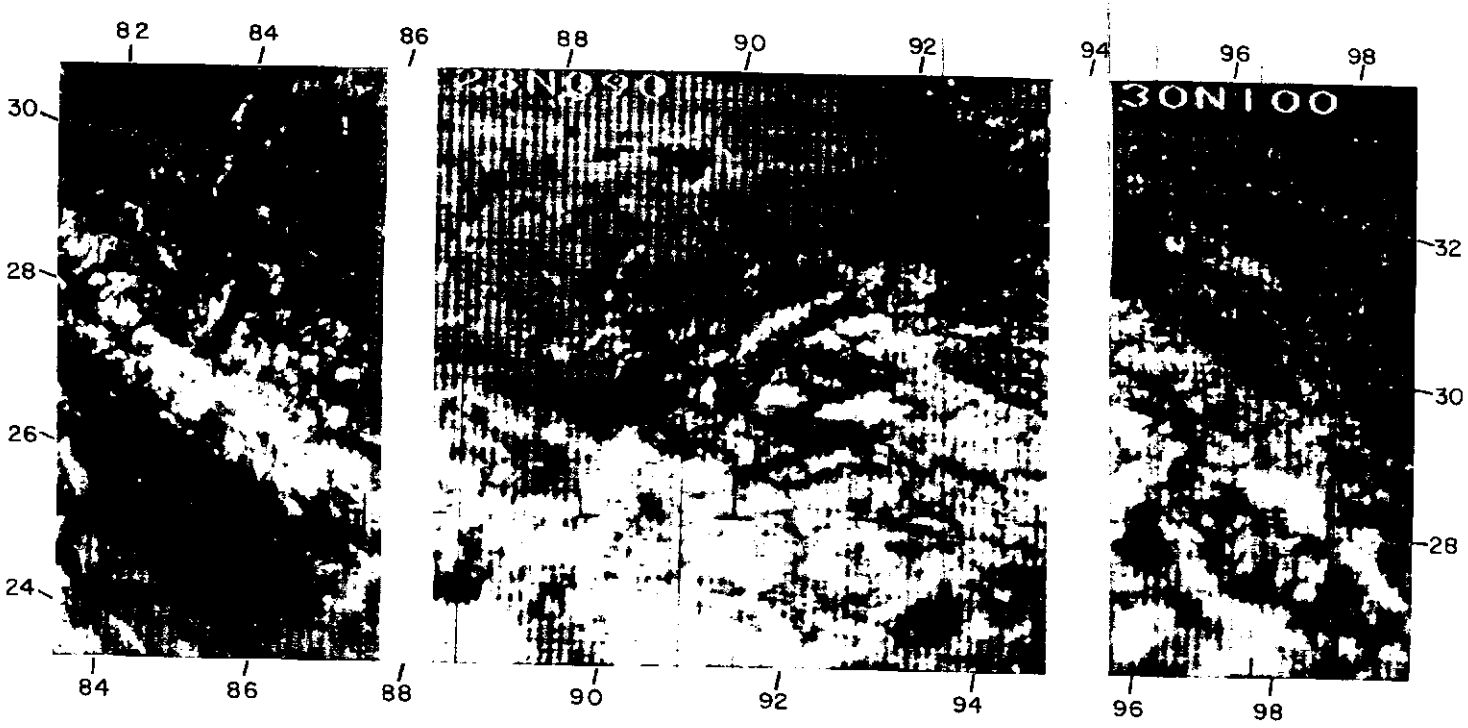

Plate 2. NIMBUS II, Orbit 478, June 20, 1966. Orographically triggered convective cells over SE Tibet. Note the lakes of south-central Tibet.

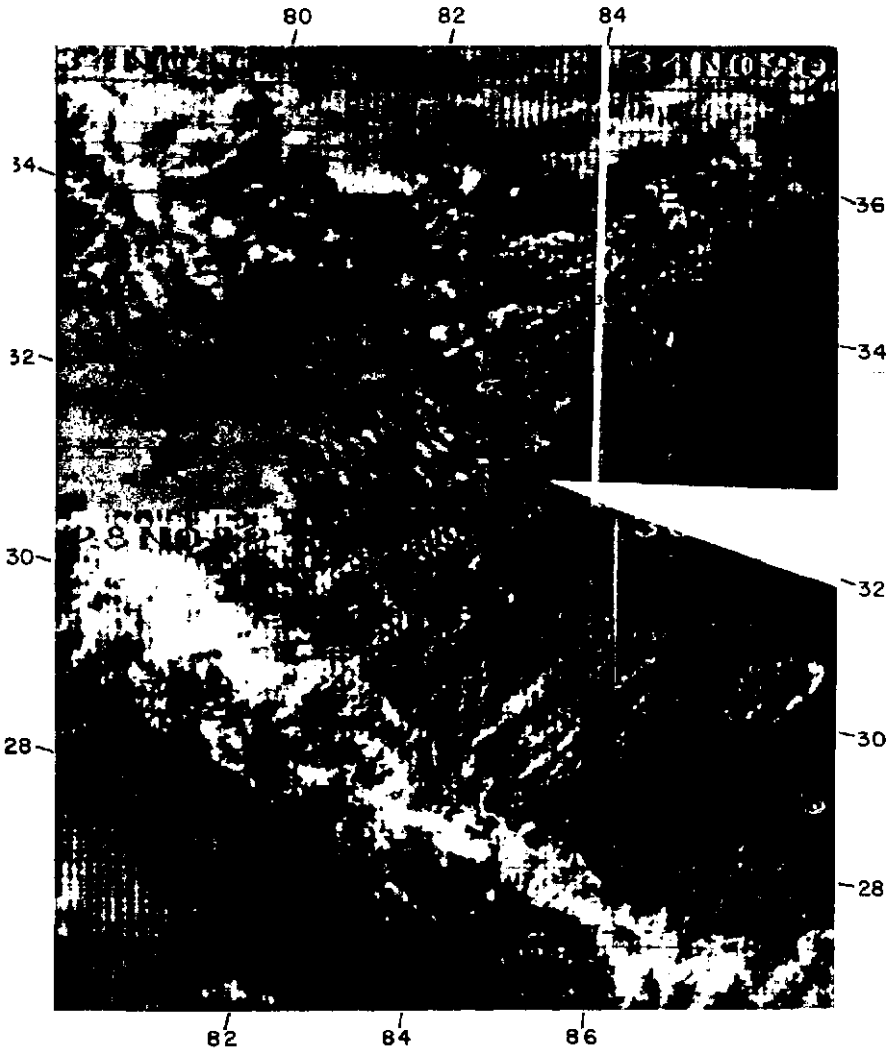

Plate 3. NIMBUS II, Orbit 678, July 5, 1966. Mountain waves and cumuli in the lee of the Karakorums and Himalayas.

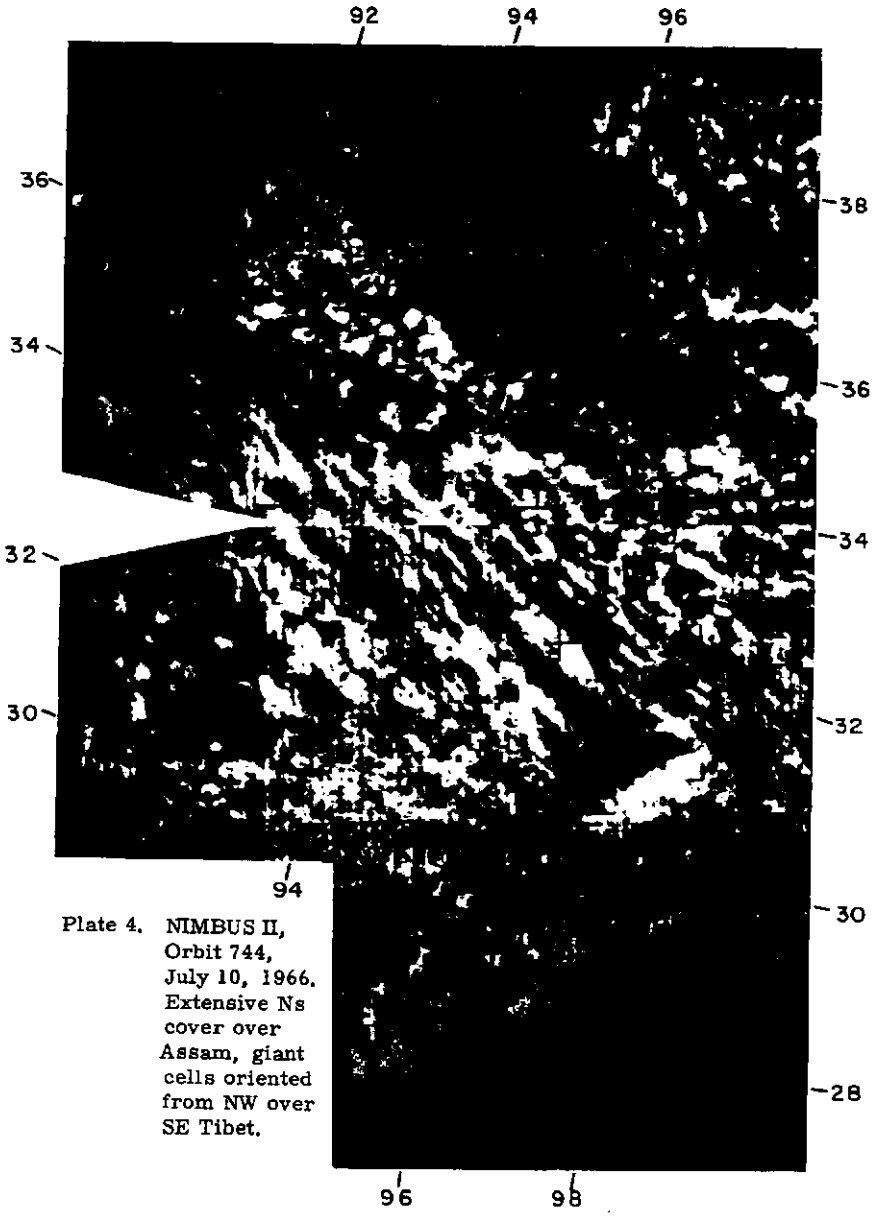

Plate 4. NIMBUS II, Orbit 744, July 10, 1966. Extensive Ns cover over Assam, giant cells oriented from NW over SE Tibet.

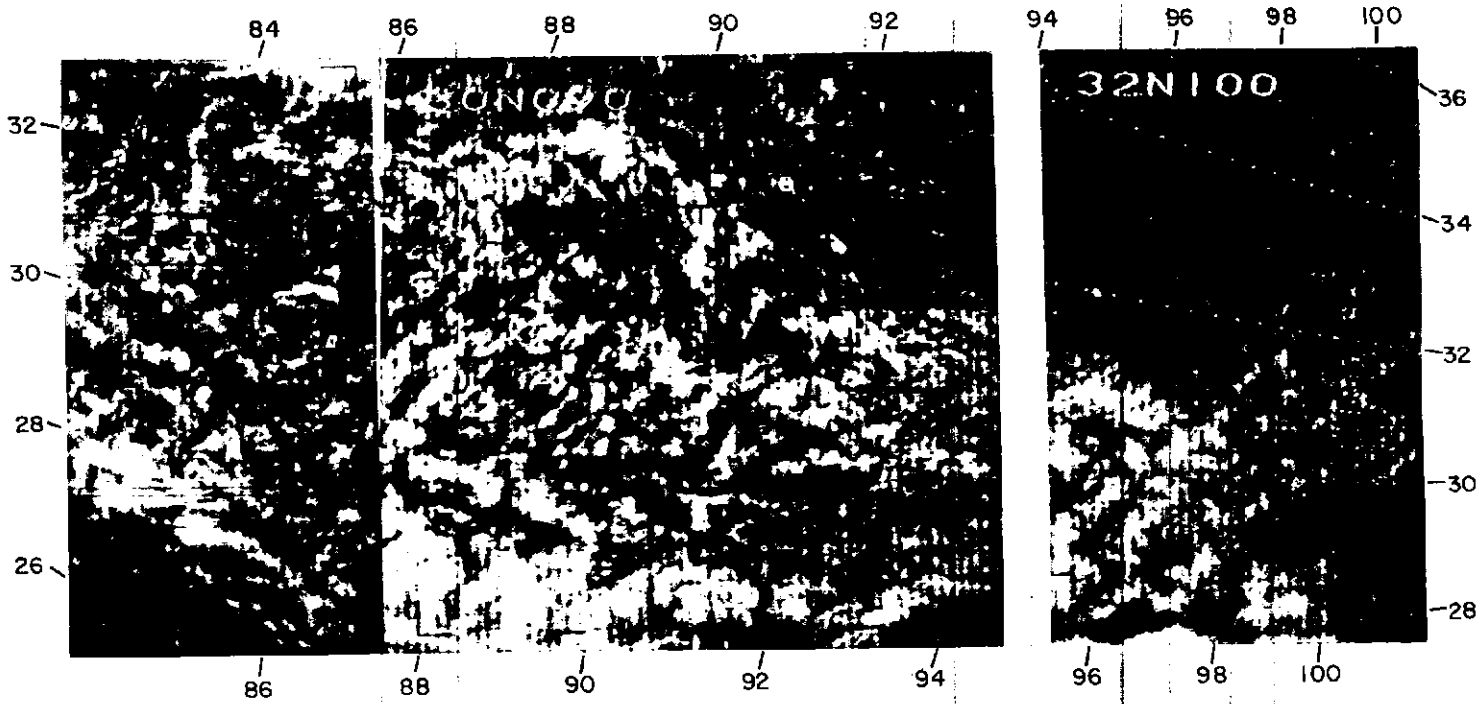

Plate 5. NIMBUS II, Orbit 904, July 22, 1966. Giant cells over S and SE Tibet, anticyclonically oriented around 32N, 86E. Note the appearance of some lakes, Tsangpo and Meridional Gorges in SE Tibet.

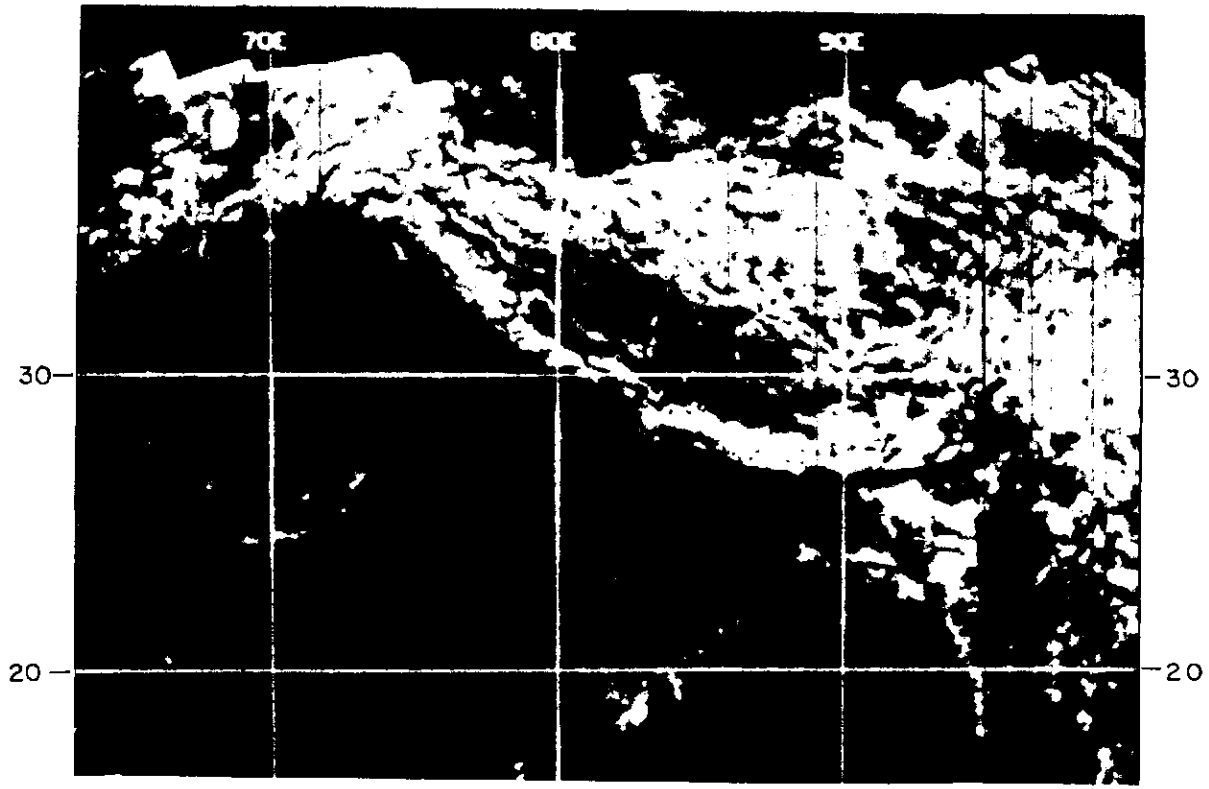

Plate 6. ESSA 3, May 7, 1967. Marginal mountains and SW Tibet mostly cloud free, central and eastern Tibet many giant Cb cells, NE India partly cloudy, especially east of 95E.

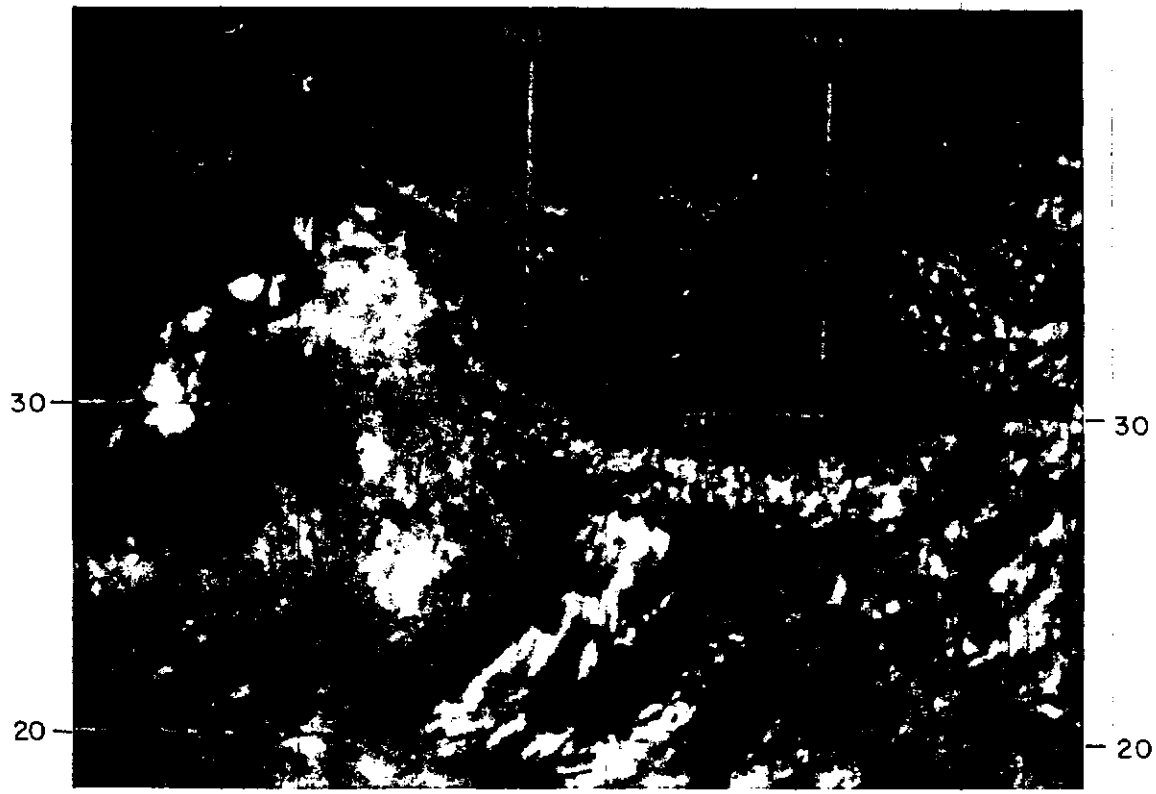

Plate 7. ESSA 5, July 22, 1967. Monsoon disturbance over Rajasthan and Punjab, giant Cb cells over most of Tibet, divergence zone at foot of the Himalayas.

APPENDIX A: DATA SOURCES

1. O. M. Chelpanova: Climate of the U. S. S. R. , Vol. 3 (in Russian language), Leningrad, 1963.

2. ESSA/WMO: Monthly Climatic Data for the World, Vol. 16-20, Asheville, 1963-68.

3. Geographical Faculty, Lomonossov University, Moscow: Data from Pamir Expeditions 1957-59, Vol. I, Aerological Observations (in Russian language), Moscow 1962, 234 p.

4. Meteorological Department, Bangkok, Thailand: Upper Winds over Southeast Asia and Neighbouring Areas (1961, 1965).

5. Meteorological Department, Govt. Union of Burma: Pilot Balloon Data and Frequency Tables, 1956-57.

6. India Meteorological Department: Monthly and Annual Normals of Rainfall and of Rainy Days (up to 1940), Mem. Ind. Meteor. Dept. 27, 5 (1949).

7. _____: Monthly and Annual Normals of Rainfall and of Rainy Days (1901-50), Mem. Ind. Meteor. Dept. 31, 3 (1962).

8. _____: Climatological Tables of Observatories in India, Delhi, 1953, XXXV and 508 p.

9. _____: Monthly Weather Review, 1955-61.

10 _____: Indian Daily Weather Report, 1962-63.

11. Institut fur Meteorologie und Geophysik, Fr. Univ. Berlin, Meteorologische Abhandlungen Vol. 64, No. 5-7 (May-July 1966), Berlin 1966.

12. Japan Meteorological Agency: Daily Weather Maps, Sea Level, 850 mb, 700 mb and 500 mb Charts with Synoptic Data Tabulations, Tokyo, 195660, 1964, 1966.

13. USAF Operational Navigation Chart, Sheets G6-G7-G8, H9-H10 (Scale 1:1 million).

14. U.S. Weather Bureau: Northern Hemisphere Data Tabulations, 1956. 61.

15. _____: An Annotated Bibliography on the Climate of the Tibetan Highlands, Washington 1965 (49 entries, road map)

16. West Pakistan Water and Power Development Authority: Annual Report of River and Climatological Data of West Pakistan, Lahore 1960-64.

17. World Meteorological Organization: Short-Period Averages for 1951-60 and Provisional Average Values for Climate Temp and Climate Temp Ship Stations, WMO/OMM-No. 170, TP 84, Geneva 1965.

APPENDIX B: METEOROLOGICAL STATIONS IN TIBET

Unlike other countries, the coordinates of aerological and synoptic stations in Tibet are still in part uncertain. Since the Chinese People's Republic is not a member of the World Meteorological Organization, only unofficial sources are available which apparently give only approximate coordinates for some stations. Furthermore, Chinese place names do not always coincide with the traditional Tibetan names and transcriptions are manifold. In the extensive highlands, height determinations are subject to large sources of error.

Some detective work was therefore necessary to identify the proper station coordinates, especially those of the key stations Karmu and Heiho. Main sources were the International World Map, the World Aeronautical Chart and the USAF Operational Navigation Chart (all 1:1 million) together with the Times Atlas (Sheets 21-23) and other atlas publications. Certainly all previously published maps are not free from error; our proposed corrections are therefore only tentative.

Table 1 shows the semi-official coordinates as used by the meteorological services of several countries (U. S. A. , Japan and Federal Republic of Germany). With the exception of Lhasa, all meteorological stations have been installed since the occupation of Tibet by Chinese forces. The aerological data were not available to the German Weather Service before 1956. Most probably all aerological stations are situated along the newly constructed highways which allow inexpensive supply.

The position of Mangya lies on the caravan trail (highway?) from Lhasa to the Charkhlik oasis (near station 51777, Nochiang) at the southern edge of the Tarim Basin; Mangya is situated at the southeastern edge of the Tsaidam plain.

Shahiullah Mazar (51915) is situated on the highway from central Tibet to Yarkand-Kashgar, at a sharp bend of the Kara-Kash-Darja, where the valley flows from SSW to NNE, with a tributary coming in from the west. Only a few observations are available.

TABLE 1: NAMES AND COORDINATES OF TIBETAN METEOROLOGICAL STATIONS

Code No.	Station	Tibetan Name	Abbr.[2]	Lat.	Long.	Height
51895	Mangya*		Ma	37°51'N	91°39'E	3060 m
51915	Shahiullah Mazar	Sai-Tu-La	SM	36°20	7 8°00	3669
52818	Karmu*	Golmo	Ka	36°12	94°39	2850
55228	Dar Gunsh	Gar Dzong	GD	32°11	79°59	(4287)
55299	Heiho*	Nag-chu Dzong	H	32°00[1]	92° 07	4000[1]
55472	Hsian Shatsung	Shensa Dzong	SD	30°50	88°45	(-4710)
55578	Jih Kentsheh	Shikatse	Sh	29°13	88°55	3800)
55591	Lasa*	Lhasa	Lh	29°43	91°02	3658
55680	Gyangtse		Gy	28°57	89°38	4000)
55773	Pali	Phari Dzong	P	27°44	89°05	(-4500)
56029	Yushu	Iyekundo	Y	33°06	96°42	3873
56137	Changtu*	Chiamdo	Ch	31°10	97°16	3200[1]
56146	Kantze*	Kantzu	Kz	31°38	99°59	3320[1]
56533	Tzukei*	Lawang	L	27°40	98°23	(-1800)
56571	Hsihchang*		Hs	27°53	102°18	1599[1]
56739	Tengchung*			25°07	98°29	1627

1) cf. discussion in the notes

2) Abbreviation used on the maps

* Aerological

TABLE la: COORDINATES OF ADDITIONAL AEROLOGICAL STATIONS

Code No.	Station (Country)	Abbr. [1]	Lat.	Long.	Height
38613	Jalalabad (USSR)		40°55'N	72°57'E	771 m
38954	Khorog (USSR)	Kh	37°30	71°30	2080
	Kosharyl (Pamir, USSR)	~ Mu	~38°30	~74°	3710
40498	Kabul (Afghanistan)	Kb	34°33	69°12	1803
41530	Peshawar (Pakistan)	Pe	34°01	71°35	359
42071	Amritsar (India)	Am	31 °38	74°52	234
42182	New Delhi (India)	D	28°35	77°12	216
42410	Gauhati (India)	Gh	26°05	91°43	54
42475	Allahabad (India)		25°27	81°44	98
43540	Srinagar (Kashmir)	Sr	34° 05	74°50	1505
51706	Keshih (=Kashgar, Chinese P. R.)	Kg	39°32	76°06	1530
51777	Nochiang (=Charkhlik, Chinese P. R.)	N	39°05	88°03	960
51828	Hotien (=Khotan, Chinese P. R.)	Ho	37°07	79°55	1389
56294	Chengtu (Chinese P. R.)	CT	30°04	104°04	498
57516	Paishihlu (Chinese P. R.)		29°29	106°20	?

1) Abbreviation used on the maps

Karmu (52818) is situated at the southern edge of the great Tsaidam salt plain and is characterized by an extremely arid continental climate. The official coordinates (Table 1) are inconsistent with the maps which show this point within a mountainous area at an elevation between 3500 and 4000 meters. The NJ46 International World Map shows a place called Ka-erh-mu = Golmo *on* the former main Lhasa-Lanchow caravan trail (now highway), while on the NJ46 map, Golmo is situated at 36 27N, 94 56E at 2752 m. Prom this evidence it seems rather likely that Karmu is approximately identical with Golmo; there is hardly any reason to doubt the official elevation of 2850 m. On the IJSAP Operational Navigation Chart (Sheet G8) the airport of Ka-erh-mu is situated right in the center of the Tsaidam salt swamp at latitude 36°45N and longitude 95°34E, with an elevation of 9000 ft = 2743 m. This position does not seem to be quite consistent with the prevailing northerly winds at 1800 LT. Here hardly more can be said than that Karmu should be situated at the southern edge of the Tsaidam plain near latitude 36°25N, between longitudes 94.5° and 95.7°.

Gar Dzong (55228), near the administrative center of Gartok, is situated in the marked broad valley of the Gartang River, one of the sources of the Indus which runs from SE to NW. The elevation of 14058 ft. = 4287 m is derived from the USAF Navigation Chart.

Assuming that the semi-official coordinates of Heiho (55299) are correct, this station (airport?) is situated in the upper catchment area of the Salween River at an elevation of nearly 5000 m, at a place named Adag Mamar. Obviously all geopotential data from Heiho before 1962 are inconsistent with the neighboring stations; similarly the low surface temperatures (Table 4) are inconsistent with Lhasa and Yushu if the height of Heiho is not more than 4000 m. Day-to-day analyses of 500 mb maps--as performed by my collaborator Mr. H. S. Anand during 1961--demonstrated that internal consistency of the data could only be achieved after applying a correction of +150 gpt m to all geopotential heights (with an error of hardly more than 10 gpt m). The Times Atlas indicates the name Heiho in brackets at the well-known Tibetan place Nag-chu Dzong (3I°28'N, 92°00'E) on the Lhasa-Lanchow highway. This identification is confirmed by other sources and would be more consistent with all meteorological data; thus it is preferred here.

Mountain ridges above 6000 m are visible to the south, southeast and north of Heiho, with a pass at 16600 ft. = 5060 m. Temperature data (Tables 16, 18) suggest an elevation of at least 4500 m.

Shensa Dzong (55472) coincides well with a place named on the USAF Navigation Chart (30°58'N, 88°41'E) near Lake Kyaring Tso, at an elevation of 15448 ft. = 4708 m, in a valley running from SE to NW. Only a few observations are available.

Shikatse (5557 8) is'.iust south bi* the Tsangpo Vailfiy in a tributary running from SE to NW.

Gyangtse (55680) is in a valley running SE-NW, about 80 km upstream from Shikatse. A former British-Indian meteorological station (elevation 3996 m) was destroyed in 1954 by an inundation.

Phari Dzong (5577 8), on the highway from Lhasa to Sikkim, is situated near the source of a valley running toward the south (Ama Chu catchment, through western Bhutan to lower Brahmaputra = Tsangpo), only 10 km south of the watershed.

Yushu (56029) is identical with the Tibetan town Iyekundo (or Djekundo). Its elevation of 3873 m seems to be more consistent with the temperature data than that of the NJ47 International World Map of 3658 m. The station is situated in a W-E oriented tributary of the upper Yang-tse-Kiang, imbedded in high plateaus of more than 4500 m elevation.

Changtu (56137) is identical with the Tibetan town Chiamdo, situated on the Lhasa-Chungking Highway in a N-S oriented section of the upper Mekong River, imbedded in high plateaus of 4500-5000 m elevation, but opened toward the west through a tributary. After a comparison of the 500 mb height with neighboring stations (Karmu, Lhasa, Hsihchang) for eight months (July-August, 1957-60), a correction of +60 gpt m (with an error less than 10 gpt m) was applied.

Kantze is situated at the northern flank of the Yalung River (Ye-lung- chang) which here turns from ESE to SSE, and on the Lhasa-Chungking Highway.

On the Navigation Chart (Sheet H10) an elevation of 11500 ft. = 3505 m is given; the adjacent mountain passes are at elevations between 4200 and 4900 m. After a comparison of the 500 mb heights with neighboring stations a correction of +50 gpt m (+10 gpt m) was applied.

Lawang (Tzukei, 56533) is situated in a N-S running valley, parallel to the meridional gorges of the Salween, Mekong, and Yangtse, at an elevation of approximately 6000 ft and only about 30 km west of the Salween gorge. Immediately south of the position, the valley bends sharply toward the west and runs into the upper Irawaddy River while the original direction is followed from the south by another tributary of the Irawaddy.

Hsihchang (56571), apparently identical with Ning-yuan, is situated on a tributary of the Yalung River, similarly running from north to south. The elevation is also given as 1200 m.

Tengchung (56739) lies south of the gorges in a more hilly, open country.

APPENDIX C: DESCRIPTION OF INDIVIDUAL WEATHER SITUATIONS (1966)

May 25 (Orbit 132): A large Cs-Ns system above Karakorum extends to about 80E. North-central and eastern Tibet development of giant cells over mountain areas. Himalayas, Upper Sutlej Basin and south-central Tibet cloudless or few cells developing under the control of a weak warm ridge near 85E. Assam arc giant cells under large Cs sheets expanding to NE.

May 26 (Orbit 145, incomplete): Assam arc dense Ns system encircled by the snow-covered mountains, eastern Tibet giant cells elongated from 240° with anvils extending to NE. In the area of Yangtse Valley (33-34E) lee waves from 240°, wave length about 8 km. Central Tsaidam some streets of Sc casting shadows, mountains north of Tsaidam orographic clouds and Cs waves extending towards NE. Ascents from Lhasa and Tengchung confirm tropospheric warming (+1 -4°C) and humidity increase to near saturation (including Changtu). Surface low in Upper Burma has deepened (6 mb), westerlies extend to 500 mb south to about 20N, to 300 mb down to 15N with a marked trough near 90E.

June 3 (Orbit 252, incomplete and poorly gridded): Western mountains, Himalayas and Upper Sutlej Basin cloud-free or small-scale Cu convection. Northern and central Tibet strong cloudiness, above Astin-Tagh in broad-scaled rows from 240°, coinciding with a 500 mb low centered near 36N, 87E.

June 5 (Orbits 278/9): Western mountains few clouds, NW Himalayas Ns, with upgliding Cs extending to Karakorums correlated with a 500 mb low near 36N, 74E and a marked 300 mb trough along 70E (ridge at 90E). Similar, but stronger, situation above E Tibet. Assam arc and Gorges Ns with few gaps, As extending up to 33N. S Tibet (Upper Sutlej-Tsangpo Basin) nearly cloud free, central Himalayas few orographic cells, Assam plain extended Ns, giant orographical cells in central Tibet (oriented 230-260°), NE Tibet cloudless. At 700 mb a remarkable contrast: Karmu T = 18°C, T_d = -21°C compared with Hsihchang T = 10°C, T_d = 9°C.

June II (Orbits 358/9): Central Himalayas (76-82E) cloudy, possibly in relation to fibrous Cs over the Indo-Gangetic Plain at the same longitudes; other western mountains few clouds. West and central Tibet giant cells, Astyn-Tagh (85-89E) covered by Ns. Assam arc surface low, dense Ns covers Himalayas toward the west to 89E. E Tibet strong cloudiness (probably giant cells with extended medium and high clouds), orography only partly discernible. 500 mb high near 40N, 67E, NW flow above all of Tibetan Highlands up to trough near 110E (300 mb near 102E).

June 14 (Orbits 398/9): Western mountains few crouds, south of Himalayas (76-82E) dense, but broken, clouds, apparently residual of a disturbance. Himalayas and Karakorums orographic clouds. Upper Sutlej Basin and S Tibet west of 86E and south of 31N small-scale convection in rows from 300°; Gentral Tibet beginning small-scale convection. North of 33N and NE Tibet many giant orographic cells. Himalayas east of 90E and Assam arc extended medium and high clouds with some gaps, apparently veiling giant cells; Gorges mostly invisible, Cs extending up to 32N, 97E-34N, 102E--orographical NW-SE orientation discernible. 500 mb high near 35N, 85E; zonal trough about 30N, 75E-28N, 105E.

June 16 (Orbit 425): Western mountains and Astin-Tagh few clouds, Himalayas orographic cloudiness, Punjab several extended Cb-Ns cells, northern, central and southern Tibet unusually strong convective cloudiness, mostly giant cells--lakes partly visible. Bright Ns-Cs area elongated from 32N, 88E to 34N, 93E, north of it rows oriented from 40-60°. Assam arc Ns-As, Cs, extending towards north up to 33N; NW-SE oriented valleys weakly discernible. 500 mb marked anticyclonic cell above Tarim Basin (cloud-free) centered near 40N, 85E; cyclonic trough extends from about 26N, 75E to 36N, 100E as indicated by the above-mentioned Ns-Cs area.

June 18 (Orbits 451/2): Western mountains cloud free, only NW Himalayas some orographic cells. Northern, central, southern and eastern Tibet mostly cloud free; only over the highest mountains (Mustagh-Ata) Cb cells in development. East of 83E Himalayas partly cloudy, giant cells developing. Assam arc dense Ns, above mountains only broken Cs- As. Small-scale convective clouds oriented in rows from 40-50°--east of

30N, 91E to 33N, 96E. Towards the east they turn into giant orographic cells south of 33N. At 700 mb and 500 mb trough with marked cyclonic shear from 25N, 90E to 32N, 115E, above Lhasa NE flow; 500 mb and 300 mb anticyclonic cell still near 37N, 85E.

June 20 (Orbits 478/9): Alai, eastern Hindukush, NW Himalayas, Karakorums and Punjab few giant cells, surface cyclone above Baluchistan, western and central Tibet few orographic cells (as June 18), central Tarim Basin zonally oriented convergence line and surface front. Himalayas east of 83E cloudy. Upper Tsangpo Basin and southeastern Tibet many orograph- ical cells south of about 32N as seen in Plate 2. Assam arc giant cells covered by Cs sheets. Gorges partly discernible. Eastern Tibet mostly cloud-free, except convective cells south of 32N. Warm 500 mb anticyclone above SE Tibet, centered near 26N, 96E with ridge along about 100E, zonal trough along 23N; 300 mb easterlies south of 26N. The frequent apparent anticyclonic cloud pattern above SE Tibet produced by the orographic structure--mountain ridges oriented 240-250° at longitudes 90- 94E, but 300-320° at longitudes 96-100E.

June 26 (Orbit 558): Western mountains cloud-free except central Karakorums where bright orographic clouds appear. Himalayas cloudy, but large valleys visible. Northwestern Tibet and Upper Sutlej Basin mostly cloud-free. Central, southeastern, eastern and northern Tibet many giant cells, mostly orographic (big lakes and NW-SE oriented valleys visible), NE Tibet (Kuku-Nor area) broken Cs-As sheets. Assam arc dense Cs, apparently covering giant cells, extending towards NE, Gorges not visible. 500 mb anticyclonic cell near 33N, 90E; cyclonic trough extending from 26N, 90E to 32N, 105E.

June 28 (Orbits 584/5): Western mountains mostly cloud-free, except some bright orographic clouds in Alai, central Pamir (perhaps), central Karakorums. NW Himalayas giant orographic cells, east of 7 6E monsoon disturbance with Cs-As covering giant Cb cells. Southern Tibet many convective cells south of 32N (lakes visible), apparently small-scale convection rows oriented 40°. Eastern Tibet confused Cs pattern with some giant cells; apparent anticyclonic center near 34N, 93E. Central and northern Tibet (west of 90E) mostly cloud-free. Assam arc giant Cb cells with Cs

sheets extending towards NE up to 31N. 500 mb anticyclonic axis in eastern Tibet along 34N, trough extending from 26N, 80E to 32N, 102E (similar to June 26).

June 29 (Orbit 598): Pamir and Alai cloudy, to the east giant cells, strong convergence zone south of Tienshan. Central Karakorums and notably central Kuenlun bright orographic clouds, weak clouds along Astin-Tagh. Southern, central and eastern Tibet giant orographic cells, big lakes visible, small-scale convection on plains south of 33N. Himalayas east of T&E mostly'cloudy, valleys partly visible, Upper Tsangpo Basin strong convective cloudiness. Assam arc Cs with few giant Cb cells. Gorges only visible north of 30N. 500 mb anticyclonic cell centered near 33N, 95E with ridge along 95E; cyclonic trough from about 27N, 80E extending to 31N, 105E (similar to June 26, 28); 300 mb easterlies south of 30N.

July 2 (Orbit 638): Alai, Pamir and Hindukush mostly cloud-free, few giant cells in development. Karakorums and Himalayas north of Sutlej Valley large-scale cloud system from south with varying intensity. Western Tibet giant cells, apparently small-scale cloud streaks from 230°, Kuenlun cloudfree, Astin-Tagh weak orographic clouds. Central and eastern Himalayas large orographic clouds, east of 84E closed cloud system from south. Southern, central and eastern Tibet south of 34N small-scale convection together with few orographic cells in development, lakes mostly visible. Assam arc scattered Cs-As fields. Gorges hardly discernible, northeastern Tibet giant cells. 500 mb only weak anticyclonic cells centered above Tarim Basin and near 33N, 98E; weak trough along 85E; 300 mb high near 28N, 100E.

July 3 (Orbit 652, only west of 7 8E): Large-scale cloud system (Cs, As, Ns) extending between 29N and 40N; Alai, Pamir and Hindukush west of 74E only orographic convection. 500 mb trough from 46N, 90E to about 32N, 70E, similar at 300 mb, high same as July 2.

July 4 (Orbits 664/5): Extensive cloud system with giant cells and large Cs-As sheets in eastern Pamir, Kuenlun and northern Karakorums. Between 30N and 33N mountain waves east of Himalayas—direction of flow 240°, number of waves up to 14, wave length 12-18 km, horizontal extension up to 300 km off the wave-producing ridge. Himalayas west of 81E orographic

cloudiness with extended medium and/or high clouds, Kashmir Basin and Indus Valley below Gilgit River cloud-free, Hindukush orographic clouds. East of Kuenlun broad Cs-As-Ns system, especially 33-37N, 94-99E. Southern and central Tibet between 83E and 90E mostly cloud-free, very few orographic cells. Eastern Tibet many small-scale convective cloud rows oriented from 220-240°, spaced 5-10 km apart, interrupted by giant orographic cells, diagonal valleys partly discernible. Himalayas east of 87E and Assam arc diffuse giant cells. Gorges partly visible. Marked 500 mb trough extending from 43N, 90E to about 32N, 65E, Tibet mostly SW flow, high tropospheric moisture. Unusually deep 300 mb trough along 68E, extending to 25N, strong SW flow between 70E and 90E.

July 5 (Orbits 677/8): Alai, Pamir, Hindukush, and Himalayas west of 75E only orographic clouds, but eastern portion (especially between 35. 5 and 38N) extended Cs-Ns system, apparently with diffuse giant cells (such as above central Kuenlun) extending towards east along Astin-Tagh to another large Ns system above NE Tibet (96-100E); Kuku-Nor and Upper Hoangho Basin cloud-free. East of the Himalayas between 30 and 32N again widespread mountain waves (cf. July 4), wave length 15-20 km, number of waves 9-12 (see Plate 3). On both flanks of this lee wave system small-scale convective cloud rows (distance 5-10 km) oriented similarly from 220-240° and interrupted by giant isolated orographic cells. This system covers large areas of Tibet south of 3IN, extending from about 83E to 93E; lakes discernible. Eastern Himalayas and Assam arc diffuse giant cells. Gorges covered by an extensive bright Ns system, probably related to a surface frontal system extending to 25N, 110E and farther east. 300 mb and 500 mb main trough areas along 73E, another trough (cf. July 4) above Tarim Basin, probably 45N, 92E to 37N, 83E; above Tibet strong SW flow prevails at 300 mb. Eastern Tibet mostly cloudy, irregular pattern of diffuse convective cells, diagonal valleys partly discernible.

July 7 (Orbits 704/5): Alai, Pamir, Hindukush cloud-free, Karakorums and Himalayas west of 84E only few orographic clouds. West central Tibet and Upper Sutlej Basin small-scale convective cloud streets from 230° (in advance part of a deep 300 mb trough along 75E). Kuenlun, Astyn-Tagh and northeastern mountains extensive dense frontal clouds. Central Tibet east of 90E giant cells, mostly oriented SW-NE; Nepal, Sikkim, Bhutan and Assam

dense cloudiness with few gaps; SE Tibet many giant cells, diagonal valleys visible. 300 mb anticyclone above S China.

July 9 (Orbit 731, Orbit 730 not usable): Mountains west of 85E, western and central Tibet, Upper Sutlej Basin mostly cloud-free. Anticyclonic cell at 500 mb and 300 mb ridge at 75-80E. East of 88E many giant cells, Upper Tsangpo Basin small-scale convection, Himalayas east of 86E orographic clouds; all east of a 300 mb trough extending from 50N, 100E to about 32N, 86E.

July 10 (Orbits 744/5): Himalayas and western mountains few clouds, central Tibet mostly cloud-free. East of 90E many giant cells, as shown in Plate 4, mostly oriented from NW-SE (diagonal valleys visible). Tsaidam small-scale convection, .Assam arc dense Ns extending only slightly into the mountains. 300 mb ridge at 75-80E, main anticyclone along 28N, 90-120E, both separated by indefinite trough.

July 18 (Orbits 850/1): Marginal mountains, Kuenlun, Mustagh-Ata orographic clouds. Northern and central Tibet nearly cloudless, except few orographic Cb in development, no indication of a surface front along 35N. Southern and eastern Tibet many giant cells--between 87 and 92E apparently with plumes from 40°—extended cloud system above Gorges and SE Tibet south of 34N, with gaps along valleys, few orographic Cu in NE Tibet, Kuku-Nor visible. Assam arc nearly cloud-free, giant cells south of 26N only. 500 mb two anticyclonic cells near 33N, 78E and along 30N, 90-1 30E with weak col near 86E; 300 mb anticyclone above south-central China in similar position.

July 19 (Orbit 864): Northwestern mountains, western and northern Tibet few orographic clouds, no indication of surface front along 33N, however extended orographical clouds (As, Ns) above Himalayas about 78-86E, apparently not correlated with monsoon low. Tibet east of 85E many giant Cb cells and/or small-scale convection; Gorges and Assam arc similar to July 18, N"E Tibet extensive Cs sheets. 500 mb high near 40N, 7 8E, large anticyclone along 32N from SE Tibet to China, weak col near 86E. 300 mb similar large anticyclone SE Tibet and China.

July 21 (Orbit 891): Northwestern mountains few orographic clouds, SE Kashmir extensive Ns system with patches up to 83E. Northern Tibet few convective cells; southern, central and eastern Tibet many giant cells developing, in the east oriented from 230°. Assam arc, Gorges and SE Tibet high but patchy cloudiness, Tsaidam mostly cloud-free. 500 mb anticyclone near 35N, 78E, trough from 40N, 105E to 32N, 90E; 300 mb high above southern China, extension to N India interrupted by col near 90E; surface front running east from 85E along 30N not consistent with cloud pattern.

July 22 (Orbits 904/5): Northwestern mountains (including Kuenlun and Karakorums) only few orographic clouds, western Himalayas and Kashmir N with extended Cs sheets, northern Tibet Cs sheets with developing giant cells. Central, southern and southeastern Tibet including Gorges strong convective cloudiness with many developing giant cells, valleys discernible (see Plate 5). Central plains of Assam arc, eastern Tibet and Tsaidam nearly cloud-free.

July 24 (Orbit 931): Central Himalayas 78-88E extensive Ns system, marginal Cs, other mountains orographic clouds. Northern Tibet weak convection, Tarim Basin patchy Cs sheets. Southern, central and parts of eastern Tibet developing giant cells, anticyclonic ally oriented around a nearly cloud-free area near 32N, 9IE; Assam Cs plumes from 40°. Surface monsoon lows above Punjab and Assam, 500 and 300 mb anticyclonic cell above central Tibet with unusually high temperatures aloft (Changtu 500 mb + 5°C, Lhasa 300 mb - 18°C).

July 25 (Orbit 944): Monsoon disturbance with extensive Ns area along Himalayas, 78-83E, and strong cloudiness up to 90E. Karakorums and NW Tibet cloudy, northern and central Tibet extensive Cs sheets with developing giant cells, eastern Tibet and Gorges comparatively weak convective cloudiness. Cloud pattern suggests (cf. July 24) anticyclonic center near 31N, 90E. Assam few giant cells with Cs plumes from 60°, central plain nearly cloud-free. Surface frontal system above NW Tibet, 500 mb weak trough near 88E separating anticyclonic cells near 25N, 83E and 29N, 108E; Gorges area still high temperatures (Tengchung 500 mb - 0°C, 400 mb - 9°C); 300 mb anticyclonic belt elongated along 30N from 40E to 120E.

July 28 (Orbit 984): Northwestern mountains few orographic clouds, Tarim Basin cloud-free (inconsistent with a frontal system along 39N). Western Tibet, Upper Sutlej Basin patchy Cs and small-scale convection; central, southern, and eastern Tibet many giant cells. 500 and 300 mb weak trough near 85-90E, surface monsoon trough in its normal position.

July 30 (Orbit 1011): Western mountains and northern Tibet nearly cloud-free, Pamir and Alai few orographic clouds. Southern and central Tibet giant cells developing, SE Tibet extensive Ns sheet centered 31N, 94E reaching from 29-32. 5N, widespread convective cloudiness (valleys discernible) above E Tibet up to Kuku-Nor region. 500 mb anticyclonic cell near 35N, 85E, weak col near 100E, temperatures +1°C. 300 mb high east of 100E, weak trough near 80E.

July 31 (Orbit 1026): Northwestern mountains few orographic cells, except NW and central Himalayas (including Kashmir) covered by dense Ns. Central, southern and southeastern Tibet many giant cells with Cs patches, Upper Trangpo Basin small-scale convection. Assam are giant cells with dense Cs, Gorges cloudy, valleys discernible. NE Tibet and around 33N, 91E nearly cloud-free. Surface monsoon trough in usual position, 500 mb high cell near 35N, 90E, trough along 80E; 300 mb anticyclonic cell near 30N, 92E.

DESCRIPTION OF INDIVIDUAL WEATHER SITUATIONS (1964)

NIMBUS I cloud pictures usually have a much better resolution than those of NIMBUS II--the central camera reproduces even small-scale cumulus cells with a diameter of 0. 8-1.0 km. Unfortunately, the useful lifetime of NIMBUS I was limited to about four weeks after launching (August 28, 1964). Pictures were taken near 0500 GMT or 1100 LT. This evaluation is restricted to a very small and incomplete sample, but may serve as a useful comparison representing conditions in the transition period between late summer and early fall, still with strong convective activity.

August 31 (Orbit 43): Narrow zone of frontal clouds in southern Tarim Basin. Southern Tibet 81-84E rows of convective clouds oriented from 240° ahead of a weak 300 mb trough, towards east dense clouds.

September 1 (Orbit 57, only east of 82E): Extensive frontal system across northern Tibet, Ns-Cs clouds, between 86E and 90E dissolving into medium and giant convective cells; Tsaidam few Cu with shadows; 94-98E again Ns with high albedo, Lake Kuku-Nor cloud-free. Himalayas overcast, southern Tibet medium and giant cells, central area Cs-As-Ns. Between upper Tsangpo and Mekong many streets of convective clouds (orographically reinforced), slight anticyclonic curvature from 230° to 250°; SE Tibet heavy cloudiness with giant cells and a few gaps, east of 99E transition into strong convective pattern, with indications of meridional gorges. 500 mb trough near 90E, upper anticyclonic cell near 110E.

September 8 (Orbit 160): Trans-Himalaya (north of Upper Sutlej Basin) and central Tibet giant cells, Himalayas on both sides of Sutlej Valley cloudfree and snow, near 77E and east of 80E strong orographical clouds (large valleys open), small-scale Cu rows from 210° west of Lake Manasarovar (see Plate 1). Kashmir Basin, valleys of Indus, Gilgit/Hunza and Khunar cloudless; mountain chains, including Hindukush, individual (mostly circular shaped) Cu cells. 500 mb trough near 35E between two anticyclonic cells near 33N, 75E and east of 100E.

September 11 (Orbit 204): Diffuse, but not closed, frontal cloud zone SE of 30N, 78E to 34N, 85E, apparently oriented from about 230° (300 mb trough near 7 5E) with some mountain waves. Central and NW Tibet mostly cloud-free, few orographic Cu. Dense Ns with monsoon disturbance around 28N, 81E.

September 14 (Orbit 250, only west of 83E): Himalayas, Karakorums, Astyn-Tagh and Kuenlun snow-covered and cloud-free, only orographic Cu in the outer ranges of Himalayas 77-79E, together with small-scale Cu in the Gangetic plain; Trans-Himalaya north of cloudless Upper Sutlej Basin giant cells, north and south of Lake Panggong Cu rows from 220°. 500 mb ridge near 75E.

September 19 (Orbit 320): Extensive frontal Ns system above eastern Tibet, towards NW transition to Cs-As, towards SE into Cu streets. 28-30N, 97-102E distinct row structure (oriented from 230°) only partly interrupted by meridional gorges. 500 mb well-marked trough along 90E, ridge near 100E.

September 21 (Orbit 350): Mountains with extensive snow cover, Kuenlun orographic clouds at southern flank. Central Tibet giant cells, partly merging into Ns, Upper Sutlej Basin and northern Tibet rows of convective clouds with few giant cells; mostly-oriented from 250° (500 mb trough near 85E), lakes partly visible. SE Tibet strong convective cloudiness, big lakes visible, irregular rows oriented from 230°; 300 mb anti-cyclonic cell near 28N, 98E.

An approximate idea of the conditions during the early night can be obtained from a small sample of HRIR (high-resolution infrared) pictures from NIMBUS I (Orbits 36, 109, 124, 197, 284, 299 and 343). Inmost of these cases the western mountain areas (Hindukush, Karakorum, NW Himalaya, also with two exceptions Pamir) seem to be cloud-free; the larger valleys (Amu-Darja, Indus with Gilgit/Hunza Valley, Sutlej and/or Ganges) are visible due to their higher temperatures; and the larger glacial regions (central Pamir, central Hindukush, Karakorum, Kuenlun) show up because of their lower temperatures. Central and southern Tibet are also mostly cloud-free; in only one case (Orbit 343, September 20) many cloud cells dot central Tibet between latitude 33N and 36N.

Unfortunately, only three orbits from east of 82E are available (September 16, 17 and 20); in each case cloudiness increases towards the east and southeast and giant Cb cells are visible above the Himalayas and the Assam region. The few HRIR data available are consistent with the results of the daytime pictures; if truly representative, they indicate the early disappearance of convective clouds in west-central and southern Tibet after sunset.

APPENDIX D: SYNOPTIC DATA

Before the installation of regular meteorological stations in Tibet in 1956, meteorological information was restricted to a number of climatological stations. Only the results of Leh and Lhasa have been published and referenced frequently. The reports from scientific travelers like Sven Hedin (cf. Table 17) contain many interesting weather descriptions, notably the large frequency of afternoon showers and thunderstorms during the warm season with sleet, graupel and/or hail, and heavy gusts.

Since 1958, synoptic weather messages have been distributed from the Tibetan stations, and 1200 GMT data have been published in available sources, although incomplete and unchecked. These data were compiled, as far as possible, for the period 1958-1962 (Yushu only 1960-1962) including some winter months for comparison. A more complete survey was made for a selection of stations mainly covering the period 1960-1963; at seven stations fairly complete records of eight daily observations were studied (Tables 2-6). They largely confirm all travelers reports and reveal many interesting climatological details. Of particular interest are the reports from Heiho in the central part of the Tibetan Highlands, and Karmu, at the southern edge of the arid Tsaidam salt plain.

At Karmu the frequency of precipitation during the afternoon is only 12 (4) percent during summer (winter). Low clouds are rare, especially during winter; during summer most of them are thermodynamically stable. In both seasons, surface winds prevail from northerly directions, in contrast to the predominantly WNW flow at 500 mb (or 3 km above the ground, cf. Table 13); this seems to be part of a diurnal circulation between the Tsaidam plain and the surrounding mountains. This daytime circulation, diverging in all directions from the extended plain towards the adjacent mountains, also seems to be responsible for the stability of the clouds in spite of the large mid-tropospheric lapse rate of 7.7 C km (Table 11) and the perennial aridity of the Tsaidam desert.

At Heiho the weather conditions are much different, particularly during summer. On 45% of all days, thunderstorms are observed during the six afternoon hours, and on 72% of all days showers or thunderstorms either

occur between 1700 and 1800 LT or are visible from the station, probably in the distant mountains. Even more impressive is the frequency of cumulo-nimbus clouds on 75% of all days, with a cloud base of 20002500 meters above ground, i. e., near 6500 m above sea level. This coincides exactly with the high (super-moist-adiabatic) lapse rate in the middle troposphere (Table 10) at all stations on the Tibetan plateau. The total amount of cloudiness at 1800 LT is high (72%); here the contribution of medium and high clouds is much smaller than at Karmu. The surface winds are well distributed over all directions. At 500 mb the resultant wind is irom the SSW, however with a constancy of not more than 30% ^ which indicates the vicinity of the 500 mb anticyclonic center above SE Tibet. Taking into account the high vertical lapse rate--and in accordance with the pilot balloon and surface wind observations at Depsang, 5362 m (cf. Flohn 1958)--the 1800 LT surface winds can be considered as first order approximations to the geostrophic flow at 1.0-1. 5 km above station level in all cases where local orographic flow deviations are negligible.

Even during winter, showers occur between 1200 and 1800 LT on 11% of all days and are visible, at 1800 LT, on 21% of all days. Surface winds from the west and northwest prevail in accordance with the westerly flow at 500 mb (Table 13). The excellent visibility during most of the year has been stressed by all travelers--the author was also much impressed by this in the Hindukush Mountains of Afghanistan and northernmost Pakistan. Even under winter conditions (cf. Appendix J) instability is not infrequent and should be mainly caused by a combination of local heating and advective processes.

00-1800 LT, JUNE-SEPTEMBER

) E	Rain 60-69	Dust, Sand 06-09, 31-35	N[1]	∇&R[2,3] in %
0	4	9	476	23
1	13	19	452	8
4	0	0	164	35
0	0	0	276	59!
2	2	0	356	67!
8	0	1	337	36
0	0	0	482	72!
3	9	1	253	33
7	0	0	366	43
1	9	0	246	62!
2	16	1	366	26
0	0	9	244	0.4
0	1	3	280	5
0	0	3	244	21

h Mazar 18%

%, Shikatse 6.3%, Kantze 4%, Hsihchang 3%

TABLE 3: PAST WEATHER (W) AT TIBETAN STATIONS, JUNE-SEPT. (LOCAL TIME 90°E)

A) Station	W =	0	1	2	3	4	5	6	7	8	9	n
Mangya	00-06 LT	137	208	51	0	0	0	20	1	6	0	423
(1957-60)	06-12	132	160	128	6	0	0	40	1	10	1	478
	12-18	79	180	109	5	0	0	28	0	45	10	456
	18-00	126	226	65	5	0	0	19	0	37	4	482
Gar Dzong	06-12 LT	38	52	22	0	1	0	1	0	16	1	131
(1961-63)	12-18	40	52	22	1	1	0	0	0	27	15	158
	18-00	56	59	8	0	0	0	0	0	23	7	153
Heiho	00-06 LT	75	133	64	0	5	1	0	0	160	7	445
(1960-63)	06-12	50	131	87	0	4	1	1	0	182	26	482
	12-18	22	74	42	0	0	0	1	0	127	214	479
	18-24	76	104	63	0	0	1	0	0	155	73	472
Shikatse	06-12 LT	38	71	62	0	0	0	0	0	160	7	291
(1961-63)	12-18	27	70	54	0	0	1	0	0	72	104	327
	18-24	25	38	32	0	0	0	0	0	81	60	236
Phari-Dzong	00-06 LT	10	65	37	0	2	0	1	0	216	1	332
(1961-63)	06-12	14	62	91	0	4	3	0	0	172	2	348
	12-18	5	25	32	0	0	0	1	0	281	20	364
	18-24	3	41	37	1	0	0	2	0	271	5	360
Kantze	00-06 LT	40	100	47	0	0	0	0	0	156	5	348
(1961-63)	06-12	37	104	56	0	0	0	4	0	158	6	365
	12-18	25	53	18	0	0	0	0	0	144	126	376
	18-24	46	86	30	0	0	0	0	0	141	61	364
Lawang (Tzukai)	06-12 LT	3	14	46	0	32	1	29	0	75	0	200
(1961-63)	12-18	2	15	12	0	4	1	5	0	117	29	185
	18-24	2	27	32	0	5	0	6	0	119	12	203
Hsih chang	00-06 LT	22	78	68	0	0	1	34	0	103	43	349
(1961-63)	06-12	36	70	114	0	0	0	44	0	89	12	365
	12-18	28	66	91	0	0	0	29	0	84	67	365
	18-24	21	80	79	0	0	0	31	0	97	57	365
B) Supplement. June-September, 12-18 LT only												
Lhasa (1958-62)		35	98	66	1	0	0	0	0	57	74	331
Karmu (1958-62)		126	155	115	2	0	0	35	0	14	5	452
Yushu (19 60-62)		21	51	28	1	0	2	22	0	72	52	249
C) Supplement, December-February, 12-18 LT only												
Lhasa (1958-61)		93	113	56	7	1	0	1	0	16	0	287
Heiho (1958-61)		51	103	50	11	0	0	0	2	28	0	245
Karmu (1958-61)		53	97	79	5	0	0	0	11	0	1	246
Yushu (1960-61)		12	79	37	0	1	0	0	4	16	0	116

TABLE 4: FREQUENCY OF PRECIPITATION (W=5-9)
AND THUNDERSTORMS (W=9) JUNE-SEPTEMBER
(IN PERCENT)

Station	All Kinds of Precipitation				Thunder storms
	00-06	06-12	12-18	18-24	12-18 LT
Lhasa	-	-	40	-	45%
Shikatse	58	41	54	60	32
Gyangtse	62	28[2]	74	38	39[1]
Phari Dzong	66	51	83	77	6
Heiho	38	44	71	59	45
Shensa Dzong	-	11[2]	63	-	40[1]
Mangya	6	11	18	12	2
Karmu	-	-	12	-	1
Shahiullah Mazar	34	16	19	36	o[1]
Gar Dzong	19	14	27	20	9
Yushu	-	-	59	-	21
Kantze	46	46	72	56	34
Lawang	69	52	82	67	16
Hsih chang	51	40	49	51	18

1) Only 50-100 observations each period

2) 06-09 LT only

TABLE 5: LOW CLOUD TYPES (C_L) AND HEIGHTS (h),
1800 LT, JUNE-SEPT. (PERCENT)

^{C}L =	0	1-3	4	9	h=	5	6	7	8	9	n
Mangya	28	13	24	29		4	30	30	6	29	474
Karmu	27	14	28	3		1	22	25	25	27	458
Shahiullah Mazar	0	31	25	39		0	I	9	89	0	93
Gar Dzong	1	24	33	40		0	2	40	56	2	165
Lhasa	<1	15	22	61		0	<1	6	86	8	340
Heiho	<1	7	16	75		0	1	15	82	1	481
Shensa Dzong	0	6	22	72		1	14	37	42	6	65
Shikatse	2	4	15	78		<1	3	10	28	59	276
Gyangtse	0	14	5	81		0	13	62	25	0	96
Phari Dzong	<1	4	22	73		49	46	4	<1	<1	356
Yushu	-	-	-	-		7	40	41	7	5	260
Kantze	2	8	30	60		0	6	20	72	2	366
Lawang	<1	5	32	55		5	35	51	7	<1	2 39
Hsih chang	1	13	47	30		1	17	69	11	2	366
For comparison: December-February											
Lhasa	24	9	45	21		<1	<1	<1	72	26	252
Heiho	14	4	38	42		4	2	9	67	19	220
Karmu	91	1	2	<1		1	1	7	2	89	250

TABLE 6: AVERAGE CLOUDINESS - TOTAL SKY COVER ($\bar{N}$) AND COVER BY LOW CLOUDS ($\bar{N}_h$) JUNE-SEPTEMBER (PERCENT, LOCAL TIME)

	$\bar{N}$						$\bar{N}_h$					
	00	06	12	15	18	Average[1]	00	06	12	15	18	Average[1]
Mangya	37	54	57	62	61	54%	6	7	22	34	29	18%
Shahiullah Mazar	49	51	54	63	63	55	38	34	42	56	54	43
Gar Dzong	36	47	57	56	55	50	26	32	42	47	43	37
Heiho	62	68	75	79	72	70	56	61	72	76	66	65
Shensa Dzong	--	64[2]	--	--	73	--	--	42[2]	--	--	66	--
Shikatse	76	78	66	68	75	73	56	59	36	44	35	46
Gyangtse[3]	--	75	73	--	77	--	--	66	57	--	70	--
Phari Dzong	82	83	81	84	84	83	79	72	76	82	80	77
Kantze	67	77	68	73	75	72	58	63	60	67	64	61
Lawang	90	90	89	84	85	88	88	86	83	80	77	82
Hsihchang	80	81	73	73	78	77	63	54	39	46	54	50
For comparison:												
Depsang[4]	44	49	54	59	45	49%						

1) Eight daily observations

2) 09 LT

3) Inhomogeneous time schedule

4) 35°17'N, 77°58'E, 5362 m, July 1914

APPENDIX E: AEROLOGICAL DATA

Since the discussion of the summertime upper-level Tibetan anticyclone is based on aerological data, it was necessary (Flohn 1964, 1965) to evaluate the existing data with great care in order to avoid any kind of systematic error. Three prominent sources of error shall be mentioned here:

a) the (real or apparent) diurnal variation of temperature;
b) the systematic differences of different types of radiosonde;
c) the selection of fair weather winds at stations using only visual measuring techniques.

Error (a) can only be avoided if the diurnal temperature variation-- largely dependent on radiosonde type and on application of radiation and lag corrections--is known or can be estimated from adjacent stations (cf. Table 10). Error (b) is most serious due to the large variation in time period over which such differences extend and because of unrecorded improvements and changes of instruments in routine use. Considering climatological averages (for at least several months), the use of the thermal wind equation

$$\frac{\partial V_g}{\partial z} = \frac{g}{f T_m} \nabla T_m$$

(V_g = geostrophic wind, g = gravitational acceleration, Coriolis parameter $f = 2_\Omega \sin\phi$ T_m = mean temperature of a layer, ∇ = horizontal gradient) provides an independent check of the horizontal temperature gradients; in this way it permits a minimization of error (b). This, however, is only true in cases of representative wind samples not affected by error (c). As a consequence of fair weather selection, the thermal wind derived from incomplete samples of visual upper wind data deviates in an anticyclonic sense from its true value so that in a westerly flow its northern component is strongly exaggerated.

In the monsoon area of northeast India and Burma the pilot balloon data were so incomplete that it was very difficult to obtain a truly representative

picture of the flow above about 800 mb (cf. Source 4, Appendix A).

Unfortunately, the average maximum height of the radiosonde data from India, Pakistan and the Chinese People's Republic was relatively low (often near or below 200 mb) so that the 100 mb data should not be taken as representative. The Chinese sondes were frequently not completely transmitted; at several Tibetan stations the values for 500 or 400 mb were more complete than those below and above.

According to existing comparisons of radiosonde ascents, the day-time sondes of India (Chronometer type) and USSR are 2-4°C warmer than a chosen reference sonde (USA) in the layers between 300 and 50 mb; while the sondes of Finland, Japan, U. K. and Germany show only minor differences, mostly below 1°C. According to available information from the Chinese People's Republic, radiosondes in use are either the USSR type or the Finnish (Vaisala) type. Their distribution at different stations is unknown. Even the nighttime ascents of India have been 1 -2°C warmer (cf. Flohn 1964, p. 15); this may be due to a relatively large time-lag of the sensor. However, these comparisons for 1956 did not apply to the period used here so that any kind of correction was impossible. The even larger differences of the humidity sensors shall not be discussed.

Samples of two complete daily observations of upper winds could be evaluated at only a few stations (Table 14). At these stations the number of available data decrease at 200 mb and considerably more at 100 mb. At the stations in southern and eastern Tibet the fair weather selection prohibited any reliable evaluation of time or space derivatives, and even the resultant winds derived from the raw data were markedly biased in an anticyclonic sense.

Table 7 gives a collection of all available temperature and dew point averages for July-August. The use of different periods is permitted here because of the remarkable constancy of the summer conditions, as shown in Table 9; all values except Srinagar are given for 0000 GMT = 0600 LT. It should be noted that the average temperature above northernmost India and southern and central Tibet is 5-8°C higher than the tropical standard

atmosphere and also significantly higher than above the Sahara or the southwestern USA during summer.

Table 8--derived from incomplete transmitted data--demonstrates the annual march of temperature and relative humidity over two stations in southern and central Tibet. Table 9 gives a selection of temperature averages for individual summers; the differences between July and August are usually below 1°C. Only the 100 mb temperatures seem to be affected by instrumental improvements; the data of other stations (Karmu, Changtu, Tengchung) are similar.

Table 11 presents an evaluation of the average vertical lapse rate of the middle troposphere, i.e., in the lower 3 km above the highlands. Compared with the tropical-standard atmosphere, the degree of instability is remarkable. While Kosharyl and Karmu represent the dry atmosphere in the northern and western area, the results of Kantze, Changtu and Lhasa truly represent the conditions in eastern, central and southern Tibet.

Table 12 contains a selection of standard deviations of temperature and dew point. In the middle troposphere (500, 300 mb) above Tibet the small temperature variance is quite remarkable, especially when compared with data from the same latitude and near the equator. Values above 4°C are affected by a few doubtful data, possibly due to transmission errors. As usual, the standard deviation of dew points is much larger because of the variance of small-scale convective activity.

Table 13 presents an evaluation of 500 mb winds at three Tibetan stations during 1957-1961. Only during July and August is a well-marked 500 mb ridge observed near 30N, 92E; however, in the transitional periods from May-June and September-October, the observed WSW flow seems to indicate a similar but weaker development. In confirmation of these results, the resultant 500 mb wind above Heiho, during July and August 19 64-19 67 is 223°, 6. 8 kt (n = 38, q = 55%) and above Lhasa, 232°, 6. 4 kt (n = 42, q = 68%).

Table 14 contains, from the more complete records, resultant winds for both 0000 GMT and 1200 GMT. From these data difference winds (cf.

Chapter 6) and thermal winds (Table 15) were derived. The thermal winds above the Chinese stations (for the 500-300 mb layer) were only computed from those ascents where both levels were available; at the Indian network the decrease in the number of available data with height was generally small (cf. Table 14). In the upper layer (500-300 mb) the diurnal variation of the thermal wind was minor.

VERAGES, JULY-AUGUST, 0600 LT

	300 mb		200 mb	100 mb	
	T	T_d	T	T	Period
1	-28.0	-34.6	-45.8	-67.6	1957-60
0	-26.7	-32.8	-45.8	-69.2	1957-60
8	-25.8	-30.3	-47.2	-72.4	1959-62(i)
3	-23.9	-29.2	-45.8	-73.6	1957-60
4	-24.9	-30.2	-46.5	-72.9	1960-67(i)
2	-23.9	-29.7	-45.8	-74.0	1957-60
3	-23.8	-28.8	-45.6	-73.2	1957-60
5	-24.5	-31.2	-45.3	-73.5	1960-67
3	-25.2	-34.6	-46.9	-75.2	1960-61
5	-25.4	-31.3	-46.7	-74.7	1957-60
	-31.4	--	-44.4	-62.0	1950-59
1	-27.0	-35.6	-44.2	-68.0	1959-60
0	-30.2	-36.6	-45.1	-64.6	1957-60
9	-29.2	-39.3	-44.2	-66.6	1960-67
0	-26.6	-34.4	-44.5	-67.6	1957-60
7	-25.4	-33.8	-46.0	-71.5	1960-67
0	-25.3	-33.5	-46.2	-75.1	1964-67(i)
0	-25.9	-32.6	-47.2	-73.6	1957-60(i)
	-23.7	--	-44.1	--	1957-59
	-23.6	--	-44.7	--	1959-61
	-23.8	--	-43.6	--	1959-61
	-24.6	--	-43.3	-67.4	1963-67
	-27.6	-46.6	-46.2	-69.4	1965-66

ND HUMIDITIES,

0600 LT

Rel.Humidity (%)			
500 mb	400 mb	300 mb	n
38	46		49
35	50		51
43	50		51
38	38		48
45	43	58	52
76	69	62	74
76	70	61	98
78	72	62	101
64	58	51	51
65	52	53	53
44	41		55
40	43		56
37	44		56
39	45		52
45	49		42
44	43	57	58
60	57	59	58
72	66	58	97
80	75	63	105
84	75	64	107
62	57	57	27
59	55	40	54
38	34		57
36	35		60

TABLE 9: UPPER AIR TEMPERATURES, 0600 LT,
JULY-AUGUST, INDIVIDUAL YEARS AND PERIODS

		500 mb	400 mb	300 mb	200 mb	100 mb
Heiho	1957	-0.1	-10.6	-23.0	-44.4	--
	1958	-0.2	-11.2	-23.6	-44.3	-70.2
	1959	-0.9	-12.0	-25.0	-47.0	-74.4
	1960	-1.0	-11.5	-24.4	-46.2	-75.6
	1961	-0.4	-11.0	-23.4	-45.4	-73.7
	1962	-0.8	-11.2	-24.2	-46.6	-73.3
	Average 1965-67	-2.6[1]	-11.5	-23.5	-45.7	-71.0[1]
Lhasa	1957	-0.8	-10.7	-23.8	-45.2	-70.4
	1958	-0.6	-10.6	-23.2	-44.4	-70.9
	1959	-1.2	-11.3	-24.0	-45.8	-73.6
	1960	-1.0	-10.6	-23.6	-45.4	-75.3
	1961	-0.7	-10.7	-24.0	-46.4	-75.1
	1962	-1.3	-10.8	-24.0	-46.6	-74.1
	Average 1965-67	-1.2	-11.2	-23.4	-45.0	-74.6
Kantze	1960	-2.0	-12.1	-24.9	-46.4	-72.6
	1961	--	--	--	--	--
	1962	-2.4	-11.6	-24.8	-46.1	-73.4
	1963	-2.4	-11.8	-25.6	-46.6	-72.7
	Average 1965-67	-2.3	-11.6	-24.7	-46.6	-72.9
Hsih chang	1960	-1.5	-10.7	-24.0	-44.2	-71.4
	1961	-1.7	-11.0	-24.0	-45.6	-74.1
	1962	-1.6	-10.7	-24.3	-45.7	-74.0
	1963	-1.9	-11.0	-24.9	-46.0	-73.4
	Average 1957-60	-1.9	-11.4	-25.0	-46.2	--
	Average 1964-67	-1.7	-10.9	-24.7	-45.2	-73.8

1) Less than 20 observations

TABLE 10: AVERAGE TEMPERATURE DIFFERENCES 1800-0600 LT (°C)

	700	500	400	300	200 (mb)	Period
Karmu	7. 9	1.7	1.6	1.7	0.5	
Changtu	-	2.5	1.1	0.9	0.9	
Lhasa	-	3.3	1.3	1.1	1.4	June-August 1958-60
Tengchung	-	1.2	0.8	0. 6	0.4	
Heiho	-	-	0.9	0. 9	2.4	July-August 1965-67
Kantze	-	0.1	0.3	1.7	1.8	July-August 1960-67
Hsihchang	3.3	1.0	0.1	0. 8	0.4	
Average	-	1.6	0.9	1. 1	1.1	
Nochiang	1.8	1.3	1.4	0.7	0.5	July-August 1964-67
Chengtu	0.7	0.5	0.2	0.4	0.4	July-August 1960-67
Paishihlu	2.8	0.8	0.4	0.9	0.4	
Average	1.8	0.9	0.7	0.7	0.4	
Amritsar	2.5	1.9	1.3	1.2	0.7	June-August 1957-59
New Delhi	1.6	1.2	0.8	0.5	0.4	
Allahabad	1.0	0.9	0.7	0.5	0.6	June-August 1959-61
Gauhati	1.3	1.6	1.3	1.1	0.4	
Average	1.6	1.4	1.0	0.8	0.5	

TABLE 11: AEROLOGICAL CONDITIONS DURING AFTERNOON, 1800 LT

	Temperature			Lapse Rate	
	Surface	500 mb	400 mb	4-7 km	n
Kosharyl[1]	16.8	-3.8	-17.8	9. 0°C/km	58
Karmu	20.8[2]	-2.9	-13.7	7.7	120
Kantze	19.1	-2.2	-11.4	7.1	35
Changtu	20.2	+1.1	-10.5	7.2	105
Lhasa	17.6	+2.3	-9.4	7.2	47
Hsih chang	15.7[2]	-0.7	-10.8	5.9	52
Tengchung	12.6[2]	-1.3	-10.9	5.3	64
For comparison:					
Tropical Standard Atmosphere	8.9[2]	-6.4	-17.3	5.8	

n = number of available ascents

1) Rayon Murgab, Pamir, High Badakhshan, H = 3710 m

2) 700 mb temperature

TABLE 12: STANDARD DEVIATION OF TEMPERATURE (T)
AND DEW POINT (T_d) JULY-AUGUST, 0600 LT

Temperature (C)

	700 mb	500 mb	300 mb	200 mb	100 mb	n
Nochiang	3.5	2.3	3.2	3.4	2.5	146
Karmu (1800 LT)	4.4	2.7	2.8	4.2	2.9	117
Heiho	-	1.5	2.0	2.4	3.2	269
Changtu	-	1.6	2.2	2.4	2.6	297
Lhasa	-	1.3	1.7	2.4	2.9	320
Chengtu	1.8	2.2	2.2	3.1	2.8	160
Lawang	1.5	1.1	1.7	4.3	2.8	83
Hsih chang	1.6	1.6	(5.0)	3.8	3.5	258
Tengchung	1.3	1.0	1.9	2.5	2.1	296
For comparison:						
Benina (32. 1°N)	2.5	2.6	2.9	2.8	3.1	310
Bahrein (26. 3°N)	2.2	2.6	2.3	2.8	3.0	287
Lagos (6. 6°N)	1.2	1.4	1.2	1.7	2.8	240

Dew Point (°C)

	700 mb	500 mb	400 mb	300 mb	n
Nochiang	4.0	6.7	7.8	7.6	146
Karmu (1800 LT)	5.4	9.0	8.9	6.5	117
Kantze	-	7.2	7.1	7.7	179
Chengtu	4.4	4.8	5.9	6.3	160
Lawang	7.3	9.3	9.6	10.4	83
Hsih chang	4.2	6.6	5.6	6.2	258

Parentheses indicate doubtful data

TABLE 13: SEASONAL VARIATION OF 500 MB WINDS, 1957-1961

	Karmu				Heiho				Lhasa			
	n	α	V	q	n	α	V	q	n	α	V	q
January - February	42	284°	11.0	93%	62	272°	11.9	92%	139	256°	9.0	84%
March - April	25	300	8.4	94	82	27 3	9.7	88	111	253	4.7	63
May - June	27	284	6.0	76	76	256	7.9	73	130	239	3.9	73
July - August	105	284	4.1	67	116	208	1.8	30	127	219	3.5	47
September - October	60	286	8.3	84	81	256	7.9	68	114	249	6.0	66
November - December	33	284	11.8	92	90	270	13.7	94	129	265	10.2	85
November - April	100	287	10.5	92	234	271	11.8	92	379	261	8.2	80

n = number of ascents
α = direction of resultant wind (270^{o} = W)
V= speed of resultant wind (knots)
q= constancy

TABLE 14; MEAN RESULTANT WINDS (m sec^{-1}),
600 AND 1800 LT, JULY-AUGUST

Station	Level	α 0600	|V| (0500)	α 1800	|V| (1700)	α Sum	|V|	0600 LT No. of Observations	1800 LT No. of Observations
Peshawar	0.6 km	356°	1.8	54°	1.9	26°	1.6	186	186
	3.0	273	3.6	256	2.5	266	3.0	140	161
Amritsar	0.6 km	159°	4.7	130°	1.7	152°	3.2	162	172
	3.0	316	3.3	325	5.6	321	4.5	164	173
	5.4	266	3.6	297	5.9	286	4.6	158	166
	9.0	262	12.6	255	14.8	258	13.7	131	138
Allahabad	0.6 km	232°	0.6	54°	0.3	230°	0.16	175	179
	3.0	86	2.0	95	2.0	90	2.0	171	177
	5.4	101	3.6	82	3.7	91	3.6	168	176
	9.0	94	7.5	87	7.2	90	7.4	135	139
Gauhati	0.6 km	32°	0.6	347°	0.5	12°	0.5	184	186
	3.0	172	2.0	165	2.8	168	2.4	182	184
	5.4	145	2.6	125	2.5	135	2.5	178	179
	9.0	90	4.8	78	5.1	84	4.9	147	149
Hsih chang	700 mb	199°	3.2	165°	3.1	183°	3.0	191	100
	500	103	2.0	315	0.6	90	0.8	70	56
	300	62	7.6	74	3.9	66	5.8	50	27
Kantze	500 mb	260°	3.0	287°	1.6	271°	2.2	75	23
	300	310	5.6	275	4.9	294	5.0	46	29
Chengtu	850 mb	61°	1.6	73°	1.8	67°	1.7	155	175
	700	166	1.4	118	1.3	144	1.2	154	174
	500	221	3.1	233	1.8	227	2.5	155	173
	300	285	4.6	290	5.2	287	4.9	123	162
	200	357	3.7	316	2.2	341	2.8	37	52
Karmu	700 mb	278°	6.8	308°	2.9	287°	4.4	64	110
	500	286	2.1	287	4.0	286	3.0	50	93
	300	277	18.0	279	20.9	278	19.4	37	54
Nochiang	850 mb	74°	5.8	36°	5.2	56°	5.3	134	171
	700	15	1.3	62	2.2	45	1.6	124	156
	500	266	6.8	259	8.3	262	7.5	87	115
	300	276	22.4	271	24.8	273	23.5	61	94
Kosharyl	500 mb	261°	5.7	261°	5.6	261°	5.7	102	101
	300	271	22.0	267	22.4	270	22.2	102	101
	200	270	29.5	268	28.0	270	28.7	94	81

TABLE 15: MEAN THERMAL WINDS (m sec^{-1}),
0600 and 1800 LT, JULY-AUGUST

Station	Layer	α 0600	V (0500) LT	α 1800	V (1700) LT	α Sum	V
Peshawar	0.6-3.0 km	245°	1.9	247°	1.8	246°	1.8
	3.0-5.4	281	1.4[1]				
	5.4-9.0	282	1.7[1]				
Allahabad	0.6-3.0 km	79°	2.6	102°	1.7	87°	2.1
	3.0-5.4	117	1.8	69	1.8	93	1.7
	5.4-9.0	87	4.0	94	3.5	90	3.7
Gauhati	0.6-3.0 km	181°	2.4	166°	3.2	172°	2.8
	3.0-5.4	99	1.3	46	1.8	69	1.4
	5.4-9.0	57	3.3	50	3.9	53	3.8
Hsih chang	700-500 mb	49°	4.0	340°	3.8	17°	3.3
	500-300	31	2.6	85	4.4	65	3.2
Kantz e	500-300 mb	307°	6.0	287°	3.1	300°	4.4
Chengtu	700-500 mb	247°	2.7	259°	2.7	253°	2.7
	500-300	328	3.9	309	4.0	318	3.9
Karmu	700-500 mb	93°	4.8	248°	1.6	107°	1.6
	500-300	273	15.1	27 6	15.9	275	15.5
Nochiang	850-700 mb	266°	5.5	200°	3.5	241°	3.8
	700-500	256	7.4	256	10.7	256	9.0
	500-300	277	16.3	274	16.0	276	16.1
Kosharyl	500-300 mb	268°	16.4	268°	16.8	268°	16.6

1) 1100 LT

APPENDIX F: SURFACE TEMPERATURES REDUCED TO SELECTED ALTITUDES

In extensive mountain areas like Tibet average surface temperatures are only comparable when reduced to standard height levels. Here it would be utterly meaningless to reduce temperature averages from stations at elevations between 3000 and 5400 m to sea level; such values depend mainly on the hypothetically assumed vertical lapse rate. In order to minimize these errors, the average temperatures from all climatological data have been reduced to selected altitudes (2300, 3300, and 4000 meters) by using an average lapse rate of 6°C/km. This value was chosen to replace the usually adopted value of 5°C/km since above, say 3000 meters the average free air lapse rate is near 6. 5°C/km.

In Table 16, all available temperature averages--except most values from the Tian-Shan and other areas of northern central Asia--have been collected for comparison. Only a few comments in regard to these records shall be given here.

At the 2300 m level a contrast from east to west is immediately visible. All stations in the valleys (Skardu, Kargil) have a more continental type of annual temperature variation, while all of the famous "Hill Stations" from Murree to Darjiling show the same moderate seasonal variation with cool summers and mild winters. The dry and sunny interior valleys, like Kargil, Skardu and Batang are much warmer during summer than the rainy and misty hill stations, where the ascending air is constantly cooled under near moist - adiabatic conditions. The daily temperature variation AT very clearly distinguishes the valley stations (AT > 12°C) from the hill stations (AT = 6-8°C).

At the 3300 m level there is only one group of hill stations which are situated on both sides of the Salang Pass in the Afghan Hindukush. While during winter the western mountains and valleys are usually rather cold, under the influence of a permanent snow-cover together with frequent clear nights, the valleys of southern and eastern Tibet (with little snow) are still mild, as well as those at Batang in section B. During summer the high valleys of southern Tibet are also warmer in an absolute sense than some of the Indian hill stations; the non-reduced averages from Lhasa (3675 m,

June X7°C) and Leh (3514 m, July 17. 4°C) are higher than those from Darjiling (2265 m, June 16. 3°C, July 16. 5°C). The most remarkable result is that even the annual averages of interior Tibet (Leh, Lhasa, Chiamdo, and Taining) are up to 10°C higher than those of Salang Pass, where the northern entrance of the highway tunnel is more frequently in clouds than the southern entrance. Sary Tash in the broad Alai Valley is exceptionally cold during the entire year. For July, the following reduced values can also be added from Table 16: Mangya 14.8, Kantze 14.8.

Most stations at the 4000 m level lexeept Lokpal and Fedtchenko Glacier) are from the interior highlands. While the summer temperatures are remarkably high, the winter temperatures in southern Tibet are relatively mild which results in a high annual mean. For July, the following reduced values can be added from Table 18: Shahiullah Mazar 10.9, Heiho 10.2, Gar Dzong 16.5 (if the height is reliable!), Shikatse 13.1, Phari Dzong 11.1; the new record from Gyangtse (July 12. 5) is apparently inconsistent with the former results. The records of "Central Tibet" and "Eastern Tibet" have been derived from non-stationary observations published by scientific expeditions, among which those of Sven Hedin are especially important (cf. Flohn 1958). These observations have been made at varying places and at varying heights; they have been reduced here to 4000 m in order to facilitate comparison, although 4500 m would certainly be a better approximation to the average true height. Such non-stationary averages are, if carefully observed and evaluated, nearly as representative as averages for ocean areas. The great diurnal variation of temperature shows the high frequency of nighttime freezing; Table 17 shows some (non-reduced) averages from Sven Hedin[1] s expeditions and from Depsang near Karakorum Pass.

Table 18 shows the temperature averages at synoptic stations, including average temperatures at 1200 GMT (1800 LT) as evaluated from the (incomplete) synoptic data published in two sources (12, 14, cf. Appendix A). While Lhasa, Yushu and Changtu are relatively moist during summer, the air at Heiho and especially at Karmu is much drier. During winter the eastern valleys are not as extremely dry as Lhasa, Karmu and especially Heiho. Table 19 contains relative humidities for the synoptic stations.

TABLE 16: MEAN TEMPERATURE (SURFACE STATIONS) REDUCED TO SELECTED ALTITUDES

Station[2]	Jan.	April	June	July	Oct.	Year	ΔT[1]
A) Reduced (by 0. 6°C/l00 m) to an altitude of 2300 meters							
Ghazni (2183 m)	-5.3	9.7	20.2	22.3	8.0	8.9	15. 6
Murree (2168 m)	+2.5	12.6	20.6	18.9	13.8	11.2	7.7
Skardu (2284 m)	-4.0	11.3	20.3	23.6	11.9	10.7	12. 4
Kargil (2682 m)	-5.2	10.8	21.5	26.3	14.3	11.2	12.0
Simla (2202 m)"	+4.7	14.0	19.2	17.7	14.5	12.7	7.2
Mussoorie (2115 m)	+4.9	14.7	18.8	17.1	13.1	12.7	7.4
Mukteshwar (2314 m)	+6.0	15.2	18.8	17.7	14.2	13.2	8.1
Jomosom (2800 m)	9.0	15.0	20.8	22.2	15.4	(15.3)	(12.6)
Lachen (2697 m)	5.1	13.1	16.8	18.0	10.9	11.7	8.4
Darjiling (2265 m)	+4.9	12.6	16.1	16.4	13.1	11.6	5.9
Batang (2685 m)	7.1	16.7	23.0	23.8	14.8	15.3	13.8
FOR COMPARISON:							
Khorog (2080 m)	-8.8	7.8	17.4	20.7	9.5	7.2	--
Sining (2295 m)	-7.1	6.5	15.3	18.1	11.1	9.8	--
Tali (2086 m)	+8.0	15.2	17.0	20.5	14.7	14.1	11.2
B) Reduced (by 0. 6°C/l00 m) to an altitude of 3300 meters							
Salang North (3350 m)	-9.7	+0.1		7.7	0.9	-0.4	7.2
Salang South (3100 m)	-9.0	+0.7		10.9	3.7	+1.2	6.6
Misgar (3102 m)	-6.9	+4.3		15.8	5.8	4.5	13.2
Leh (3514 m)	-7.2	+6.9		18.7	8.0	6.8	14.0
Dras (3066 m)	-17.1	-1.9		15.6	4.3	+0.4	14.4
Wallungchung Gola (3048 m)	-0.3	+6.7		11.8	7.7	6.1	9.2
Yatung (2987 m)	-1.5	+5.9		12.7	6.9	5.9	11.4
Lhasa (3675 m)	+2.2	11.8		18.5	11.3	10.8	15.5
Changtu (3200 m)	+0.1	10.2		17.7	10.7	9.4	18.5
FOR COMPARISON:							
Ansobski Pass (3583 m)	-11.3	-1.3		12.7	+1.1	+0.1	--
Sary Tash (3207 m)	-19.6	-3.4		8.4	-3.2	-4.3	--
Murgab (3640 m)	-15.7	+2.2		15.6	+1.6	+1.0	--
Dmeishan (3137 m)	-5.0	+1.9		11.6	4.2	+2.8	--
Sungpan (2882 m)	-4.8	+5.1		12.7	4.8	4.3	--

TABLE 16: CONTINUED

Station[2]	Jan.	April	July	Oct.	Year	ΔT[1]
C) Reduced (by 0.6°C/100 m) to an altitude of 4000 meters						
Lokpal (4267 m)	-8.0	-1.3	8.7	+2.4	+0.8	5.8
Gyangtse (3996 m)	-3.8	+4.9	14.3	+7.0	+5.5	16.6
Lhasa (3675 m)	-1.9	+7.7	14.4	+7.2	+6.7	15.5
Heiho (4150 m)[3]	-10.0	+2.0	10.0	+2.0	+1.0	--
Central Tibet[4]	-9.4	+3.2	11.7	+1.4	+2.3	17.4[5]
Eastern Tibet[4]	-12.9	(+2.1)	8.7	-3.2	-2.2	--
Taining (3690 m)	-9.6	+1.0	11.2	+3.7	+2.2	--
Fedtchenko Glacier (4169 m)	-16.2	-7.4	4.3	-5.9	-6.1	--
FOR COMPARISON:						
Latitude Average 35° N	-10.3	-4.8	5.0	-1.6	-3.0	--

1) ΔT = daily temperature amplitude (Max. -Min.) not reduced

2) Positions cf. Tables 1.1 a (Appendix B) and Table 21 (Appendix G)

3) Estimated from 1800 LT temperatures (Table 18a)

4) Expedition records at varying places, reduced to 4000 m, cf. Table 17

5) 1300 LT temperature minus daily minimum (slightly less than ΔT)

TABLE 17: SUMMER CLIMATIC DATA FROM NORTHERN AND WESTERN TIBET (EXPEDITIONS)

					Mean Temperature (°C)					Mean Cloudiness (%)				Resultant Wind 13^h			
Year	Month	$\bar{\phi}$(°N)	$\bar{\lambda}$(°E)	$\bar{H}$(m)	07^h	13^h	21^h	Min.	Ave.	07^h	13^h	21^h	Ave.	dd	q(%)	R(%)	n
1900	July	37.3	90.5	4020	6.1	14.7	6.2	-0.9	8.3	41	47	22	37	--	--	70	10
1900	August	35.7	90.0	4865	4.3	10.8	5.0	-1.2	6.3	66	61	62	63	--	--	67	31
1901	June	36.9	88.7	4465	2.8	12.2	2.6	-4.8	5.1	49	59	38	49	--	--	43	30
1901	July	34.3	88.5	5065	4.5	12.2	4.4	-3.6	6.4	53	58	36	49	--	--	49	31
1901	August	33.1	89.2	5022	5.1	12.7	5.0	+0.4	7.9	64	70	53	62	--	--	66	28
1906	August	34.0	78.4	4556	6.4	14.8	9.5	+1.5	10.1	58	58	30	49	233	26	38	16
1907	June	29.5	84.5	4602	7.4	14.6	3.7	-5.8	7.5	32	43	29	35	225	71	10	30
1907	July	30.3	82.5	4769	8.9	13.8	4.3	-2.8	7.9	61	52	38	50	223	85	22	31
1907	August	30.6	81.4	4608	10.6	15.7	7.0	+1.9	10.2	45	48	42	45	232	46	22	31
1908	June	-31	~84	4949	6.3	14.5	4.6	-2.7	7.5	18	47	8	24	216	56	37	30
1908	July	~ 31	~83	4803	6.9	13.2	6.1	-0.3	8.1	54	59	42	52	198	57	66	31
1908	August	~ 31	~82	4198	10.5	16.0	10.4	+4.5	11.8	57	66	50	58	238	37	57	31
Depsang (for comparison)					06^h	15^h				06^h	15^h	21^h		15^h			
1914	June	35.3	78.0	5362	-5.6	+6.2	-1.4	-7.6	-0.3	--	--	--	--	--	--	--	26
1914	July	35.3	78.0	5362	-1.0	+9.0	+1.8	-3.5	+3.2	49	59	36	49	271	--	--	31
1914	August	35.3	78.0	5362	-5.4	+2.8	-2.1	-6.6	-1.1	--	--	--	--	--	--	--	16

$\bar{\phi}$ ($\bar{\lambda}$) = average latitude (longitude) of observations

$\bar{H}$ = average height above sea level

$\bar{R}$ = relative frequency of rain days

n = number of days

dd = direction of resultant wind (270^o = W)

q = constancy (in percent)

TABLE 1 8: MONTHLY AVERAGES AND DAILY VARIATION OF AIR TEMPERATURE (°C), JUNE-SEPTEMBER

Station	June	July	Aug.	Sept.	00	06	12	15	18	ΔT[3]
					(July-August)					
Mangya	12.4	16.2	14.8	9.7	11.6	9.1	20.1	21.6	20.1	12.5
Shahiullah Mazar [1,2]	--	12.9	12.2	6.6	10.9	7.9	15.6	18.1	15.7	10.2
Gar Dzong[2]	12.2	14.8	14.6	9.6	11.8	8.7	16.8	19.4	18.4	10.7
Heiho	7.8	9.3	8.6	6.1	6.3	4.9	12.3	13.0	11.3	8.0
Shensa Dzong[2]	9.1	9.6	9.4	-6.2	--	--	--	--	12.0	--
Shikatse	14.0	14.3	12.4	11.9	11.1	9.5	15.9	17.4	16.3	7.9
Gyangtse[2]	12.8	12.5	12.1	9.3	--	8.3	15.3	17.3	14.3	9.0
Phari Dzong	7.1	8.1	7.7	5.9	6.5	5.2	11.1	10.6[4]	8.4	5.9
Kantze	12.5	14.4	13.7	11.6	11.2	10.6	18.2	19.1	15.8	8.5
Lawang[2]	19.2	20.9	19.5	18.6	18.5	17.9	23.2	23.3	20.6	5.4
Hsihchang	21.6	23.3	22.5	21.7	20.9	20.1	26.0	26.6	24.0	6.5
Depsang (5362 m)[5]	-0.3	3.2	-1.1	--	-2.2	-3.2	5.4	5.9	3.8	9.1
Tengchung[6]	19.9	20.3	20.4	19.8						

1) 1957 only
2) Reduced to eight observations daily
3) AT = difference 1500 (1200) - 0600 LT (90E)
4) Temperature drop probably caused by ascending valley winds
5) 1914 only
6) Average 1916-1937

AVERAGE TEMPERATURES AND DEW POINTS AT 1200 GMT (1800 LT)

	Lhasa		Heiho		Karmu		Yushu		Changtu	
	$\overline{T}$	$\overline{T}_d$	$\overline{T}$	$\overline{T}_d$	$\overline{T}$	$\overline{T}_d$	$\overline{T}$	$\overline{T}_d$	$\overline{T}$	$\overline{T}_d$
June	18.4	4.9	10.6	-1.2	19.2	-3.7	14.0	4.4	17.0	4.4
July	19.4	7.5	11.9	3.4	22.4	1.6	16.5	6.7	22.8	5.0
August	17.4	8.2	10.8	4.3	21.4	0.8	14.1	6.2	21.0	1.4
Sept.	15.1	4.7	8.1	0.3	14.6	-2.6	10.9	3.0	--	--
For comparison:										
Jan.	1.6	-22.7	-8.4	-29.3	-9.3	-23.6	-4.6	-19.0	3.1	-16.9
Feb.	5.0	-20.9	-5.4	-30.0	-3.4	-23.4	-2.1	-17.2	2.5	-16.5

Period: 1958-1962 incomplete (Yushu 1960-1962, Changtu 1958-1960)

TABLE 19: RELATIVE HUMIDITY (AVERAGES IN PERCENT), JUNE-SEPTEMBER (LOCAL TIME)

$\overline{RH}$ at	00	06	12	15	18	Ave.[1]
Mangya	37	43	20	18	20	28
Shahiullah Mazar	48	58	30	24	34	41
Gar Dzong	43	59	31	25	26	37
Heiho	84	88	54	51	62	68
Shikatse	76	84	54	50	54	64
Gyangtse	--	87	54	52	55	(64)
Phari Dzong	89	91	68	72	81	80
Kantze	83	86	52	48	63	66
Lawang	90	94	73	69	77	81
Hsihchang	79	84	59	57	68	69
For comparison:						
Depsang[2]	(70)	67	35	33	40	51

1) Eight observations

2) 35°I7'N, 77°58'E, 5362 m, June-July 1914

APPENDIX G: PRECIPITATION AND WATER BUDGET

The Tibetan Highlands are surrounded (from the Punjab through Afghanistan, Turkestan, Sinkiang and into northeastern China) by large arid or semi- arid areas with a relatively dense, growing population. Their water supply depends to a large extent on the runoff of rivers coming from the marginal mountains (Himalaya, Karakorum, Hindukush, Pamir, Alai, Kuenlun, Astyn Tagh, etc.), i.e. from the excess of the hydrologic balance in the high mountains. Because of the scarcity of available data for the terms of the hydrologic balance equation no complete budget can be given. However, it seems to be advisable to compile the available data as far as possible--some collected from private sources, others from unpublished official records (Tables Z0-Z2). Most of the data cover the mountains at the southern margins; only data from Pakistan have been published extensively (Source 16, Appendix A). USSR sources certainly contain much more highly valuable data; some published results are given for comparison in Table 22.

In the western mountains and valleys (Table 20, A-C) the largest portion of rainfall is produced by the traveling disturbances of the westerlies (mainly upper troughs) during winter and spring. In a highly interesting transition zone--cf. stations like Khost (Afghanistan), Peshawar, Cherat, Malakand and Saidu Sharif (N. Pakistan), Srinagar (Kashmir), Murree (Pakistan), Dalhousie and Joshimath (India)--the monsoon rains during summer overlap with these winter rains. This is an unique type of climate, rarely adequately treated in textbooks of climatology. This transition zone extends for more than 1500 km, from 70E to 84E (Jomosom, Nepal).

The belt of winter precipitations can be readily followed along the Himalaya Mountains right across Sikkim and Assam into upper Burma (cf. Pasighat or Htawgaw) with only slightly decreasing intensity (monthly averages for February-March may reach 100-150 mm in Assam and upper Burma, compared with 200-250 mm in the Hindukush). Due to the special flow patterns in NE India (Chapter 5, 8) during spring, no dry season separates the two rainy seasons, and the spring rains of NE India proceed immediately into the summer rains in spite of the complete reversal of the upper wind field during that transition. With the exception of the high Hindukush

area, November and/or December are frequently the driest months of the year; travel during late October or November is usually favoured because of the stability of the weather, the incredible blueness of the sky, the bright autumn colors and the excellent visibility.

In tropical and subtropical mountains a hierarchy of diurnal circulations to a large extent control the patterns of clouds and precipitation, taking into account the fact that traveling disturbances increase or decrease the moisture content and the vertical stability of the atmosphere. Since the daytime circulation is nearly everywhere much stronger than the reversed nighttime circulation, the area-averaged precipitation is to a large extent concentrated along the mountain ridges, while the larger valleys (with diameters on the order of 10-20 km) are locally characterized by arid conditions. Troll and Schweinfurth have reported this phenomenon from the Himalayas as well; in Table 20, stations like Misgar, Gilgit, Bunji, Kyelong and Jomosom represent these arid valleys. They contrast sharply with the adjacent mountains where 50-80 km long glaciers indicate much higher precipitation. In the Karakorum and at Nanga Parbat, glaciologists have estimated the average annual precipitation at up to 3000 or even 6000 mm compared with 100 mm in the valleys.

In fact, the valley data (hitherto the only available data) are largely unrepresentative. The western mountains receive enormous amounts of winter snow as shown by stations like Salang Pass (Afghanistan) and Kalam (Swat River) in northern Pakistan, as well as Chodko-Obi or even Pedtchenko Glacier (locally protected from the westerly winds). Thus, it is not astonishing that large towns like Kabul--in spite of only 32 cm rain per year--do not suffer at all from insufficient water supply, but rather from a lack of drainage of the high ground water level.

This is reflected in the high runoff values (Table 22) which implies even higher area-averaged precipitation rates. Any estimates of these precipitation rates from valley data alone are misleading; in the higher mountains (with peaks above 3500 m) precipitation amounts of more than 100 cm are very likely, and values of 200-500 cm should not be uncommon on the western and northwestern slopes of the highest ridges.

The area evaporation (Table 22) is determined as the difference between measured runoff and an estimated precipitation; not much emphasis can be laid upon the accordance of these values. Naturally the potential evaporation data based on Class A pans is much larger. Assuming a correction coefficient of 0.74, fairly representative evaporation values (of small open water surfaces) are as follows: Mangla (Chenab River) 17 5 cm, Saidu Sharif 141 cm, Balakot (34°33'N, $73^0$21'E, 1080 m) 176 cm and Tarbela Dam (Indus River, 34°04'N, 72°40'E, 353 m) as much as 209 cm per year.

Very little is known about precipitation and evaporation above the Tibetan Highlands. Precipitation data from Sinkiang are scarce; all oases at the edges of the Tarim Basin receive less than 10 cm/year. In the SE corner of Tibet rainfall is much greater and varies between 50 and 200 cm/year while Lhasa, Gyangtse and Chiamdo receive 25-50 cm/year. Since > 40 per cent of central and northern Tibet have only internal drainage, this area should be even drier.

Using the foregoing estimates of the thermally driven circulation, and the heat budget, one can also try to obtain reasonable estimates of the water budget terms. The local rainfall P due to evaporation E is one part, the advective rainfall P_a due to the transport of water vapor W = -div ($\overline{vq}$) across the marginal mountains is the other part. The storage of water vapor in the atmosphere (S_a) is small but not always negligible; the storage in the soil (S_S) including snow-cover maintains to a large extent the external runoff Rf. Now we may distinguish between a local water cycle ($E-P_\ell = 0$) and a regional water cycle ($P_a - Rf - S_S + S_a = 0$). The complete water balance equation may then be written as follows:

$$P_a + P_\ell = Rf + E + S_S - S_a$$

The first attempt considers the highlands, as a whole. Here one may assume that during summer $P_\ell - E = 0$, $S_a = 0$ and $Rf - S_S = 0$; then $W = P_a$. The average mass inflow in the 500-600 mb layer has been estimated at 360 cm sec^{-1}. Over the southeastern highlands this layer contains nearly 0.6 g precipitable water; averaged over the whole circumference 0.5 g is chosen as a more realistic value. Then the water vapor

transport, W, into the highlands is

$$W = 360 \text{ cm sec}^{-1} \times 0.5 \text{ g cm}^{-2} = 180 \text{ g cm}^{-1} \text{ sec}^{-1}.$$

Or, integrated over a circle with the radius R = 800 km

$$\Sigma W = 180 \times 2\pi \times 8 \times 10^{7} \text{ g sec}^{-1} = 0.90 \times 10^{11} \text{ g sec}^{-1} .$$

Assuming (Chapter 3) 300 giant cells each with a rain area having a diameter of 10 km, the total rain area in a given time unit (e. g. one hour) is $300 \times \pi \times 5^2 = 2.36 \times 10^4$ km^2 (neglecting the displacement of the cells with the average flow). Under these assumptions, the rainfall intensity in these 300 cells is

$$J_R = 0.9 \times 10^{11} \times 3600/2.36 \times 10^{14} \text{ g cm}^{-2}\text{h}^{-1} = 1.37 \text{ g cm}^{-2}\text{h}^{-1} \text{ or } 13.7 \text{ mm h}^{-1}$$

which is a quite realistic value.

Next, averaging the rainfall produced by the giant cells over the total area of the Tibetan Highlands for an entire day, the 12-hour inflow of water vapour gives

$$P_a = 0.9 \times 10^{11} \times 4.32 \times 10^{4}/2 \times 10^{16} \text{ g cm}^{-2}\text{d}^{-1} \sim 0.20 \text{ g cm}^{-2}\text{d}^{-1}$$

equivalent to 2 mm per day or 60 mm per month.

The rainfall P_ℓ from local sources must be added to this. From the surface heat budget considerations (Chapter 7) an average value of LE = 90 ly d^{-1} may be estimated as typical for high-level grasslands; this is equivalent to an evaporation of 1.5 mm d^{-1} or 45 mm per month. Neglecting and assuming $Rf = S_S$ (mainly in the marginal mountains), an estimate of local rainfall is given as $P_\ell \sim E$. Thus the area average of summer rainfall for the Tibetan Highlands should be on the order of 100 mm per month. This is not an unrealistic value, taking into account the fact that the valley stations of SE Tibet observe monthly rainfall amounts of 100-250 mm and Gyangtse in the arid upper Tsangpo Basin receives 80-90 mm (Table 20).

A further estimate of P can be derived from the relatively large daily variations of precipitable water in the atmosphere (S_a). The following values were obtained from aerologica1 data in the 300-600 mb layer:

Local Time	Lhasa	Heiho	Kantze	Karmu	Lawang	Nochiang
					(for comparison)	
0600	1.38	1.30	1.23	0.57	1.19	0.38 cm
1800	1.24	1.15	1.21	0.48	--	0.28
0600-1800	0.14	0.15	0.02	0.09	--	0.10

Assuming, as above, Rf = S_S and P_a = W, then P_ℓ = E + S_a. During daytime, the average loss of precipitable water is S_a = -0.10 cm (in south-central Tibet -0.15 cm); this must be replenished during the night by a part of W. The local evaporation (E) is mostly restricted to the daylight hours; during the night E may even be negative when and where dew is produced. Thus, an estimate of rainfall due to local sources during daytime (0600-1800 LT) is

$$P_\ell = E + S_a = 0.\ 15 + 0.10 \text{ cm } d^{-1} = 0.25 \text{ (in central Tibet 0.30) cm } d^{-1}.$$

It must be realized, however, that the rainfall obtained from is, in fact, part of the advective rainfall P_a= W. Near the geographical center of the highlands, W should be small. If W = S_a, this value of P may give a lower limit of the total amount of precipitation during the summer rain period in central Tibet, i.e. about 90 mm/month.

TABLE 20: AVERAGE AMOUNT OF PRECIPITATION (mm)

Station	J	F	M	A	M	J	J	A	S	O	N	D	Year
A) Eastern Afghanistan													
Kabul	33	38	91	84	22	4	2	2	1	10	15	14	316
Karizimir	42	65	106	140	37	1	8	1	2	4	41	30	477
Jabul Saraj	55	88	115	170	40	1	4	0	2	4	29	38	545
Salang South	112	206	244	346	106	3	4	0	6	18	74	96	1214
Salang North	92	205	241	308	164	6	9	1	7	30	74	108	1244
Faizabad	32	107	103	67	44	2	11	2	2	21	25	25	443
Ghazni	44	57	68	99	25	3	17	0	0	1	21	33	368
Khost	13	40	65	102	59	23	123	70	53	8	10	16	583
Jalalabad	20	25	40	58	27	0	9	3	1	3	18	18	221
B) Pakistan (west of Indus, 70-73°E)													
Chitral	22	37	87	92	33	9	4	6	8	20	6	21	346
Drosh	35	39	95	104	49	17	15	17	18	32	9	30	459
Kalam	73	110	205	267	96	5	43	25	34	36	46	71	1011[1]
Saidu Sharif	84	87	128	89	54	45	124	110	56	25	23	53	87 8
Malakand	75	98	119	73	24	22	128	187	59	19	8	53	865
Mardan	43	46	58	36	16	17	80	120	43	8	10	21	500
Peshawar	37	40	62	45	20	8	32	52	21	6	8	17	345
Landikotal	33	43	69	65	28	10	23	38	18	8	5	20	360
Cherat	59	82	109	71	42	29	92	125	53	14	9	40	725
Parachinar	52	67	110	102	159	51	89	94	54	24	20	30	744
Ft. Lockhart	57	71	88	79	63	61	142	143	77	25	30	26	843

1) Reduced to Saidu Sharif 908 mm

C) Pakistan (east of Indus) and Kashmir (73-76°E)													
Misgar	8	5	11	15	18	6	9	10	7	3	3	5	100
Gilgit	7	7	20	24	22	10	10	14	10	6	1	3	134
Bunji	7	7	22	27	27	17	14	21	9	2	2	2	158
Astor	35	21	98	80	47	27	7	30	22	8	10	18	403
Srinagar	74	72	92	93	60	36	59	61	39	30	11	33	640
Abbottabad	87	104	114	89	56	79	228	250	94	35	18	46	1200
Murree	96	112	122	105	66	101	315	351	138	40	19	46	1508

TABLE 20: CONTINUED

Station	J	F	M	A	M	J	J	A	S	O	N	D	Year
C) Pakistan (east of Indus) and Kashmir (73-76°E) cont'd.													
Skardu	22	18	26	25	20	6	10	9	10	4	2	10	162
Kargil	37	38	60	42	25	7	7	10	10	6	3	21	264
Dras	97	97	138	104	62	17	16	14	18	22	12	54	649
Dalhousie	181	169	98	76	54	130	557	563	174	34	19	98	2153
D) Central Himalayas (77-80°E)													
Leh	10	8	7	6	6	5	12	15	7	3	1	5	83
Kyelong	59	64	102	79	56	23	23	33	52	21	7	26	555
Kulu	105	113	131	80	54	54	128	147	75	27	15	51	981
Simla	65	70	64	46	60	149	416	419	182	33	10	28	1542
Lokpal	247	125	179	82	49	117	483	372	238	129	31	127	2179
Joshimath	66	93	98	54	35	89	176	185	108	28	12	27	973
Mussoorie	69	87	57	34	42	223	698	695	253	29	4	35	2225
Mukteswar	57	62	48	36	56	176	316	306	202	43	9	25	1337
Nainital	70	73	53	38	84	391	769	750	363	61	13	25	2690
E) Nepal (83-87°E)													
Jomosom	30	22	40	21	13	10	42	46	30	23	1	2	281
Beni	26	28	42	34	78	212	320	414	187	46	8	9	1406
Butwal	16	15	15	21	58	405	673	812	330	31	9	4	2451
Kathmandu	10	42	15	26	129	246	373	347	182	36	2	8	1416
Namche Bazar	34	24	32	27	43	139	212	210	140	51	15	13	939
Chaunrikharka	8	11	30	49	124	376	621	615	362	78	9	7	2284
Jiri	18	26	46	87	107	419	613	617	396	88	18	7	2522
Wallungchung Gola	31	23	60	62	84	191	301	349	229	126	7	5	1468
F) Sikkim and Tibet (88-90°E)													
Gyangtse	0	1	3	5	12	38	78	94	35	4	1	0	271
Lachen	56	58	149	105	149	256	294	265	243	129	17	20	1741
Chungtang	36	57	261	182	350	439	523	521	183	220	5	32	2799
Yatung	14	55	52	81	103	145	163	155	110	49	11	9	947

TABLE 20: CONTINUED

Station	J	F	M	A	M	J	J	A	S	O	N	D	Year
F) Sikkim and Tibet (88-90°E) cont'd.													
Gangtok	25	68	129	294	436	545	664	593	478	147	46	27	3452
Darjiling	11	32	54	115	231	597	792	643	446	142	25	4	3082
G) Assam and Burma (95-99°E)													
Pasighat	55	96	138	273	466	967	975	622	585	261	33	24	4491
Sadiya	44	82	128	251	274	492	508	418	305	143	27	21	2693
Putao	17	52	74	124	204	705	931	934	733	182	28	9	4042
Htawgaw	33	101	98	161	235	405	344	266	194	170	78	25	2131
Myitkyina	10	23	23	46	160	493	477	434	257	183	39	12	2147
Tengchung (China)	13	38	39	66	124	242	316	260	168	165	47	16	1496
H) USSR (Turkestan and Pamir) for comparison													
Dushanbe	79	74	108	111	73	19	1	3	1	19	45	71	604
Chodko-Obi	221	182	240	182	136	47	14	5	9	75	125	192	1428
Ansobski Pass	20	20	29	37	47	36	8	7	3	13	21	18	259
Khorog	27	23	23	29	18	5	3	1	3	10	22	20	183
Sary Tash	13	18	25	23	55	63	38	16	12	17	17	18	315
Irkeshtam	5	5	10	14	28	30	25	15	12	7	6	6	164
Murgab	5	3	4	6	11	14	8	8	7	2	2	2	72
Fedtchenko Glacier	82	75	92	87	86	65	27	16	20	69	87	92	798
J) Sinkiang and Northeastern Margins													
Kashgar	15	3	12	5	7	5	10	7	3	2	5	8	81
An-hsi	2	1	4	5	3	6	15	10	3	1	2	5	57
Tun-hwang	1	1	3	3	6	9	15	9	2	0	1	2	52
Chiuchuan	1	3	5	4	8	10	17	28	5	1	3	2	87
Tsaidam (~Karmu)													108
Sining	1	3	5	4	26	48	71	94	72	25	5	1	365
Lanchow	3	3	7	13	28	38	67	92	55	16	3	1	326

TABLE 20: CONTINUED

Station	J	F	M	A	M	J	J	A	S	O	N	D	Year
J) Sinkiang and Northeastern Margins Cont'd.													
Sunpan	5	13	27	62	99	124	158	92	119	65	18	7	789
Taining	1	7	18	73	76	166	102	76	174	36	5	2	736?
K) Eastern Tibet and Southeastern Margins													
Changtu	0	3	5	10	65	129	96	77	93	10	2	2	491
Lhasa	0	6	4	3	21	70	147	114	59	10	3	0	437
Batang (Pa’ an)	0	2	0	8	28	109	140	127	127	28	0	0	569
Tali	2	57	101	27	147	315	271	198	197	99	62	13	1488
Tatsienlu	10	10	18	58	84	160	86	96	140	64	8	3	737
Ya'an	15	25	40	91	97	154	474	418	218	120	55	18	1725
Hsih chang	8	10	28	30	86	272	180	208	231	112	33	3	1202
Kunming	5	24	19	26	135	201	291	278	180	73	46	13	1284

TABLE 21: COORDINATES OF CLIMATIC STATIONS

Station	Lat. (N)	Long. (E)	Height (m)	Code No.	n
A) Eastern Afghanistan					
Kabul	34°33'	69°12'	1803	40 948	45
Karizimir	34°40'	69°05'	1860	40 949	9
Jabul Saraj	35°08'	69°15'	1628	40 952	6
Salang South	35°21'	69°03'	3100	40 937	5
Salang North	35°22'	69°03'	3350	40 938	5
Faizabad	37°09'	70°29'	1200	40 913	4
Ghazni	33°32'	68°25'	2183	40 961	9
Khost	33°40'	69°55'	1185	40 959	5
Jalalabad	34°26'	70°28'	551	40 950	9
B) Pakistan (west of Indus)					
Chitral	35°51'	71°50'	1439	41 506	31
Drosh	35°34'	71°47'	1509	41 515	40
Kalam	35°30'	72°35'	2290	-	4
Saidu Sharif	34°47[1]	72°22'	900	-	26
Malakand	34°33'	71°55'	~800	-	38
Mardan	34°12'	72°03'	~350	-	57
Peshawar	34°01'	71°35'	360	41 530	60
Landi Kotal	34°06'	71°08'	1067	41 528	38
Cherat	33°49'	71°53'	1302	41 565	45
Parachinar	33°52'	70°04'	1728	41 560	40
Ft. Lockhart	33°33'	70°55'	1998	-	43
C) Pakistan (east of Indus) and Kashmir					
Misgar	36°47'	74°46'	3102	41 502	15
Gilgit	35°55'	74°23'	1488	?	47
Bunji	35°39'	74°38'	~1400	-	7
Skardu	35°18'	75°37'	2284	?	47
Astor	35°22'	74°52'	2350	-	7
Kargil	34°34'	76°08'	2682	-	41
Dras	34°26'	75°46'	3066	43 542	45
Abbottabad	34°09'	73°13'	~1400	-	75

TABLE 21: CONTINUED

Station	Lat. (N)	Long. (E)	Height (m)	Code No.	n
C) Pakistan (east of Indus) and Kashmir cont'd.					
Murree	33°54'	73°24'	2168	41 573	60
Dalhousie (India)	32°32'	75°58'	1959	42 059	~10
D) Central Himalaya (77-80°E)					
Leh	34°09'	77°34'	3514	43 544	60
Kyelong (Chenab Valley)	32°35'	77°04'	?	-	50
Kulu (Seraj-Tahsil)	31°57'	77°07'	1370	-	50
Simla	31°06'	77°10'	2202	42 083	50
Lokpal	30°44'	79°38'	4267	-	~7
Joshimath (Garhval)	30°33'	79°34'	187 5	42 416	50
Mussoorie	30°27'	78°05'	2115	42 112	15
Mukteshwar (Kumaon)	29°28'	79°39'	2310	42 147	50
Nainital	29°24'	79°28'	1953	42 146	50
E) Nepal (83-87°E)					
Jomosom	28°47'	83 43'	2800	-	9
Beni	28°21'	83°34'	915	-	9
Butwal	27°42'	83°28'	263	-	9
Kathmandu	27°42'	85°20'	1324	42 289	40
Jiri	27°38'	86°14'	1895	-	3-4
Chaunrikharka	27°42'	86°44'	~2700	-	14
Namche Bazar	27°50'	86°43'	~3400	-	14
Wallungchung Gola	27°42'	87°47[1]	3048	-	5
F) Sikkim and Tibet (88-90°E)					
Gyangtse (Tibet)	28°56'	89°36'	3996	-	41
Lachen (Sikkim)	27°43'	88°32'	2697	-	9-11
Chungtang	27°36'	88°30'	1637	-	4
Yatung (Tibet)	27°29'	88°55'	2987	-	45

TABLE 21: CONTINUED

Station	Lat. (N)	Long. (E)	Height (m)	Code No.	n
F) Sikkim and Tibet (88-90°E) cont'd.					
Gangtok (Sikkim)	27°20'	88°37'	1764	42 299	27
Darjiling (India)	27°03'	88°16'	2265	42 295	50
G) Assam and Burma (95-99°E)					
Pasighat (Assam)	28°06'	95°23'	?	-	35
Sadiya (Assam)	27°50'	95°40'	?	-	50
Putao (Burma)	27°20'	97°25'	409	48 001	17
Htawgaw[2]	?	?	?	-	27
Myitkyina (Burma)	25°22'	97°24'	145	48 008	45
Tengchung (China)	25°07'	98°29'	1628	56 739	24
2) Burma, District Myitkyina					
H) USSR (Turkestan and Pamir, for comparison)					
Dushanbe	38°35'	68°47'	824	38 836	?
Chodko-Obi-Farm	~38.9	~69.5	1807	-	?
Ansobski Pass	39°04'	68°52'	3583	-	?
Khorog	37°30'	71°30'	2080	38 954	22
Sary Tash (Alai)	39°44'	73°15'	3207	?	?
Irkeshtam	39°42'	73°54'	2819	?	30
Murgab[3]	38°10'	73°58'	3640	?	?
Fedtchenko Glacier	38°50'	72°13'	4169	?	?
3) Formerly Pamirski Post					
J) Sinkiang and Northeastern Margins					
An-hsi	40°43'	95°57'	1182	52 424	9
Tun-hwang	40°08'	94°47'	1100	?	14
Chinchuan	39°45'	98°33'	1470	52 533	17
Sining	36°37'	101°55'	2295	52 866	4
Lanchow	36°03'	103°51'	1506	52 889	19
Sunpan	32°39'	103°34'	2882	56 182	12
Taining	30°53'	101°29'	3690	?	3-4

TABLE 21: CONTINUED

Station	Lat. (N)	Long. (E)	Height (m)	Code No.	n
K) Eastern Tibet and Southeastern Margins					
Batang (Pa' an)	30°05'	98°55'	2700	56 247	3
Tali	25.42°	100.12°	2086	?	3
Tatsienlu	30°01'	102°09'	2520	?	8
Ya'an	30°00'	103°09'	650	56 287	14
Kunming	25°02'	102°43'	1893	56 778	13

n = length of available record (years)

TABLE 22: RUNOFF DATA (E) AND ESTIMATED WATER BUDGET (cm/year)

River	Station	Lat. (N)	Long. (E)	Catchment Area (km^2)	Period
Gilgit	Gilgit	35°56'	74°19'	12100	1962-64
Indus	Darband	34°24'	72°50'	166000	1960-64
Swat	Kalam	35°30'	72°35'	2020	1961-64
Swat	Chakdara	34°38'	72°02'	5770	1961-64
Kabul	Warsak	34°11'	71°24'	67500	1961-64
Chitral	Chitral	35°50'	71 48'	10300	1964
Jhelum	Mangla	33°08'	73 38'	33000	1922-56
Serafshan	Ustje Fass Darja	39-40°	67-69°	4650	Unknown, but long period
Rayon High-Badakhshan		37-39°	71-74°	63700	
Rayon Osh {Ferghana)		40-41°	70-73°	73900	

River	Station	Rf (cm)	F(%)	Area Precipitation (P) a)	b)	c)	d)	e)	Average (cm)	Area Evaporation (cm)
Gilgit	Gilgit	70	~65	108	128	112	129	116	119	49
Indus	Darband	46	~60	77	103	87	101	82	90	44
Swat	Kalam	132	~70	188	-	172	200	168	182	50
Swat	Chakdara	87	~65	133	145	-	147	122	137	50
Kabul	Warsak	29	~35	83	82	100 f)	81	65	82	53
Chitral	Chitral	52	~65	80	-	93	108	88	92	40
Jhelum	Mangla	83	~60	138	142	-	(144)	119	136	53
Serafshan	U. Fass D.	55	66						84g)	29
High-Badakhshan		26	61						41g)	15
Osh (Ferghana)		29	56						52g)	23

a) Estimate based on runoff factor F = P/Rf

b) Estimated after Wundt, Table 4, T_m=+10°

c) As b), but T_m = +5°

d) Formula Rf = 0.86(P - 47.3) cm, winter rain area

e) Formula Rf = P - 36 (cm)

f) As b), but T_m = 15°

g) Measurements (corrected)

APPENDIX H: LOCAL WIND SYSTEMS

Surface wind observations at Tibetan stations often reveal marked local wind systems which add to the large-scale diurnal and seasonal circulation; many stations show how this large-scale seasonal system can overwhelm local valley and mountain breezes. Since the station site and topographical features cannot be judged adequately in each case from existing maps (1:1 million), detailed interpretations are possible only at selected stations. Table 23 contains the frequency of wind directions (in 30°sections, as recommended by the Aerological Commission-of 4he WMO) and calms at these stations together with the average scalar wind speed v_S in knots; the use of detailed speed data is unnecessary here because of the positive correlation between frequency and speed in the different wind directions. Only data for the standard observing hours 0600, 1200 and 1800 local time (90°E) are used; 0600 winds represent the nocturnal, 1200 and 1800 the daytime circulation.

At Mangya, winds from the NNW or NNE prevail at early morning as well as at noon and evening, with only minor shifts. Since the prevailing geostrophic flow is from WNW, the surface wind cannot be interpreted as a deviation caused by friction. The daytime circulation is obviously an up- slope breeze at the SW edge of the Tsaidam Basin; the dawn wind (0600 LT) may be interpreted as the large-scale seasonal circulation triggered by the Tibetan plateau (cf. Chapter 6) and overwhelming the expected weak down- slope wind. Conditions at Karmu (evening) and at Shahiullah Mazar (broad meandering and converging valleys) are essentially similar.

At Gar Dzong, in the broad valley oriented from SSE to NNW, a simple valley and mountain breeze circulation should be expected. At dawn the expected mountain breeze blows from SSE but with a remarkable intensity which may be attributed to reinforcement by the seasonal large-scale circulation (from S). At noon the winds are weakest when the ascending valley breeze (NNW), the gradient flow (SW) and the large-scale circulation (down- valley from SSE) are all of nearly equal intensity. At evening, the gradient flow (SW) dominates.

At Heiho, NNE winds prevail during the night; this is consistent with the assumption that Heiho = Nagchu Dzong (Appendix B) and may be interpreted as a mountain breeze from a nearby ridge. During daytime, the large vertical exchange of momentum leads to an approximate projection of the geostrophic flow (prevailing SW, but with a large variability) down to the surface (cf. Gar Dzong, 1800 LT). The resultant wind and constancy are at 0600 LT 39° (42%), at 1200 LT 239° (37%), and at 1800 LT 183° (only 5%).

At Shikatse, at dawn and in the late afternoon, ascending valley breezes (NNW) and descending mountain breezes as well as the large- scale circulation (SSE) contribute nearly equally; at noon ascending valley breezes prevail.

At Phari Dzong, near the origin of a valley running southward and crossing the Himalayas, the ascending valley breeze prevails during the entire day, even at dawn (with many calms); here the southerly seasonal circulation overwhelms the expected weak nocturnal mountain breeze.

At Lawang, in spite of a more complex topography, the wind distribution is nearly the same as at Phari Dzong; the sa,me is also true for Hsihchang, however, with 50-90% calms during the daytime as well.

At other places (Lhasa, Shensa Dzong, Gyangtse, Kantze, Yushu) the winds are largely channelled by the local topography; no clear differentiation between local circulations, large-scale circulations and geostrophic flow seems possible.

TABLE 23: FREQUENCY AND MEAN SPEED (v_S) OF SURFACE WINDS,

JUNE-SEPTEMBER (LOCAL TIME)

	dd(10°) =	03	06	09	12	15	18	21	24	27	30	33	36	Calm	n	v_S (kt)
Karmu	1800	54	28	16	4	7	2	21	13	40	53	106	23	94	464	--
Mangya	0600	15	8	6	8	17	2	7	6	3	40	106	7	200	425	3.6
	1200	72	44	34	21	29	10	10	11	22	37	84	48	20	422	7.6
	1800	162	66	32	8	9	3	8	5	5	11	94	67	5	475	10.1
Shahiullah Mazar	0600	27	1	0	0	0	1	3	4	21	8	5	5	9	84	6.9
	1800	91	0	0	0	0	0	0	1	0	0	0	0	0	92	18.5
Gar Dzong	0600	4	0	0	2	59	26	1	2	1	1	0	4	9	109	6.5
	1200	6	3	1	6	24	9	15	8	10	2	16	8	5	113	5.3
	1800	2	0	0	3	13	8	51	33	13	4	22	10	5	165	8.4
Heiho	0600	89	14	8	14	10	4	11	4	1	0	13	18	259	445	2.2
	1200	33	7	8	20	43	39	114	32	11	15	37	30	75	464	5.6
	1800	55	24	19	43	38	30	69	36	18	14	40	37	59	482	6.2
Shikatse	0600	1	0	1	2	32	2	4	0	0	0	24	16	150	232	1.5
	1200	27	5	8	7	12	3	2	1	2	0	37	58	60	222	3.7
	1800	7	4	10	18	43	19	10	5	10	2	16	41	91	276	4.2
Phari Dzong	0600	9	2	4	9	41	10	32	9	3	1	2	3	205	330	1.7
	1200	5	0	2	37	225	31	23	6	5	1	0	1	4	340	9.3
	1800	3	1	0	19	252	36	31	3	3	0	1	1	9	359	8.2
Lawang	0600	0	0	0	0	18	5	0	0	0	0	4	1	107	135	0.6
	1200	3	0	4	10	44	25	1	0	2	0	3	1	26	119	4.6
	1800	1	1	1	4	102	35	18	2	4	2	7	3	66	245	3.3
Hsihchang	0600	5	1	1	0	0	1	12	4	8	1	8	6	304	351	0.4
	1200	4	2	11	8	43	24	57	13	6	5	9	4	173	349	1.9
	1800	17	1	4	3	21	17	42	4	1	1	17	16	222	366	1.8

APPENDIX J: WINTER CONDITIONS IN THE TIBETAN HIGHLANDS

As a supplement to this investigation devoted to the summer conditions in the Tibetan Highlands, a few notes regarding the winter conditions seem to be appropriate. Tables 16 and 20 contain climatological data, mainly in the marginal mountains, for the whole year; Tables 8 and 13 give year-long aerological data; and furthermore. Tables 2, 3, 5 and 18a include additional statistics of meteorological data during winter for comparison.

The most essential question deals with the extension and duration of the winter snow cover. If Tibet can, in fact, act as a cold source (Flohn 1958, Rangajanan 1963), this should be expected during the winter when all of the high mountains are more or less snow-covered. In this case, the continuous drainage of freshly produced cold air through the mountain gaps toward the south should contribute to the remarkable strength and persistency of the subtropical jet south of the Himalayas. However, a preliminary (and necessarily incomplete) study of satellite pictures from ESSA 3 (January 4-23, 1967) and from ESSA 6 (February-March 1968, not rectified) revealed that large sections of the Tibetan Highlands, except the mountains, are mostly cloud-free. From the first series, January 4, 6, 8, 13, 15 and 20 are cases where the bulk of western, central and southern Tibet is cloud-free and snow-free. This is especially true for the elongated basins of the upper Indus, upper Sutlej and upper Tsangpo between longitudes 7 8E and 92E, which are apparently snow-free in more than 80 percent of all pictures examined. Central Tibet (31-34N, 83-90E) appears to be snow-free in about 50 percent of all cases. The visual albedo from the satellite pictures closely resembles that of central India (except for a dark strip just south of the Himalayas, about 100 km wide); it is definitely lower than that of the sandy Arabian Desert (Rub'al Khali). Since snowfall certainly occurs, this lack of a permanent snow cover may be interpreted as a result of the strong solar radiation in the subtropical highlands, together with the high evaporative power of the dry winter air (Table 18a). Tables 3 and 5 show the low cloudiness of this season, consisting mainly of thin, medium and high clouds.

The mountains of the central and eastern Himalayas are mostly snow-capped but separated by large snow-free valleys; the western mountains, however, are nearly always covered by extensive snow and only the large arid valleys can be easily discerned.

RECENT ATMOSPHERIC SCIENCE PAPERS

121. Atmospheric Water Balance *of* the Upper Colorado River Basin. J. L. Rasmussen. Prepared with support from contract NONR 1610(06) Office of Naval Research. February 1968.

122. Proceedings of the Symposium on Mountain Meteorology, 26 June 1967, Fort Collins, Colorado. Edited by E. R. Reiter and J. L. Rasmussen. Cost: $3.50 per copy.

123. The Sessile Drop as a Heterogeneous Nucleation Embryo. W. R. Barchet. Prepared with support from National Science Foundation Grant No. GA-930. June 1968.

124. Investigation of the Importance of Cumulus Convection and Ventilation in Early Tropical Storm Development. Raul Erlando Lopez. Prepared with support from NSF GF-287 and ESSA E-22-80-68(G) grants. June 1968.

125. Numerical Simulation of the Blocking Process. Y. Kikuchi. Supported in part with funds from National Science Foundation Grant No. Ga-761, June 1968.

126. Studies on Interaction Between Synoptic and Mesoscale Weather Elements in the Tropics. Part I: Some Aspects of Cumulus-Scale Down- drafts; Herbert Riehl. Part II: Vorticity Budgets Derived from Caribbean Data; Robert P. Pearce, Imperial College, London.

127. A Three-Dimensional Spectral Prediction Equation. T. J. Simons. Prepared under National Science Foundation Grant No. GA-761. July 1968.

128. Anisotropy in Reflected Solar Radiation. Vincent V. Salomonson. Supported by National Aeronautics and Space Administration Grant No. NASr-147. August 1968.

129. Studies in Low-Order Spectral Systems. F. Baer. Prepared under National Science Foundation Grant No. GA-761. August 1968.

The "Atmospheric Science Papers" are intended to communicate without delay current research results to the scientific community. They usually contain more background information on data, methodology, and results than would normally be feasible to include in a professional journal. Shorter versions of these papers are usually published in standard scientific literature.

Editorial Office: Head, Department of Atmospheric Science
Colorado State University
Fort Collins, Colorado 80521